



Journal of the Geological Survey of Brazil

The Rio Piranhas-Seridó Domain, Borborema Province, Northeastern Brazil: Review of geological-geochronological data and implications for stratigraphy and crustal evolution

Vladimir Cruz de Medeiros^{1*} , Rogério Cavalcante¹ , Frank Gurgel Santos² ,
Joseneusa Brilhante Rodrigues⁴ , Jocilene dos Santos Santana³ , Alan Pereira da Costa¹ ,
Izaac Cabral Neto¹ 

¹CPRM-Serviço Geológico do Brasil (NANA/SUREG-RE), Rua Professor Antônio Henrique de Melo, 2010, Natal, RN, Brazil, CEP: 59078-580

²CPRM-Serviço Geológico do Brasil (GEREMI/SUREG-RE), Av. Sul, 2291, Recife, PE, Brazil, CEP: 50770-011.

³CPRM-Serviço Geológico do Brasil (GEREMI/SUREG-SA), Av. Ulysses Guimarães, 2862, Sussuarana - Centro Administrativo da Bahia, Salvador, BA, Brazil, CEP: 41213-000

⁴CPRM-Serviço Geológico do Brasil (SEDE), Setor Bancário Norte - SBN Quadra 02, Bloco H - Asa Norte, Brasília, DF, Brazil, CEP: 70040-904

Abstract

This paper presents a review of available lithostratigraphic and isotopic data, in addition to other information collected from projects of the Geological Survey of Brazil (SGB-CPRM), for the Rio Piranhas-Seridó Domain (PSD). This domain is one of the tectonostratigraphic compartments of the central-northeast portion of the Borborema Province (Northeast Brazil), bound by the Picuí-João Câmara, Patos and Portalegre shear zones. More recent isotopic determinations (U-Pb dating of zircon) and geological maps (usually on a 1:100000 scale) have clearly detected and/or redefined several units, e.g., the Amarante, Campo Grande, Granjeiro and Saquinho complexes, in addition to the Serra do Ingá body (Archean), Arabia Complex (Siderian), Caicó Complex and Serra da Formiga Suite (Rhyacian), Poço da Cruz Suite (Orosirian-Statherian), Seridó Group (Ediacaran) and Ediacaran to Early-Cambrian magmatic suites, in addition to pegmatites and granitic pegmatites. With respect to the supracrustal rocks of the Seridó Group, the deposition in the Ediacaran is based on field relations and on the ages of detrital zircons, which showed a greater contribution from Mesoproterozoic to Neoproterozoic sources, the vast majority of which may come from the PSD itself. Current records indicate that the evolution of the PSD started in the Eoarchean, and peaked in the Neoproterozoic with the Brasiliano event, which is characterized by sedimentation of the Seridó Group, intrusion of plutonic bodies, deformation and metamorphism (especially at the regional level), in addition to the formation or reactivation of important shear zones. Such evolution is acknowledged on the basis of the accretion of oceanic arcs during the Paleoproterozoic (containing Archean fragments), including the generation of juvenile magmas and a protocrust (Caicó Complex). The Neoproterozoic record, associated with the Brasiliano event, is considered by several authors as reworking with no or little contribution of juvenile material, with deposition of the Seridó Group, emplacement of several Ediacaran to Early-Cambrian magmatic suites, accompanied by the formation of shear zones, predominantly in the southern and eastern portion of the domain.

Article Information

Publication type: Research papers
Received 9 June 2021
Accepted 20 August 2021
Online pub. 28 September 2021
Editor: Evandro Klein

Keywords:
Rio Piranhas-Seridó Domain,
Borborema Province,
Crustal evolution,
U-Pb, Lithostratigraphy

*Corresponding author
Vladimir Cruz de Medeiros
vladimir.medeiros@cprm.gov.br

1. Introduction

The Rio Piranhas-Seridó Domain (PSD) corresponds to a segment of the Borborema Province (Almeida et al. 1977), encompassing part of the states of Ceará, Rio Grande do Norte, Paraíba and Pernambuco in northeastern Brazil. It is bounded to the east, south and west by the Portalegre, Picuí-João-Câmara and Patos shear zones, respectively, while to

the north it is covered by the Phanerozoic sedimentary rocks of the Coastal Province and the Potiguar Basin (Fig. 1).

Considering previous studies and methodologies applied in the region, the objectives of this paper are to review the lithostratigraphic units and geochronological data presented/discussed in the geological literature and cartography, present new geochronological data for the Seridó Group and re-discuss the evolutionary framework of the PSD.



This work is licensed under a Creative Commons Attribution 4.0 International License.

ISSN: 2595-1939

<https://doi.org/10.29396/jgsb.2021.v4.n3.1>

Open access at jgsb.cprm.gov.br

The boundaries of the PSD, in relation to the adjacent domains as well as to the Potiguar Basin, are highlighted by the contrast in the intensity of the magnetometric anomaly (reduction to the pole). This anomaly is strongly positive within the domain and medium to low in the adjacent domains (Fig. 2).

Inside the PSD, several Archean, Paleoproterozoic and Neoproterozoic units have been mapped, as well as important extremely large shear zones. They are essentially dextral strike-slip shear zones (Malta, Santa Monica and Frei Martinho), implemented or reactivated during the Brasiliano event, thus affecting the main units of the domain.

2. Materials and methods

2.1 Stratigraphic-geochronological review

This stratigraphic and geochronological review used information/data available in the literature (references

throughout the text, figures and tables) in the form of geological maps (especially from the Geological Survey of Brazil-CPRM), published articles, master's theses, doctoral dissertations, etc. They were analyzed together with the Seridó Group's geochronological data, which were made available in the present study.

2.2 U-Pb dating by the LA-ICP-MS technique

Fresh samples of paragneiss (1) and quartzite (2) were collected for U-Pb geochronology in detrital zircon for a possible correlation with the formations of the Seridó Group. The zircon was separated from these samples in the Grinding Laboratory of the Department of Geology, Federal University of Rio Grande do Norte (DG/UFRN). Each sample was crushed and sieved, and heavy minerals were concentrated by panning. The non-magnetic minerals from these concentrates were separated in a Frantz Isodynamic Magnetic Separator

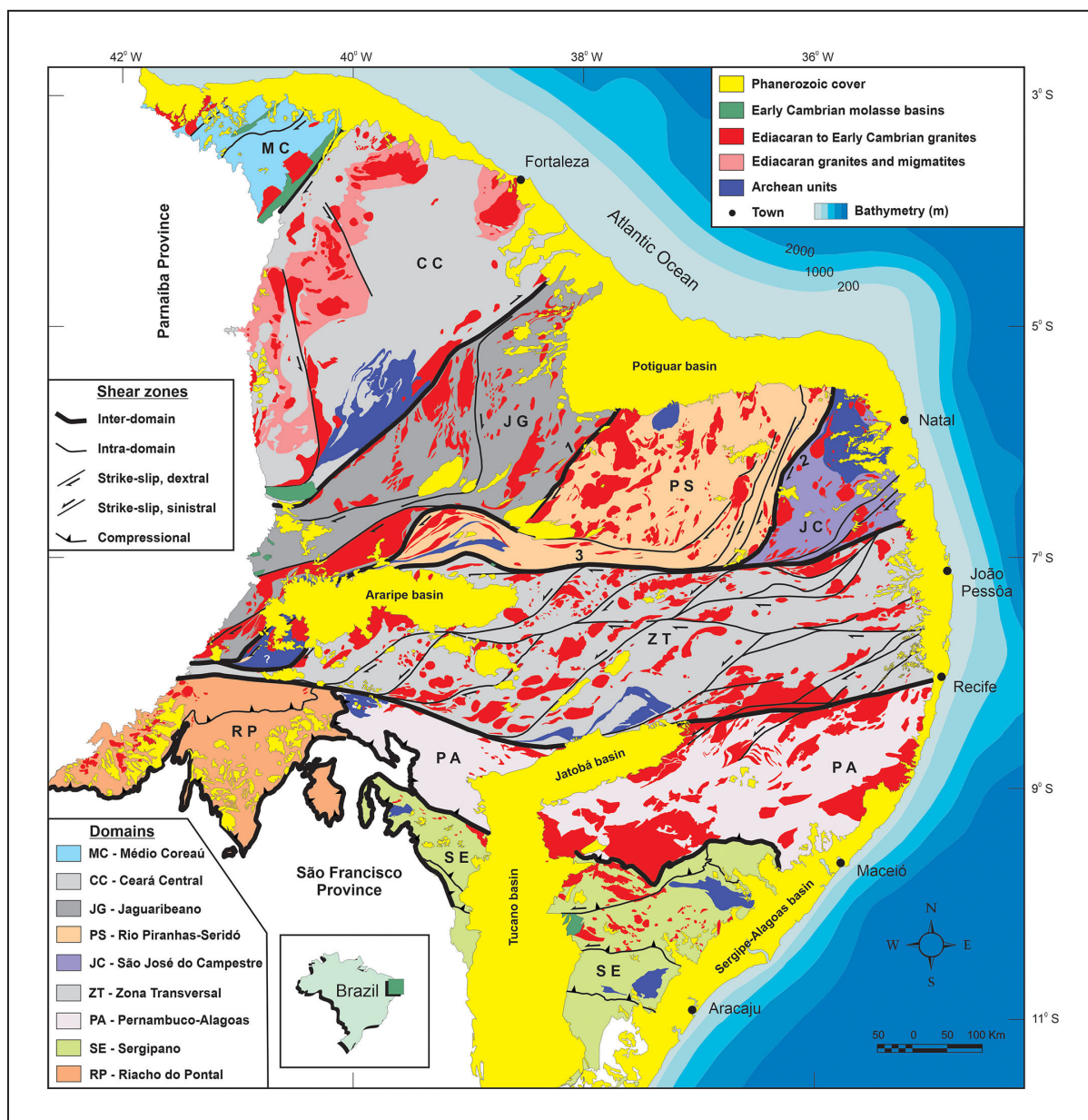


FIGURE 1. Location of the Rio Piranhas-Seridó Domain in the Borborema Province. Updated from Medeiros et al. (2017). 1 = Portalegre shear zone; 2 = Picuí-João-Câmara shear zone; 3 = Patos shear zone.

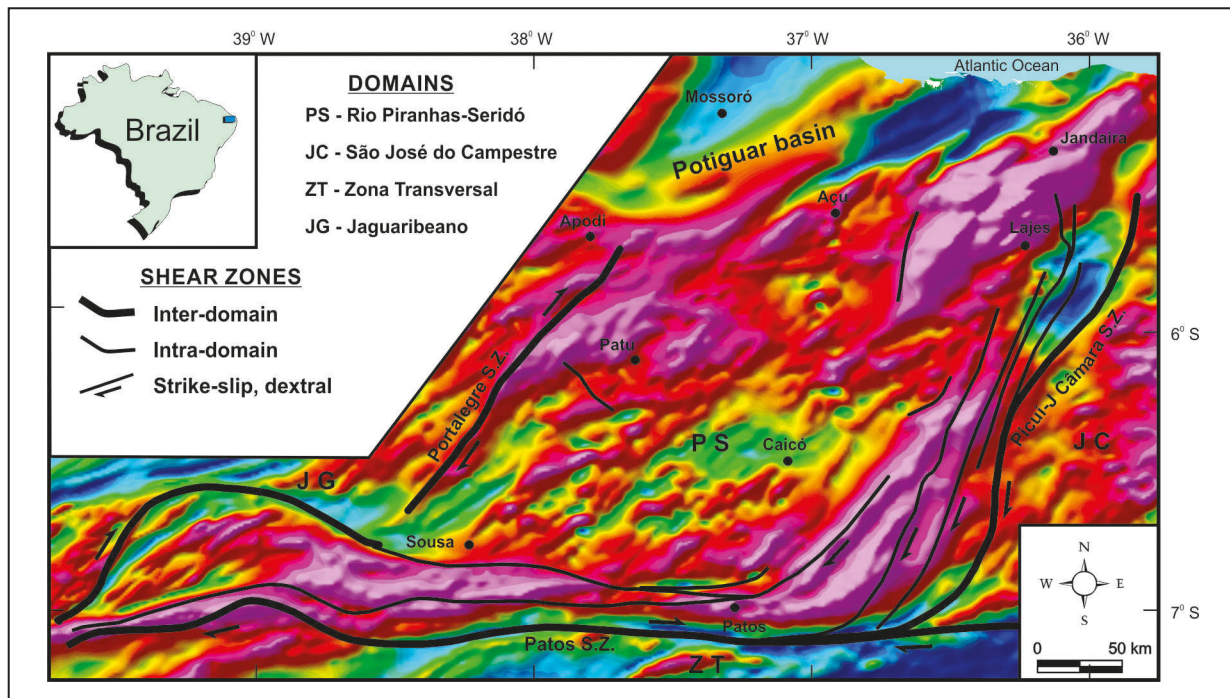


FIGURE 2. Aeromagnetometric image (magnetometric anomaly reduced to the pole), highlighting the boundaries of the PSD and its main shear zones (SZ).

and later classified using dense liquids. Mounts were made by fixing zircon crystals from the concentrates on double-sided tape, then embedding them in epoxy resin (cold), ground to expose the interior of the grains and polished with $0.25\text{ }\mu\text{m}$ diamond paste. The mounts were previously imaged via cathodoluminescence in a scanning electron microscope at the CPGeo laboratory (Research Center for Geochronology and Isotopic Geochemistry) at IGc-USP, where isotopic determinations were performed at the Neptune LAM-MC-ICP-MS instrument (Thermo-Finnigan) fitted to the ArF Excimer Laser ($\lambda=193\text{nm}$) (Photon Machines).

Ablation was performed in $32\text{ }\mu\text{m}$ spots, with frequency of 6 Hz and fluency of 6 mJ. The pulverized material was carried by a He (0.6 l/min) and Ar (0.7 l/min) flow. In all analyses, the international standard GJ-1 was used to correct instrument drift, as well as the fractionation between U and Pb isotopes. To check accuracy, analyses were performed using the TEMORA international standard of 416.78 Ma (Black et al. 2003). Data were acquired in 60 1-second cycles, following the acquisition sequence of 2 blanks, 3 standards, 12 zircon spots, 2 blanks and 2 standards. At each reading, the following mass intensity values were determined: ^{202}Hg , $^{204}(\text{Pb+Hg})$, ^{206}Pb , ^{207}Pb , ^{208}Pb and ^{238}U . The reduction of raw data, which included corrections for blanks, instrument drift and common lead, was performed using an electronic spreadsheet. Age calculations and graphs were built using ISOPLOT 3.0 (Ludwig 2003). Cumulative frequency diagrams were designed using age values $^{207}\text{Pb}/^{206}\text{Pb}$, when ages were greater than 1300 Ma, and age values $^{206}\text{Pb}/^{238}\text{U}$ for other results.

3. Lithostratigraphic Units

The PSD is composed of Archean nuclei, Siderian-Rhyacian gneissic-migmatitic blocks, bodies of augen Rhyacian-Statherian gneisses, Neoproterozoic metasupra-

crustal sequences and intense Neoproterozoic to Early-Cambrian magmatism, affected by or generated during the Brasiliano Orogenesis in the Neoproterozoic (Fig. 3).

Paleoproterozoic units (Caico and Arabia complexes, Serra da Formiga and Poço da Cruz suites) and Neoproterozoic units (Seridó Group), and Ediacaran-Cambrian igneous rocks are the most expressive units in terms of outcropping area in the PSD. However, in addition to the Granjeiro Complex, previously dated as Neoarchean by Silva et al. (1997), the discovery of Archean rocks has been reported in this domain in recent years; for example, the Amarante Complex, Campo Grande Block/Complex in Rio Grande do Norte (Fig. 2) and Serra do Ingá body.

3.1 Archean Units

3.1.1. Amarante Complex

Located in the northeastern portion of the PSD, the Amarante Complex was redefined by Dantas et al. (2019) as being composed of intercalations of felsic and mafic rocks. The former rocks consist of undifferentiated gneisses and orthogneisses of syenitic composition, white to light pink color and medium to fine equigranular granolepidoblastic texture. Their foliation is represented by the alternation of mafic bands (biotite, muscovite, \pm magnetite) and felsic ones (quartz and feldspars). The latter are formed by an association of metamafic-ultramafic rocks, with emphasis on metapyroxenites, metagabbros and amphibolites (Fig. 4A).

Geochronological data by U-Pb dating of zircon (LA-ICP-MS and SHRIMP zircon, Tab. 1) show ages determined in orthogneisses of 3528 Ma (São Tomé/RN, Cavalcante et al. 2019), 3508-3506 Ma (São Tomé/RN, Ruiz et al. 2019) and 3348 Ma (outskirts of the Bonfim/Lajes-RN mine, Oliveira et al. 2013). More recently, Santos et al. (2020) determined ages of 3526

and 3747 Ma in serpentinites from the Serra Verde (Lajes/RN) and Oiticica (São Tomé/RN) mines, respectively. These ages are interpreted as Paleoarchean to Eoarchean crystallization ages in orthogneisses, pyroxenites and serpentinites.

3.1.2. Serra do Ingá body

The Serra do Ingá unit, according to Dantas et al. (2019), consists of bodies positioned in the NE-SW direction with a width of 0.35-0.60 km and a length of 1.66-5.0 km, located about 10 km southwest of the Bonfim tungsten mine (Lajes/RN). The bodies are formed by metamorphic rocks with hornblende, plagioclase, biotite, quartz and pyroxene, intercalated by magnetite-ilmenite lenses (Fig. 4B). U-Pb geochronological dating of zircon show an age of 2678 Ma (Table 1), interpreted as the rock crystallization age by Dantas et al. (2019).

3.1.3. Campo Grande Block/Complex

The Campo Grande Complex, which makes up the homonymous tectonic block, is located in the western portion of the PSD, in the region of the city of Campo Grande/RN, recently studied and dated by Ferreira et al. (2020a). The Campo Grande Block (CGB) is composed of migmatitic gneisses with mafic-ultramafic rocks of Meso-Neoarchean ages, bordered by Paleoproterozoic orthogneisses (Fig. 3). The migmatitic gneisses have a tonalitic composition, containing

granitic leucosomes that represent various phases of partial fusion, with alternating felsic (quartz, plagioclase and potassio feldspar) and mafic (biotite, amphibole and magnetite) levels, and refolding and apical thickening features (Fig. 4C). The mafic-ultramafic rocks consist of amphibolites and pyroxenites, sometimes boudinized (Fig. 4D), probably corresponding to dykes/sills interspersed in migmatitic gneisses.

According to Ferreira et al. (2020a, 2020b), the micropetrographic and mineral chemistry data of amphibolites show a cumulative texture represented by pyroxene relics, sometimes with symplectites indicative of retrograde rocks and high-pressure environment, similar to textures found in retroeclogites.

Based on Nd isotopic and U-Pb geochronological dating on zircon, Ferreira et al. (2020a), proposed an episodic crustal growth with five short intervals of crustal accretion, and we highlight the period around 2.9 Ga and 2.65 Ga (Tab. 1).

3.1.4. Granjeiro Complex

The Granjeiro Complex occurs in the southwestern portion of the PSD, on the outskirts of the cities of Granjeiro and Ipaumirim (CE). This portion was initially characterized as an Archean-age metapluonic-sedimentary association that occurs between the Farias Brito and Patos shear zones (Silva et al. 1997; Vasconcelos and Gomes 1998), whose exhibition area was redefined by Palheta et al. (2019) on the

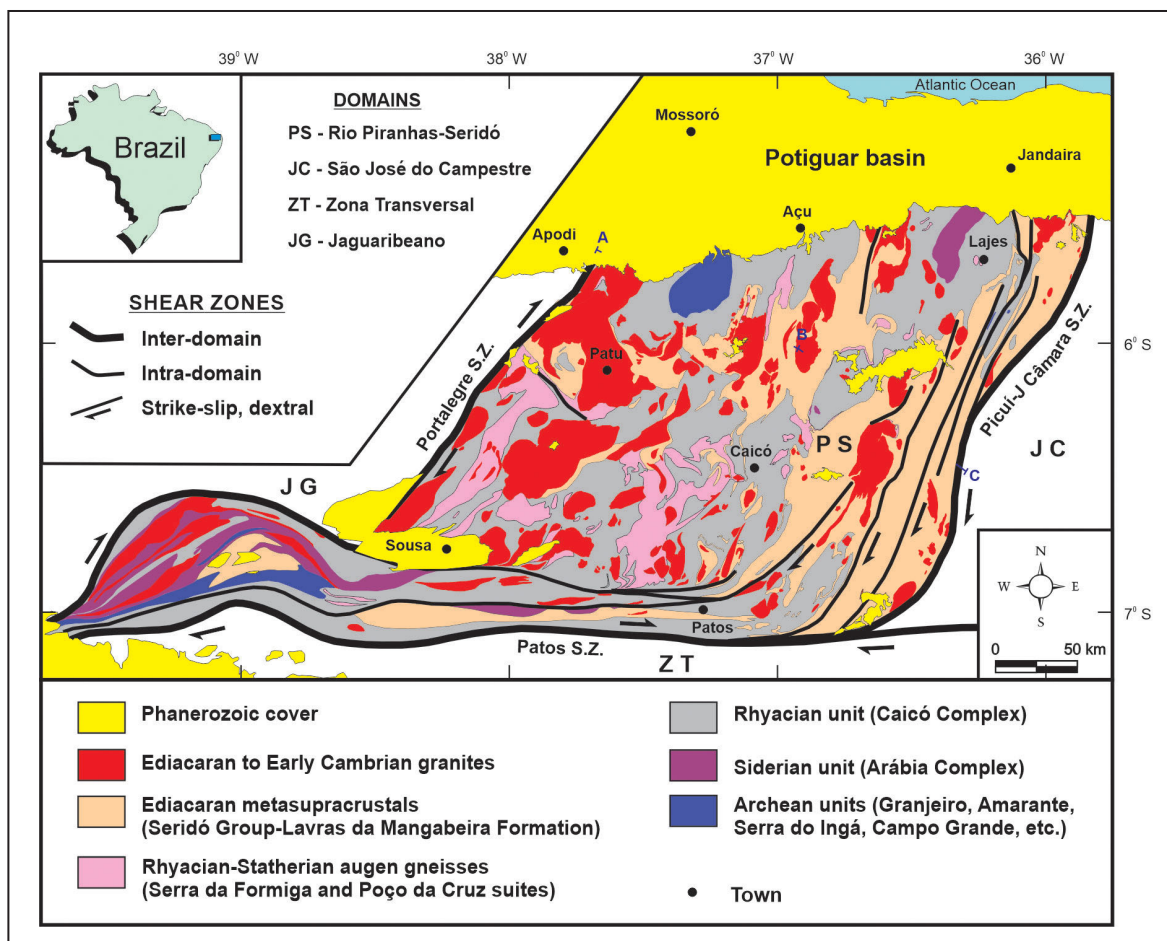


FIGURE 3. Main lithostratigraphic units and shear zones mapped in the PSD and their main shear zones (SZ). A-B-C = profile shown in Fig. 19.

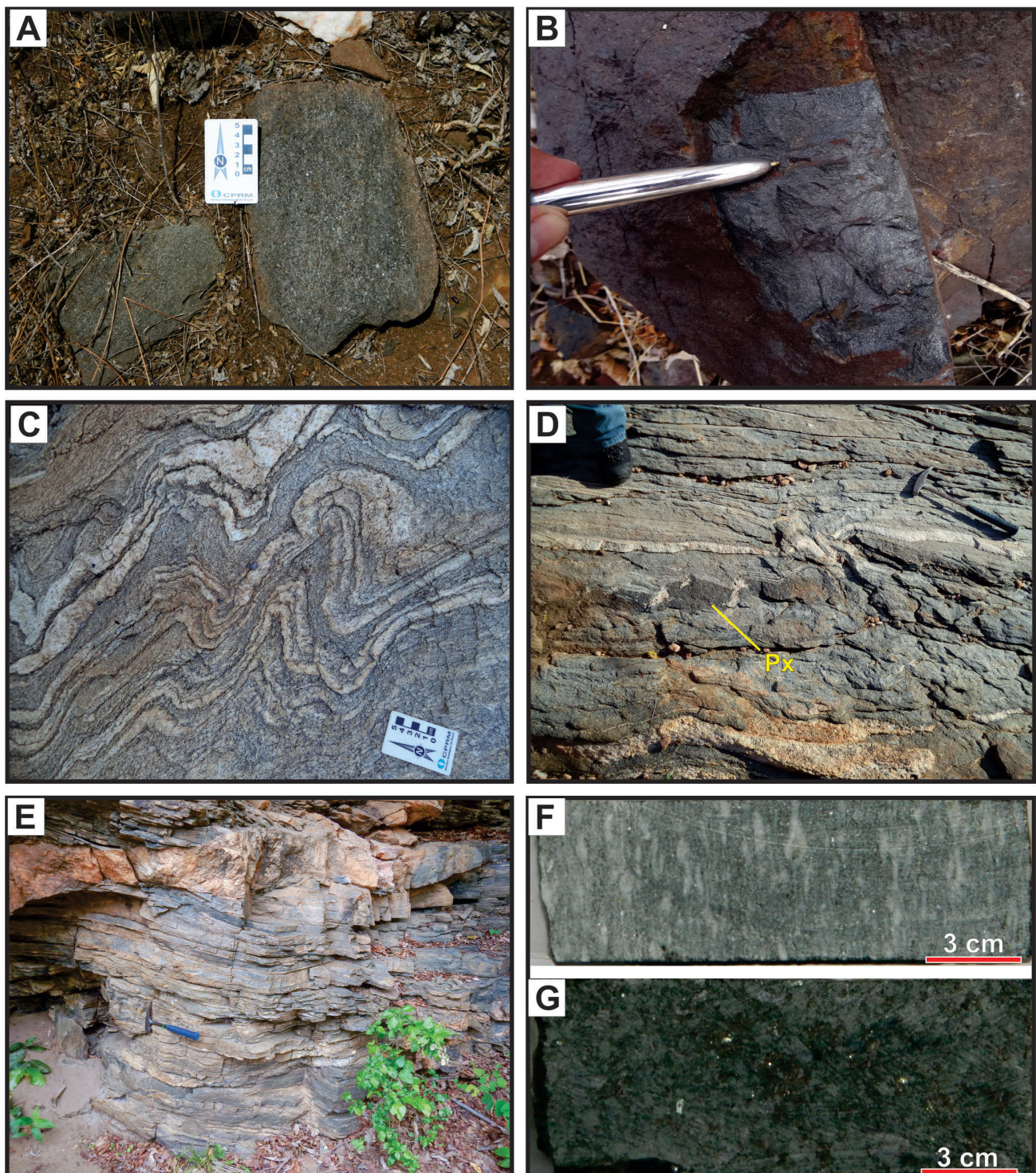


FIGURE 4. General aspects of the PSD's Archean rocks: (A) medium to coarse mafic-ultramafic rocks composed of amphibole, pyroxene and magnetite belonging to the Amarante Complex (Gameleira do Bonfim village, São Tomé/RN); (B) magnetitite lenses associated with mafic-ultramafic rock sequence of the Serra do Ingá body (Fazenda Mundo Novo, São Tomé/RN); (C) migmatitic gneiss from the Campo Grande Complex, showing folds highlighted by quartz veins; (D) Campo Grande Complex gneisses with mafic boudins composed of pyroxene (Px); (E) granodiorite orthogneiss with boudinized leucogranite sheets; (F) microaugen gneiss with plagioclase crystals (G) and gabroic metamorphic rock from the Saquinho Complex.

TABLE 1 - Relation of U-Pb ages in Archean-Statherian orthoderived rocks from the PSD, published in the literature.

| LITOSTRATIGRAPHIC UNIT | ROCK TYPE | AGE (Ma) | METHOD | REFERENCE |
|----------------------------|---|-----------|-----------------------------|--------------------------|
| Amarante Complex | Serpentinite | 3747 ± 12 | SHRIMP ¹ | Santos et al. 2020 |
| Amarante Complex | Pyroxenite | 3528 ± 66 | LA-ICP-MS ¹ | Cavalcante et al. 2019 |
| Amarante Complex | Serpentinite | 3526 ± 05 | SHRIMP ¹ | Santos et al. 2020 |
| Amarante Complex | Orthogneiss | 3508 ± 29 | LA-ICP-MS ¹ | Ruiz et al. 2019 |
| Amarante Complex | Pyroxenite | 3506 ± 29 | LA-ICP-MS ¹ | Ruiz et al. 2019 |
| Amarante Complex | Syenogranitic orthogneiss | 3348 ± 23 | LA-ICP-MS ¹ | Oliveira et al. 2013 |
| Arábia Complex | Migmatite | 2484 ± 10 | LA-ICP-MS ¹ | Ancelmi 2016 |
| Arábia Complex | Dioritic orthogneiss | 2479 ± 15 | SHRIMP ¹ | Gomes et al. 2019 |
| Arábia Complex | Orthogneiss | 2479 ± 18 | LA-ICP-MS ¹ | Ferreira et al. 2019 |
| Arábia Complex | Biotite-amphibole orthogneiss | 2456 ± 04 | SHRIMP ¹ | Costa e Dantas 2012 |
| Arábia Complex | Felsic banded gneiss | 2400 ± 40 | SHRIMP ¹ | Hollanda et al. 2011 |
| Arábia Complex | Clinopyroxene metahornblendite | 2381 ± 16 | LA-ICP-MS ¹ | Cavalcante et al. 2019 |
| Arábia Complex | Amphibolite | 2370 ± 21 | SHRIMP ¹ | Gomes et al. 2019 |
| Arábia Complex | Amphibolite | 2367 ± 12 | LA-ICP-MS ¹ | Freimann 2014 |
| Arábia Complex | Biotite gneiss | 2356 ± 12 | LA-ICP-MS ¹ | Freimann 2014 |
| Arábia Complex | Orthogneiss | 2345 ± 23 | SHRIMP ¹ | Hollanda et al. 2011 |
| Arábia Complex | Hornblende-biotite gneiss (tonalitic) | 2331 ± 37 | LA-ICP-MS ¹ | Dantas et al. 2008 |
| Arábia Complex (Ipaumirim) | Metaquartz-diorite | 2461 ± 30 | LA-ICP-MS ¹ | Ancelmi 2016 |
| Caicó Complex | Granodioritic orthogneiss | 2242 ± 06 | ID-TIMS ¹ | Legrand et al. 1991 |
| Caicó Complex | Orthogneiss | 2231 ± 11 | LA-ICP-MS ¹ | Ferreira et al. 2019 |
| Caicó Complex | Orthogneiss | 2230 ± 10 | LA-ICP-MS ¹ | Ferreira et al. 2019 |
| Caicó Complex | Granitic migmatite gneiss | 2225 ± 12 | LA-ICP-MS ¹ | Dantas et al. 2008 |
| Caicó Complex | Granodioritic orthogneiss | 2225 ± 13 | LA-ICP-MS ¹ | Souza et al. 2016 |
| Caicó Complex | Orthogneiss | 2217 ± 11 | LA-ICP-MS ¹ | Ferreira et al. 2019 |
| Caicó Complex | Leucogneiss | 2208 ± 13 | SHRIMP ¹ | Hollanda et al. 2011 |
| Caicó Complex | Metaleucogabbro | 2207 ± 35 | SHRIMP ¹ | Hollanda et al. 2011 |
| Caicó Complex | Clinopyroxenite | 2201 ± 09 | LA-ICP-MS ¹ | Ferreira et al. 2019 |
| Caicó Complex | Metahornblendite | 2198 ± 13 | LA-ICP-MS ¹ (?) | Nascimento et al. 2011 |
| Caicó Complex | Biotite-Hornblende gneiss (granodioritic) | 2193 ± 07 | SHRIMP ¹ | Silva et al. 1997 |
| Caicó Complex | Hornblendite | 2192 ± 10 | LA-ICP-MS ¹ | Ferreira et al. 2019 |
| Caicó Complex | Hornblende-biotite gneiss (tonalitic) | 2187 ± 06 | SHRIMP ¹ | Silva et al. 1997 |
| Caicó Complex | Clinopyroxenite | 2182 ± 13 | ICPMS-LA ¹ | Ferreira et al. 2019 |
| Caicó Complex | Hornblendite | 2178 ± 08 | ICPMS-LA ¹ | Ferreira et al. 2019 |
| Caicó Complex | Amphibolite | 2175 ± 71 | LA-ICP-MS ^{1,2} | Medeiros et al. 2012a |
| Caicó Complex | Migmatite | 2168 ± 09 | ICPMS-LA ¹ | Ancelmi 2016 |
| Caicó Complex | Metagabbro/Metadiorite | 2152 ± 08 | ID-TIMS | Hackspacher et al. 1990 |
| Caicó Complex | Metandesite | 2150 ± 18 | LA-ICP-MS ¹ | Souza et al. 2016 |
| Caicó Complex | Hornblende-biotite gneiss (tonalitic) | 2146 ± 04 | ID-TIMS | Hackspacher et al. 1990 |
| Caicó Complex | Metapyroxenite | 2129 ± 05 | LA-ICP-MS ¹ | Cavalcante et al. 2019 |
| Caicó Complex | "Granitic sheet" | 2113 ± 15 | LA-ICP-MS ¹ | Souza et al. 2016 |
| Campo Grande Complex | Migmatite (tonalite residue) | 2983 ± 04 | LA-ICP-MS ¹ | Ferreira et al. 2020b |
| Campo Grande Complex | Migmatite (tonalite residue) | 2911 ± 12 | LA-ICP-MS ¹ | Ferreira et al. 2020b |
| Campo Grande Complex | Amphibolite | 2692 ± 13 | LA-ICP-MS ¹ | Ferreira et al. 2020a |
| Campo Grande Complex | Amphibolite | 2675 ± 21 | LA-ICP-MS ¹ | Ferreira et al. 2020a |
| Campo Grande Complex | Amphibolite | 2663 ± 16 | LA-ICP-MS ¹ | Ferreira et al. 2020a |
| Campo Grande Complex | Amphibolite | 2657 ± 14 | LA-ICP-MS ¹ | Ferreira et al. 2020a |
| Granjeiro Complex | Epidote amphibolite | 2654 ± 26 | LA-ICP-MS ¹ | Ancelmi 2016 |
| Granjeiro Complex | Mafic metatuff | 2590 ± 11 | LA-ICP-MS ¹ | Ancelmi 2016 |
| Granjeiro Complex | Biotite-Hornblende gneiss (tonalitic) | 2541 ± 11 | SHRIMP ¹ | Silva et al. 1997 |
| Granjeiro Complex | Biotite gneiss | 3184 ± 43 | LA-ICP-MS ¹ | Freimann 2014 |
| Granjeiro Complex | Ultramafic rock | 3042 ± 43 | LA-ICP-MS ¹ | Freimann 2014 |
| Granjeiro Complex | Banded orthogneiss | 3001 ± 10 | SHRIMP ¹ | Gomes et al. 2019 |
| Granjeiro Complex | Orthogneiss | 2802 ± 03 | LA-ICP-MS ¹ | Hollanda et al. 2015 |
| Granjeiro Complex | Amphibolite | 2764 ± 53 | SHRIMP ¹ | Gomes et al. 2019 |
| Granjeiro Complex | Metarhyolite | 2715 ± 29 | LA-ICP-MS ¹ | Ancelmi 2016 |
| Granjeiro Complex | Amphibolite | 2713 ± 18 | LA-ICP-MS ¹ | Ancelmi 2016 |
| Poço da Cruz Suite | Augen gneiss | 1990 ± 10 | Pb evaporation ¹ | Jardim de Sá et al. 1995 |
| Poço da Cruz Suite | Augen gneiss | 1934 ± 12 | ID-TIMS ¹ | Legrand et al. 1991 |
| Poço da Cruz Suite | Augen gneiss | 1741 ± 10 | SHRIMP ¹ | Hollanda et al. 2011 |
| Saquinho Complex | Microaugen gneiss | 2512 ± 03 | LA-ICP-MS ¹ | Cavalcante et al. 2018 |
| Saquinho Complex | Metagabbro/Metadiorite | 2501 ± 03 | LA-ICP-MS ¹ | Cavalcante et al. 2018 |
| Serra da Formiga Suite | Augen gneiss | 2270 ± 24 | SHRIMP ¹ | Hollanda et al. 2011 |
| Serra da Formiga Suite | Augen gneiss | 2252 ± 17 | LA-ICP-MS ¹ | Medeiros et al. 2012b |
| Serra da Formiga Suite | Augen gneiss | 2248 ± 18 | SHRIMP ¹ | Hollanda et al. 2011 |
| Serra da Formiga Suite | Augen gneiss | 2236 ± 80 | SHRIMP ^{1,2} | Hollanda et al. 2011 |
| Serra da Formiga Suite | Augen gneiss | 2234 ± 07 | SHRIMP ¹ | Costa e Dantas 2014 |
| Serra da Formiga Suite | Augen gneiss | 2210 ± 13 | LA-ICP-MS ¹ | Cavalcante et al. 2018 |
| Serra da Formiga Suite | Augen gneiss | 2209 ± 12 | LA-ICP-MS ¹ | Freimann 2014 |
| Serra da Formiga Suite | Augen gneiss | 2172 ± 24 | SHRIMP ¹ | Hollanda et al. 2011 |
| Serra da Formiga Suite | Augen gneiss | 2171 ± 20 | ICPMS-LA ¹ | Medeiros et al. 2012b |
| Serra do Ingá Body | Metamafic rock | 2678 ± 04 | LA-ICP-MS ¹ | Dantas et al. 2019 |

Key to methods: 1 - Zircon; 2 - Age not considered in Fig. 1

basis of geological mapping and new geochronological data. It is predominantly formed by gray banded orthogneisses, composed of tonalite and granodiorite, with lenses of metamafic and metaultramafic rocks (Fig. 4E). Subordinately, paragneisses with lenses of iron and quartzite formations also occur, as well as acid metavolcanic ones, including, metatuffs and metaryholites.

The orthoderived rocks from the Granjeiro Complex showed U-Pb ages of zircon at different intervals, such as ~2.4 Ga (SHRIMP - Silva et al. 1997), 3.18-3.04 Ga (LA-ICP-MS - Freimann 2014), 2.71-2.59 Ga (LA-ICP-MS - Ancelmi 2016) and 3.00-2.76 Ga (SHRIMP - Gomes et al. 2019), indicating periods of formation between Mesoarchean and Neoarchean for this complex, as shown in Table 1.

3.1.5. Saquinho Complex

Drill hole surveying was used to characterize the rocks belonging to the Saquinho Complex at the Saquinho iron mine (Cruzeta/RN), located in the central portion of the PSD (Cavalcante et al. 2018). These rocks occur at a depth between 210 and 330 m and are mostly represented by amphibole-biotite microaugen gneiss of a grayish monzogranitic composition (Fig. 4F) and greenish gabbroic metamafic (biotite-pyroxene-amphibole gabbro-gabbronorite) composition (Fig. 4G).

U-Pb zircon geochronological data collected by Cavalcante et al. (2018) provided two concordant Neoarchean ages (2512 and 2501 Ma, Table 1), found respectively in microaugen gneiss and gabbroic metamafic rock - both of which were interpreted as the crystallization age of these rocks.

3.2 Paleoproterozoic Units

3.2.1. Arábia Complex

The first Siderian U-Pb ages, 2331 Ma, found in the PSD (Santa Luzia sequence) were collected by Dantas et al. (2008) in a tonalitic biotite-hornblende gneiss (Table 1). Based on isotopic data collected in an outcropping biotite-amphibole orthogneiss northwest of Lajes (RN), with U-Pb zircon age of 2456 Ma (Table 1), and T_{DM} model age of 2.56 Ga and e_{Nd} of 1.20, Costa and Dantas (2018) suggested a possibly juvenile source for the magma that gave rise to the orthogneisses.

Costa and Dantas (2018) named the Siderian lithotypes as the Arabia Complex, which is predominantly composed of orthogneisses and migmatitic gneisses. These rocks have a granodioritic to tonalitic composition (Fig. 5A), sometimes leucocratic monzogranitic, with medium to coarse to inequigranular grains. The complex includes the lithotypes dated by Dantas et al. (2008) and the banded orthogneiss in the region of Santa Luzia/PB. For the latter, Hollanda et al. (2011) found an age of around 2400 Ma (Table 1).

The Arabia Complex also contains amphibolitic rocks that have a fine to medium-grained texture and occur as embedded bodies/lenses or in the form of centimetric to metric xenoliths in the orthogneisses, as well as metaultramafic rocks mapped in the northeast region of Cruzeta-RN (central portion of the PSD). In this region, Cavalcante et al. (2019) detected the presence of clinopyroxene-metahornblendites (Fig. 5B), dated by the U-Pb dating of zircon at 2381 Ma (Table 1).

In the southwestern portion of the PSD (near the border between the states of Paraíba and Ceará), there are Siderian

rocks, which were also considered to be from the Arabia Complex. They are banded orthogneisses, with bands of granodioritic to dioritic composition, sometimes with a concentration of magnetite and amphibole, with frequent presence of migmatitic bands, in addition to granitic/pegmatitic injections (Fig. 5C) and mafic portions.

New U-Pb zircon data (Table 1) in the southwest of the PSD, of 2461 and 2484 Ma found by Ancelmi (2016), and 2479 Ma found by Ferreira et al. (2019), in addition to two disagreements of 2479 and 2370 Ma found by Gomes et al. (2019), enabled Gomes et al. (2019) to map the Arabia Complex in that region, characterizing it as composed of the Manicoba, Coqueiro and Ipaumirim units. The first three ages would correspond to the orthogneisses and metamafic-metaultramafic rocks studied by Dantas et al. (2008) and Costa and Dantas (2018), while the Manicoba unit would represent para-derived lithotypes (marbles, calc-silicate rocks, schists, quartzites, metacherts and iron formations).

3.2.2. Caicó Complex

Based on the work of Meunier (1964) and Ferreira and Albuquerque (1969), the Caicó Complex was conceived as the foundation of the Seridó Group in the states of Rio Grande do Norte and Paraíba, where this complex was generally characterized by the presence of Rhyacian-age gneisses and migmatites (Ebert 1970; Brito Neves 1975; Jardim de Sá 1984 and 1994; Dantas 1988; Souza 1991; Souza et al. 2007, 2016).

The rocks of Caicó Complex are formed by undifferentiated gneisses and migmatites, and they may contain banded gneisses (Fig. 5D), paragneiss with biotite and/or garnet, amphibolites, probable metavolcanic rocks, sometimes migmatized, also containing schists, quartzites, metamafic-metaultramafic rocks (amphibolites/hornblendites and metagabbros) and orthogneisses (granitic, granodioritic and tonalitic).

Dark to light gray, medium to coarse (hornblende)-biotite orthogneisses are predominant, indicating a strong gneiss banding. In general, this banding is composed of alternating mafic levels of gabbroic to dioritic composition, and felsic levels of monzogranitic, granodioritic to tonalitic composition. Souza et al. (2016) described the orthogneisses belonging to the Caicó Complex as having low-K (tonalite) and medium-K (granodiorite) calcium-alkaline tendencies, probably corresponding to subalkaline volcanic arc rocks.

U-Pb zircon dating carried out in recent decades on rocks from this complex had ages ranging from 2.11 to 2.24 Ga (Table 1), and they were considered to be representative of magmatic crystallization of orthogneiss protoliths.

According to Souza et al. (2007) available data from this complex indicate that the petrogenetic model involves juvenile magmas with an older crustal input ($e_{Nd2.2Ga}$ -1.87 to +0.02 and TDM = 2.70-2.53 Ga), probably extracted from a mantle with a metasomatized source.

3.2.3. Augen Gneisses (Serra da Formiga and Poço da Cruz suites)

The gneisses of the Serra da Formiga and Poço da Cruz suites are mainly composed of biotite orthogneisses and may contain amphibole. They have an augen-like structure, medium to coarse porphyro-granoblastic textures, light

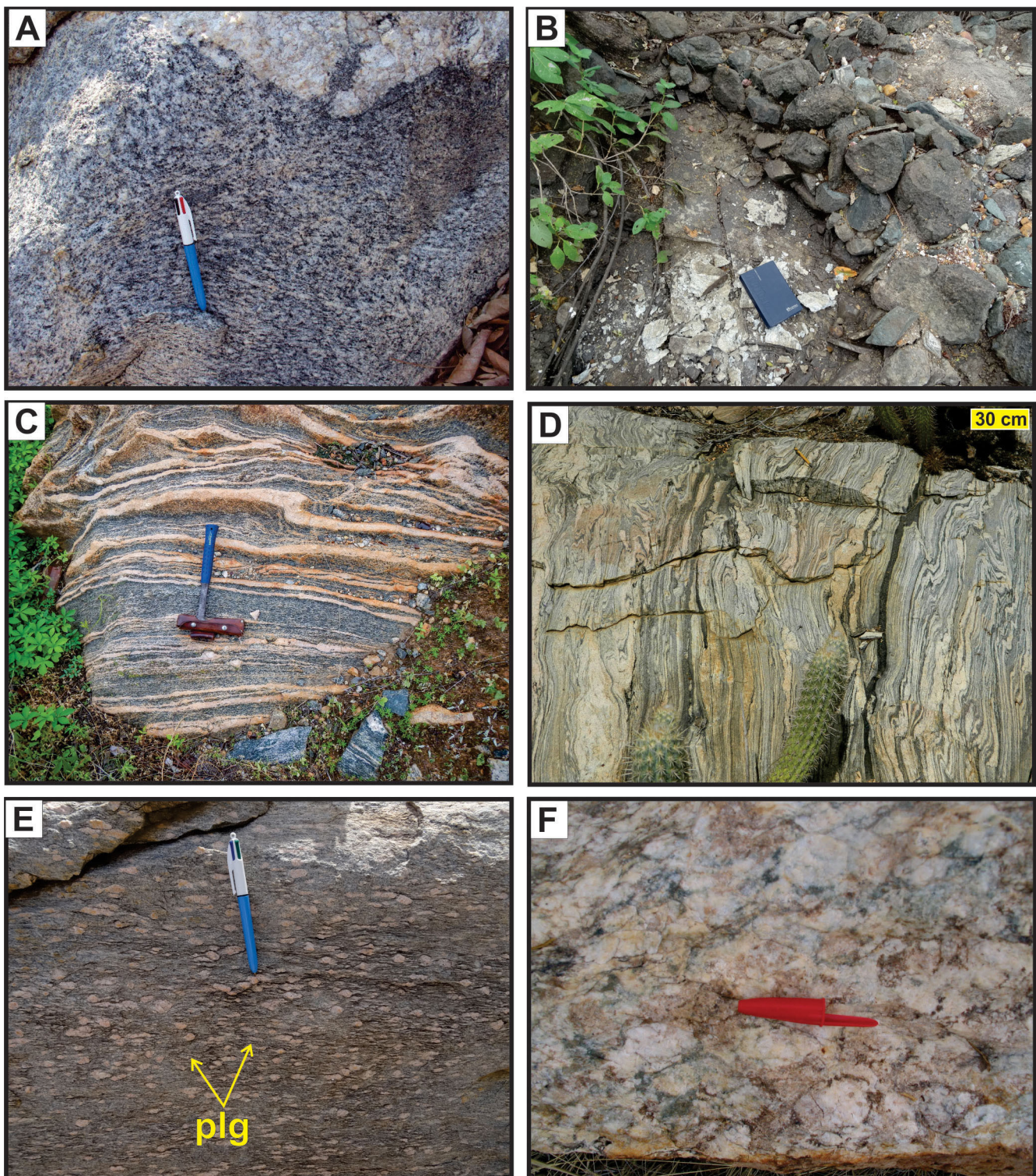


FIGURE 5. Features of PSD Paleoproterozoic rocks: (A) biotite amphibole orthogneiss of granodioritic composition from the Arabia Complex in the Pedro Avelino/RN region; (B) clinopyroxene-metahornblendite blocks from the Arabia Complex northwest of Cruzeta/RN; (C) banded and folded orthogneiss of the Arabia Complex near Marizópolis/PB; (D) banded orthogneiss of the Caicó Complex; (E) pink augen gneisses from the Serra da Formiga Suite, highlighting the plagioclase augen (Plg); (F) augen gneisses from the Poço da Cruz Suite in Serra Negra do Norte (RN).

gray or pinkish color and composition alternating between syenogranite, monzogranite, granodiorite and monzodiorite (Jardim de Sá 1994; Medeiros et al. 2012a; Costa and Dantas 2018). Texturally, the feldspar porphyroblasts in the form of augen (Fig. 5E and 5F) are particularly noteworthy.

Data (SHRIMP and LA-ICP-MS, Table 1) reported by Hollanda et al. (2011) provided U-Pb zircon ages for gneiss plutons of 2172 Ma, 2208 Ma, 2236 Ma and 2248 Ma. Medeiros et al. (2012b) ratified this age range for the augen gneisses in the Serra da Formiga and Florânia (Rio Grande do Norte) regions by the U-Pb zircon method, as they found ages with the upper intercept marking 2252 and 2171 Ma, while Cavalcante et al. (2018), using the same method, found an age of 2210 Ma for the augen gneiss from the Saquinho/Serra da Formiga region (Cruzeta/RN), while Costa and Dantas (2018) dated an amphibole-biotite augen gneiss northwest of the city of Lajes (RN) providing an age at the upper intercept of 2234 Ma. These values indicate that the magmatism occurred mainly in the range from 2270 to 2171 Ma; therefore, they are chronologically correlated with the granoblastic orthogneisses of the Caicó Complex.

Geochemical analyses performed on bodies from the Serra da Formiga region (Medeiros et al. 2012b) and from Riacho Salgado (Costa and Dantas 2018), indicate that they are peraluminous to metaluminous rocks with high-K calcium-alkaline affinity, probably related to a collisional environment. In this context, the Rhyacian augen gneisses are grouped here in the Serra da Formiga Suite (Fig. 5E); their type area is the homonymous region, and it has petrographic-lithochemical characteristics as described by Medeiros et al. (2012b).

Orosirian ages of 1934 ± 12 Ma (U-Pb in zircon) found by Legrand et al. (1991) and 1990 ± 10 Ma (Pb-Pb in zircon) by Jardim de Sá et al. (1995), led Jardim de Sá et al. (1995) to suggest that ages close to 2.0 Ga could signal a collisional event, probably related to the Transamazonian orogeny. However, Hollanda et al. (2011) found a Statherian age of 1741 ± 12 Ma (U-Pb in zircon) for an augen gneiss (Fig. 5F), which is considered to be from the Poço da Cruz Suite, as proposed by Ferreira (1998). Considering the significant difference between the available ages (1741-1990 Ma) and

the use of different methods, additional geochronological data are needed for a better consistency of the age range of this suite.

3.3. Neoproterozoic Supracrustal Rocks (Seridó Group)

The Seridó Group corresponds to a metasupracrustal sequence. Pioneering studies on this unit in the PSD are attributed to Ferreira (1967), Ebert (1969, 1970), Ferreira and Albuquerque (1969) and Santos (1973). Later, Jardim de Sá and Salim (1980), Jardim de Sá (1984, 1994) and Medeiros et al. (2012a, 2017), among others, described this unit as being composed of the Jucurutu formations (paragneisses with intercalations of marbles, calc-silicate rocks, mica schists, metavolcanic and iron formations), Equador (quartzites and metaconglomerates) and Seridó (feldspathic and aluminous mica schists, possessing subordinately intercalations of metavolcanic, marble and calci-silicate rocks), positioned respectively from the base to the top. According to Jardim de Sá (1994) and Medeiros et al. (2017), the contacts between the three formations of the Seridó Group are almost always interdigitated and/or gradational with each other, indicating a sequence of continuous deposition (Fig. 6). This relationship between the Equador and Seridó formations has also been reported by Cavalcanti Neto (2008) in the region of the eastern edge of Serra das Umburanas and Serra da Timbaúba and disclosed by drill hole surveying.

The first U-Pb ages (SHRIMP) for this group were found by Van Schmus et al. (2003) in detrital zircons from the Jucurutu and Seridó formations, whose values enabled the authors to consider the deposition of these units during the late Neoproterozoic (650 to 610 Ma). Similar ages were also found by Hollanda et al. (2015) for the same formations.

3.3.1. Jucurutu Formation

The Jucurutu Formation is essentially represented by paragneisses and marbles, with levels/layers of iron formations (Figs. 7A, 7B and 7C), amphibolites and calc-silicate rocks. The main lithotype corresponds to amphibole-

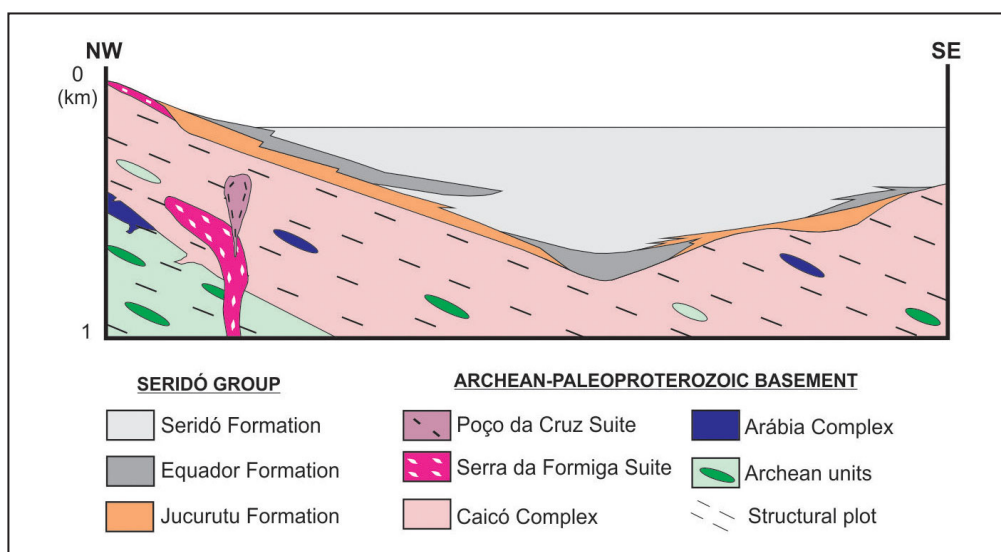


FIGURE 6. Stratigraphic relationships of formations/units that make up the Seridó Group, based on Jardim de Sá (1994) and Medeiros et al. (2017).

biotite paragneiss of generally fine-to-medium granulation and gray and/or bluish-gray color (Fig. 7A).

Marbles have a whitish-to-whitish gray color and medium to coarse grain, and they are essentially composed of calcite (Fig. 7B). Calci-silicate rocks generally have a diversified composition and granoblastic texture, with granulation ranging from fine to coarse, and they may be mainly composed of epidote, diopside, garnet, quartz and plagioclase (Fig. 7C). Granonematoblastic epidote-rich rocks of medium grain and greenish color are also common. The main tungsten (scheelite) mineralizations in the region are contained in this lithology.

The iron formations have the most expressive representatives in the areas of Saquinho (Cruzeta/RN, Fig. 7D) and Pico do Bonito (Jucurutu/RN), where the studies of Campos (2011), Sial et al. (2015), Cavalcante et al. (2018) and Dantas et al. (2017) were conducted. Cavalcante et al. (2018) described the existence of three facies (oxide, carbonate and silicate) for iron formations. The oxidized facies consists of quartz (\pm 60%), hematite (\pm 39%), magnetite, muscovite and actinolite (Fig. 7D), while in the carbonated facies (tremolite-itabirite), there is an alternation of ferruginous and amphibolite layers (quartz, hematite, magnetite, tremolite, with actinolite, hornblende and biotite as accessories). The silicate facies (quartz, hematite, actinolite and pyrite as accessories) is represented by actinolite-itabirite and cummingtonite-itabirite.

3.3.2. Ecuador Formation

The Ecuador Formation is mainly composed of quartzite muscovite, which may contain feldspar, and present medium to coarse granoblastic texture and whitish gray color. Polymitic and polymodal metaconglomerates have also been mapped, and there are fragments of quartz, orthogneisses, metagranitoids, biotite gneisses, calc-silicate rocks, metapegmatites and feldspar (Figs. 8A and 8B). These rocks range from narrow and continuous layers to large mountain ranges with a North-Northeast direction, such as Umburana and Queimadas (Equador-Parelhas-Currais Novos), which clearly bend in the northern portion of the Patos Lineament.

The geochronological data available in the literature for the lithotypes considered to belong to the Ecuador Formation were reported by Hollanda et al (2015), who highlighted a Paleoproterozoic to Archean source for the study quartzites and metaconglomerates, considering that the ages found in the detrital zircons were greater than 1800 Bad.

3.3.3. Seridó Formation

The Seridó Formation consists essentially of medium to coarse grained lepidoblastic mica schists, which may contain garnet, cordierite, staurolite, kyanite, andalusite, and/or

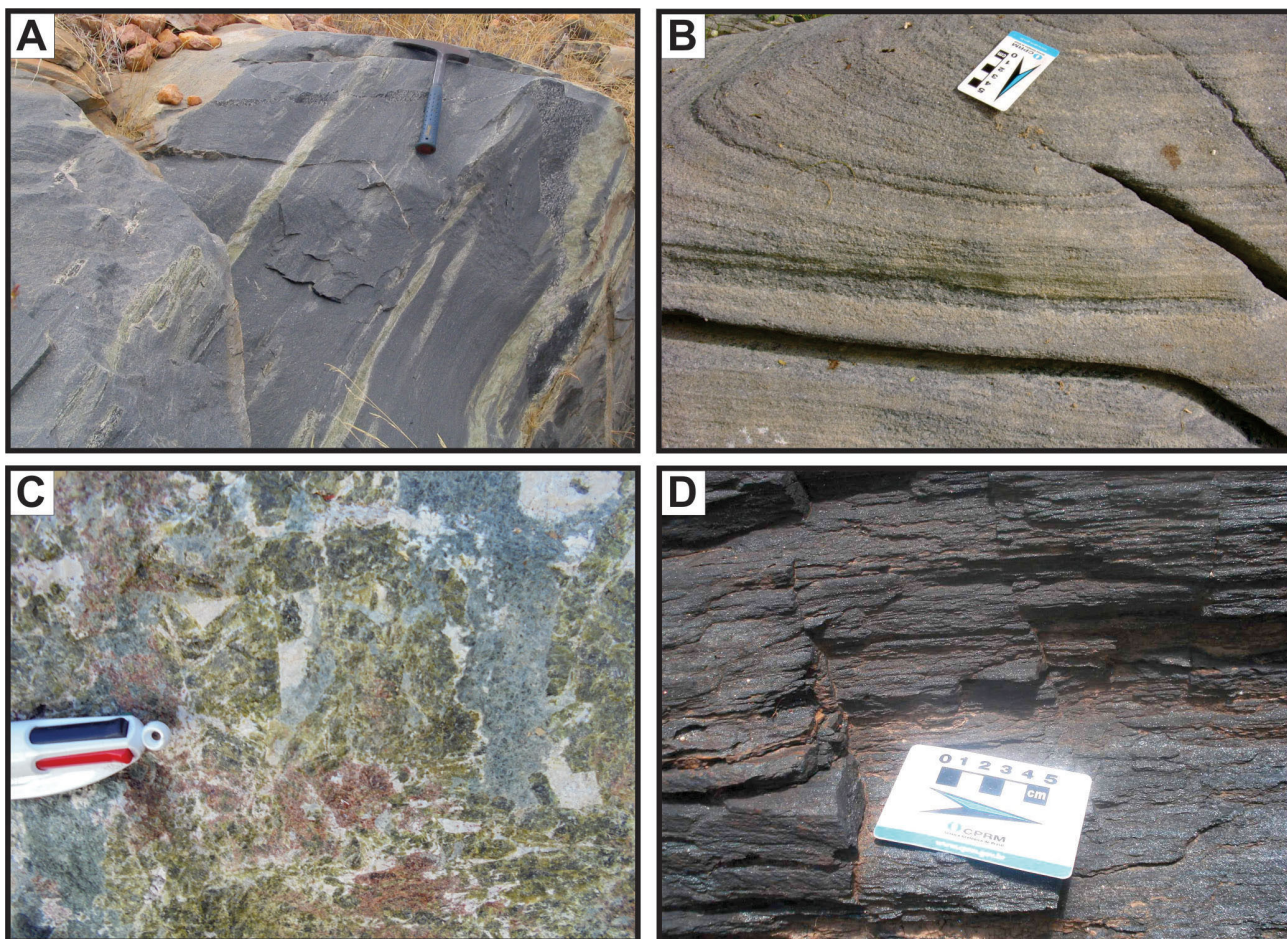


FIGURE 7. Characteristics of the rocks that make up the Jucurutu Formation: (A) amphibole-biotite paragneisses (grey color) with intercalations of calc-silicate rocks (greenish color) in the region of Jucurutu/RN; (B) marble in the region of the Brejú mine (Currais Novos/RN); (C) calc-silicate rock from the Brejú mine region (Currais Novos/RN); (D) iron formation in the Saquinho region (Cruzeta/RN).

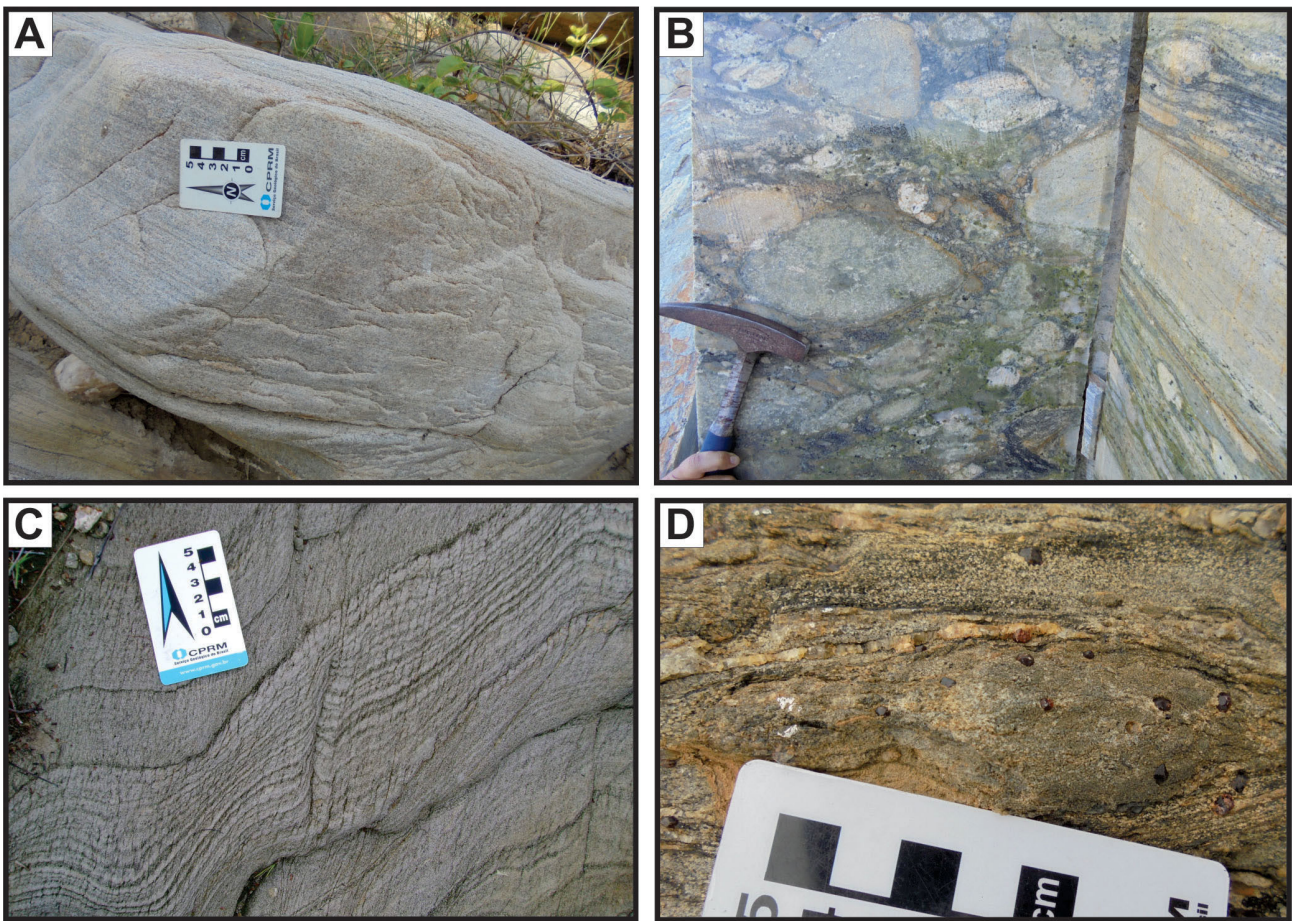


FIGURE 8. Muscovite quartzite from the Equador Formation in the Frei Martinho region/PB (A); metaconglomerate of the Equador Formation in the region of Parelhas/RN (B); schist biotite from the Seridó Formation in the region of Cruzeta/RN (C); garnet-cordierite-biotite schist of the Seridó Formation in Currais Novos/RN (D).

sillimanite, when they commonly present a porphyroblastic texture (Figs. 8C and 8D). They usually have marked schistosity, quartz veinlets and/or boudinaged/transposed veins, as well as intrusions of granitoid bodies and pegmatite veins/dikes.

3.4. Ediacaran-Cambrian Magmatism

Ediacaran magmatism in the PSD can be characterized by seven plutonic suites (Fig. 9): Jardim do Seridó, Conceição, São João do Sabugi, Itaporanga, Dona Inês, Caxexá and Umarizal, which have been described by several authors (e.g., Almeida et al. 1977, Angelim et al. 2006), Nascimento et al. 2015, Cabral Neto et al. 2019).

The Jardim do Seridó Suite is mainly formed by leucocratic monzogranites with muscovite, garnet and biotite (Fig. 10A) and, subordinately, by biotite granodiorites with fine to medium equigranular texture. Cabral Neto et al. (2019) classified this suite as peraluminous and found an age (U-Pb dating of zircon, SHRIMP) of 592 Ma (Table 2). The granitoid of Genezaré (Caicó/RN), constituted by orthogneisses of syenogranitic to monzogranitic composition (metaluminous to peraluminous), has an age of 602 Ma (Table 2) and a marked low-angle foliation (Medeiros et al. 2012a), which may be chronologically correlated with this suite.

The Conceição Suite is composed of biotite granodiorites (Fig. 10B) and tonalites, inequigranular, with medium to

coarse texture. The major example is the Serra da Garganta body (Florânia/RN). In this body, Nascimento et al. (2018) found an age of 598 Ma (U-Pb in zircon, SHRIMP, Table 2) and chemically classified as it calc-alkaline.

The São João do Sabugi Suite consists mainly of pyroxene-biotite gabbros/diorites (Fig. 10C), sometimes with amphibole, and quartz monzonites with an equigranular, fine to medium, or porphyritic texture. According to the classification by Nascimento et al. (2015), there are essentially metaluminous and shoshonitic rocks, with U-Pb zircon ages ranging from 597 to 543 Ma (Table 2).

The Itaporanga Suite is the most expressive in the PSD. It is mainly represented by biotite-amphibole monzonites (granites, granodiorites and subordinate quartz monzonites) with a marked porphyritic texture, characterized by K-feldspar phenocrysts (Fig. 10C), e.g., the Acari batholith. The main crystallization age (U-Pb in SHRIMP zircon or LA-ICP-MS) ranges from 596 to 574 Ma (Table 2), and it has been classified as high-potassium calc-alkaline by Nascimento et al. (2015).

The Dona Inês Suite consists mainly of biotite monzogranites (sometimes granodiorites), equigranular, fine or medium, leucocratic and light gray in color (Fig. 10D). According to Nascimento et al. (2015) it includes mainly metaluminous to peraluminous, high-potassium calc-alkaline rocks, with U-Pb zircon ages ranging from 579 to 527 Ma (Table 2).

The Caxexá Suite is formed by alkali feldspar granite (Fig. 10E) and, subordinately, by quartz alkali-feldspar syenite and

syenogranite with fine to medium equigranular texture. Its rocks are metaluminous to peraluminous, characterized as alkaline by Nascimento et al. (2015).

The Umarizal Suite is basically composed of quartz mangerite and charnockite (Fig. 10F), with inequigranular, medium to coarse texture. According to Nascimento et al. (2015), they correspond to essentially metaluminous rocks classified as alkaline charnockitic, whose U-Pb zircon ages range from 593 to 601 Ma (Table 2).

The expression of Cambrian magmatism in the PSD is essentially represented by pegmatic bodies and dikes on pegmatoid granites that constitute the Borborema Pegmatitic Province (PPB) - de Scorza (1944) and Cabral Neto et al. (2018) - in addition to a smaller area in the region of Tenente Ananias (RN) and rare bodies from the Dona Inês Suite that showed Eocambrian ages (Table 2).

The PPB covers a 200 km long and 40 km wide (average) NE-SW direction band in the central portion of the states of Rio Grande do Norte and Paraíba. It is mainly inserted in the eastern portion of the PSD (Fig. 9), where the vast majority of pegmatitic bodies (77%) are embedded in Neoproterozoic supracrustal rocks of the Seridó Group. According to their internal structure, there are three main types of pegmatites: homogeneous, heterogeneous (Fig. 11) and mixed, according to descriptions and/or classifications by Johnston Jr. (1945), Rolff (1945), Roy and Madon (1964) and Silva and Dantas (1997).

Homogeneous pegmatites are essentially composed of quartz, feldspars and micas, distributed regularly along the bodies, which have widths generally less than 5 m, sharp contact with watersheds, and are rarely mineralized to Ta-Nb, Be, Li and/or Sn and in the disseminated mode. Heterogeneous pegmatites present very well-defined internal zoning (zones I, II, III and IV), characterized by irregular distribution of essential minerals, and very diversified mineralogy with the presence of rare minerals (e.g., Be, Nb, Ta, Li, Sn and Cs). Mixed pegmatites comprise an intermediate type between homogeneous and heterogeneous, presenting quartz pockets instead of well-defined nuclei.

Available U-Pb geochronological data (Baumgartner et al. 2006; Beurlen et al. 2009; Santiago et al. 2019; Holland et al. 2017; Degen et al. 2019), indicate ages from 561 to 491 Ma for the pegmatites in the PPB (Table 2).

Three main models have been proposed for the generation of pegmatites in the region, namely: (i) magmatic associated with metasomatic-pneumatolytic-hydrothermal process (Rolleff 1945; Roy and Madon 1964); (ii) recrystallization/fusion of metasediments (Ebert 1970); (iii) differentiation of igneous bodies (Silva 1993; Silva et al. 1995; Beurlen et al. 2014).

The exploration of these pegmatites began with the extraction of mica during World War I, followed by the production of Ta-Nb, Be and Li (Johnston Jr. 1945; Silva and Dantas 1997; Beurlen et al. 2014). Currently, this province

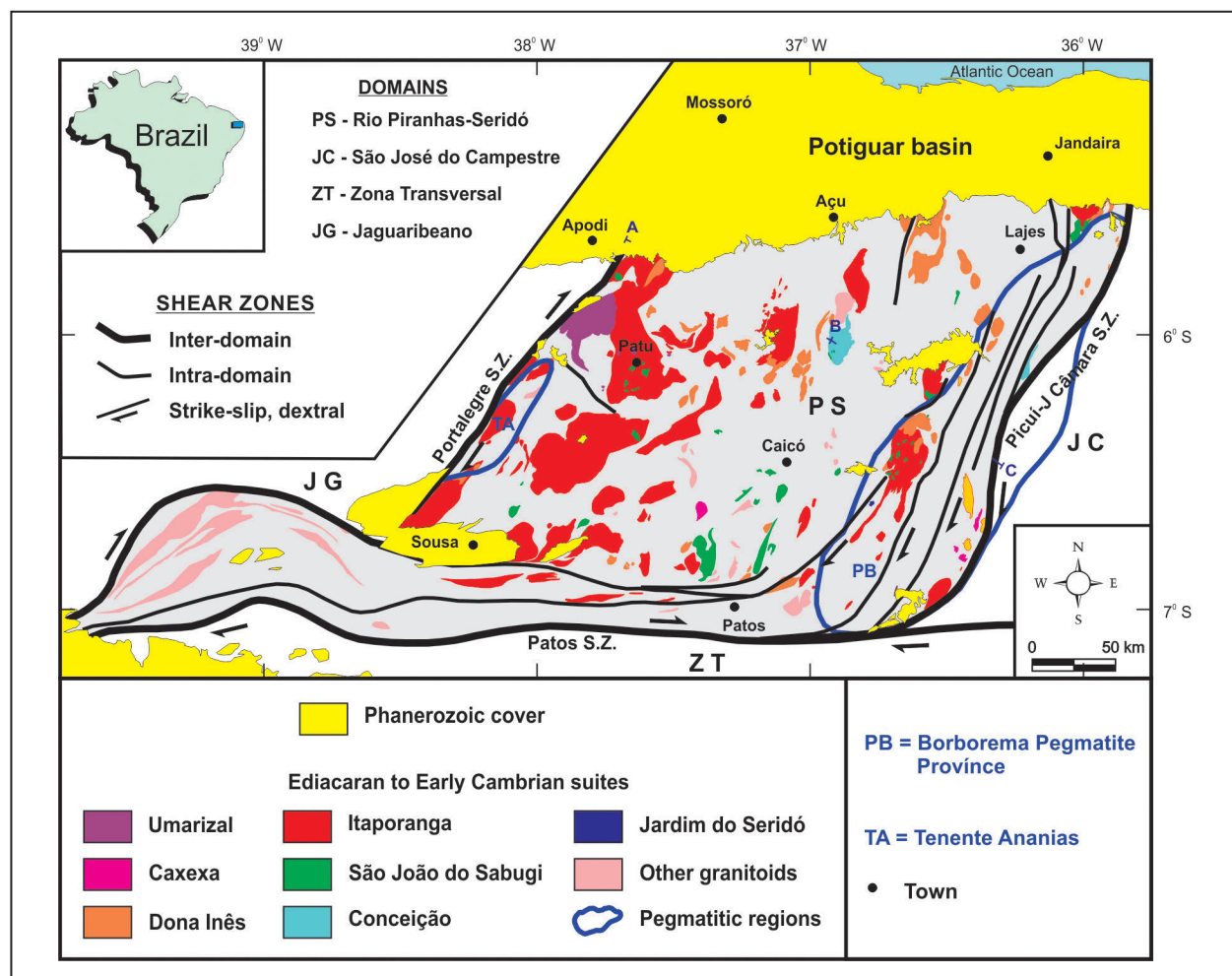


FIGURE 9. Simplified geological map of the PSD, with emphasis for the Ediacaran and Cambrian plutonic magmatism and the main shear zones (SZ). A-B-C = profile shown in Fig. 19.

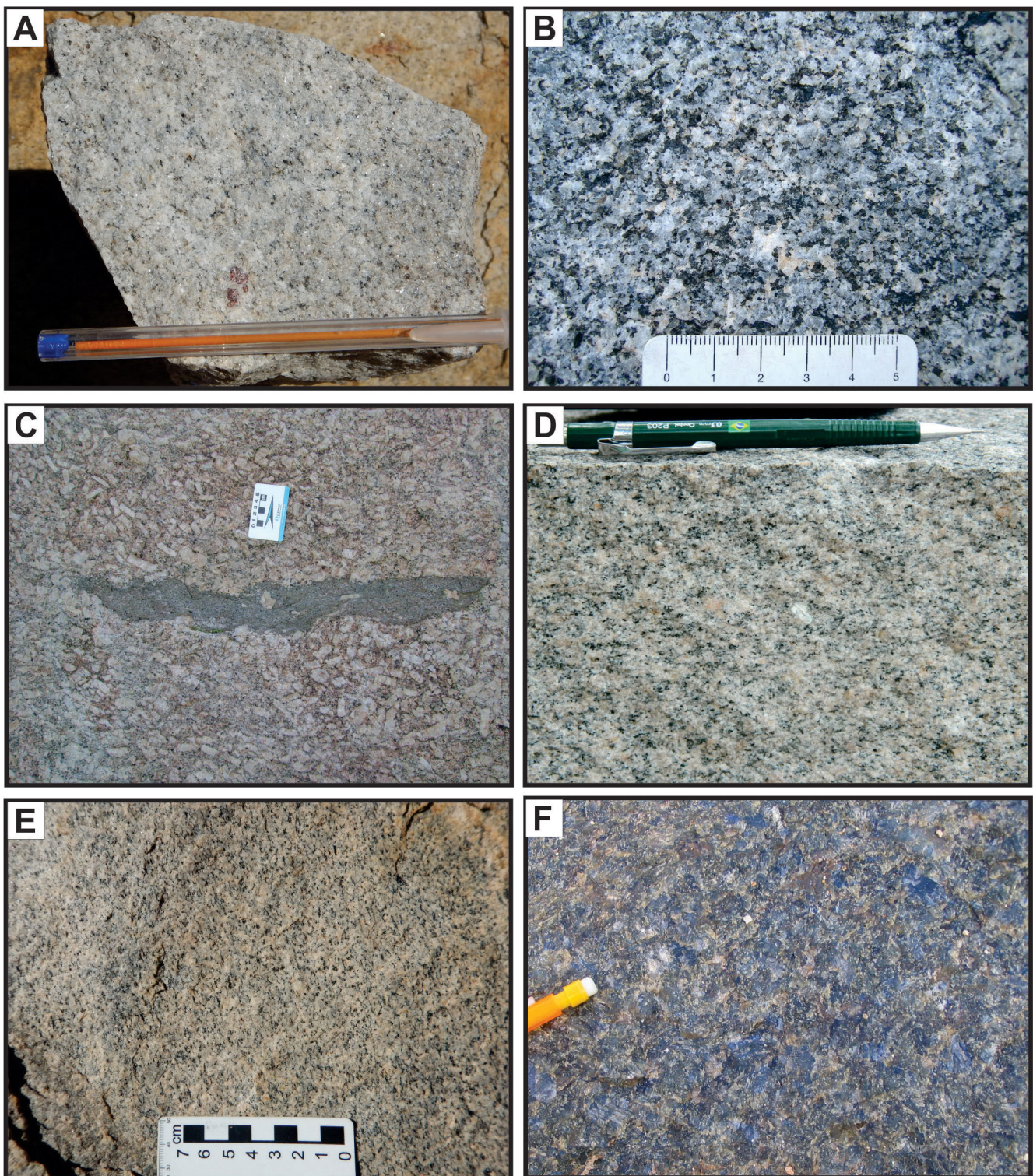


FIGURE 10. Lithotypes representative of the Ediacaran suites in the PSD: (A) monzogranite from the Jardim do Seridó Suite; (B) granodiorite from the Conceição Suite in Florânia/RN; (C) porphyritic granite from the Itaporanga Suite with dioritic/mafic enclave from the São João do Sabugi Suite in Acari/RN; (D) monzogranite from the Dona Inês Suite in Acari/RN; (E) alkaline feldspar granite from the Caxexá Suite in Pedra Lavrada/PB; (F) monzonite quartz from the Umarizal Suite in Almino Afonso/RN.

TABLE 2. Relationship of U-Pb ages in Ediacaran-Cambrian magmatic rocks of the PSD, published in the literature.

| LITOSTRATIGRAPHIC UNIT | ROCK TYPE | AGE (Ma) | METHOD | REFERENCE |
|------------------------------|---|-----------|------------------------|-------------------------|
| Ediacaran-Cambrian magmatism | Pegmatitic granite | 549 ± 04 | SHRIMP ¹ | Hollanda et al. 2017 |
| Ediacaran-Cambrian magmatism | Granite | 530 ± 42 | LA-ICP-MS ¹ | Corrêa et al. 2021 |
| Ediacaran-Cambrian magmatism | Peraluminous pegmatitic granite | 528 ± 12 | ID-TIMS ³ | Baumgartner et al. 2006 |
| Ediacaran-Cambrian magmatism | Pegmatitic granite | 528 ± 12 | LA-ICP-MS ³ | Baumgartner et al. 2006 |
| Ediacaran-Cambrian magmatism | Pegmatitic granite | 520 ± 10 | EPMA4 | Beurlen et al. 2009 |
| Ediacaran-Cambrian magmatism | Pegmatite | 515 ± 01 | LA-ICP-MS ² | Baumgartner et al. 2006 |
| Ediacaran-Cambrian magmatism | Pegmatite | 514 ± 01 | LA-ICP-MS ² | Baumgartner et al. 2006 |
| Ediacaran-Cambrian magmatism | Pegmatite | 514 ± 02 | LA-ICP-MS ² | Baumgartner et al. 2006 |
| Ediacaran-Cambrian magmatism | Pegmatite | 512 ± 03 | LA-ICP-MS ² | Baumgartner et al. 2006 |
| Ediacaran-Cambrian magmatism | Pegmatite | 510 ± 0,4 | LA-ICP-MS ² | Baumgartner et al. 2006 |
| Ediacaran-Cambrian magmatism | Pegmatite | 509 ± 03 | LA-ICP-MS ² | Baumgartner et al. 2006 |
| Ediacaran-Cambrian magmatism | Pegmatitic granite | 491 ± 26 | LA-ICP-MS ¹ | Degen et al. 2019 |
| Genezará body | Granite | 602 ± 02 | LA-ICP-MS ¹ | Medeiros et al. 2012a |
| Pegmatitic granite | Albite granite | 561 ± 04 | LA-ICP-MS ¹ | Santiago et al. 2019 |
| Granito Quixaba | Quartz monzonite | 618 ± 09 | LA-ICP-MS ¹ | Sá et al. 2013 |
| Conceição Suite | Amphibole-biotite granite | 598 ± 05 | SHRIMP ¹ | Nascimento et al. 2018 |
| Dona Inês Suite | Biotite monzogranite (equigranular) | 579 ± 07 | LA-ICP-MS ¹ | Fonseca 2019 |
| Dona Inês Suite | Biotite monzogranite (equigranular) | 579 ± 03 | SHRIMP ¹ | Silva et al. 2017 |
| Dona Inês Suite | Leucogranite | 577 ± 05 | SHRIMP ¹ | Hollanda et al. 2017 |
| Dona Inês Suite | Biotite granite (equigranular) | 572 ± 02 | SHRIMP ¹ | Cunha et al. 2017 |
| Dona Inês Suite | Leucogranite | 572 ± 05 | SHRIMP ¹ | Archanjo et al. 2013 |
| Dona Inês Suite | Biotite monzogranite (porphyritic) | 570 ± 27 | LA-ICP-MS ¹ | Souza et al. 2016 |
| Dona Inês Suite | Biotite monzogranite | 561 ± 04 | LA-ICP-MS ¹ | Medeiros et al. 2017 |
| Dona Inês Suite | Biotite monzogranite (porphyritic) | 560 ± 06 | LA-ICP-MS ¹ | Souza et al. 2016 |
| Dona Inês Suite | Biotite monzogranite | 557 ± 13 | LA-ICP-MS ¹ | Costa et al. 2015 |
| Dona Inês Suite | Granite | 545 ± 08 | LA-ICP-MS ¹ | Souza et al. 2016 |
| Dona Inês Suite | Biotite granite | 540 ± 04 | SHRIMP ¹ | Hollanda et al. 2017 |
| Dona Inês Suite | Biotite syenogranite (porphyritic) | 538 ± 02 | SHRIMP ¹ | Oliveira e Cunha 2018 |
| Dona Inês Suite | Leucogranite | 527 ± 08 | SHRIMP ¹ | Hollanda et al. 2017 |
| Itaporanga Suite | Monzogranite (porphyritic) | 596 ± 03 | SHRIMP ¹ | Hollanda et al. 2015 |
| Itaporanga Suite | Porphyritic granite | 591 ± 04 | SHRIMP ¹ | Archanjo et al. 2013 |
| Itaporanga Suite | Porphyritic granite | 580 ± 04 | ID-TIMS | Trindade et al. 1999 |
| Itaporanga Suite | Porphyritic granite | 580 ± 09 | SHRIMP ¹ | Long et al. 2019 |
| Itaporanga Suite | Biotite monzogranite (microporphyritic) | 577 ± 03 | SHRIMP ¹ | Medeiros et al. 2017 |
| Itaporanga Suite | Porphyritic granite | 577 ± 05 | SHRIMP ¹ | Archanjo et al. 2013 |
| Itaporanga Suite | Porphyritic granite | 574 ± 10 | ID-TIMS | Trindade et al. 1999 |
| Itaporanga Suite | Biotite syenogranite (porphyritic) | 574 ± 03 | LA-ICP-MS ¹ | Medeiros et al. 2008 |
| Itaporanga Suite | Porphyritic granite | 555 ± 05 | ID-TIMS | Legrand et al. 1991 |
| Jardim do Seridó Suite | Monzogranite (porphyritic) | 592 ± 02 | SHRIMP ¹ | Cabral Neto et al. 2019 |
| São João do Sabugi Suite | Gabbronorite | 597 ± 06 | SHRIMP ¹ | Archanjo et al. 2013 |
| São João do Sabugi Suite | Diorite | 595 ± 03 | SHRIMP ¹ | Archanjo et al. 2013 |
| São João do Sabugi Suite | Diorite | 579 ± 07 | ID-TIMS | Jardim de Sá 1994 |
| São João do Sabugi Suite | Monzogranite (porphyritic) | 573 ± 22 | ID-TIMS | Jardim de Sá 1994 |
| São João do Sabugi Suite | Gabbro | 543 ± 21 | LA-ICP-MS ¹ | Souza et al. 2016 |
| Umarizal Suite | Quartz monzonite | 601 ± 11 | LA-ICP-MS ¹ | Sá et al. 2013 |
| Umarizal Suite | Quartz monzonite | 593 ± 05 | ID-TIMS | McReath et al. 2002 |

Key to method: 1 - Zircon; 2 - Columbite; 3 - Monazite; 4 - Xenotime-Uraninite

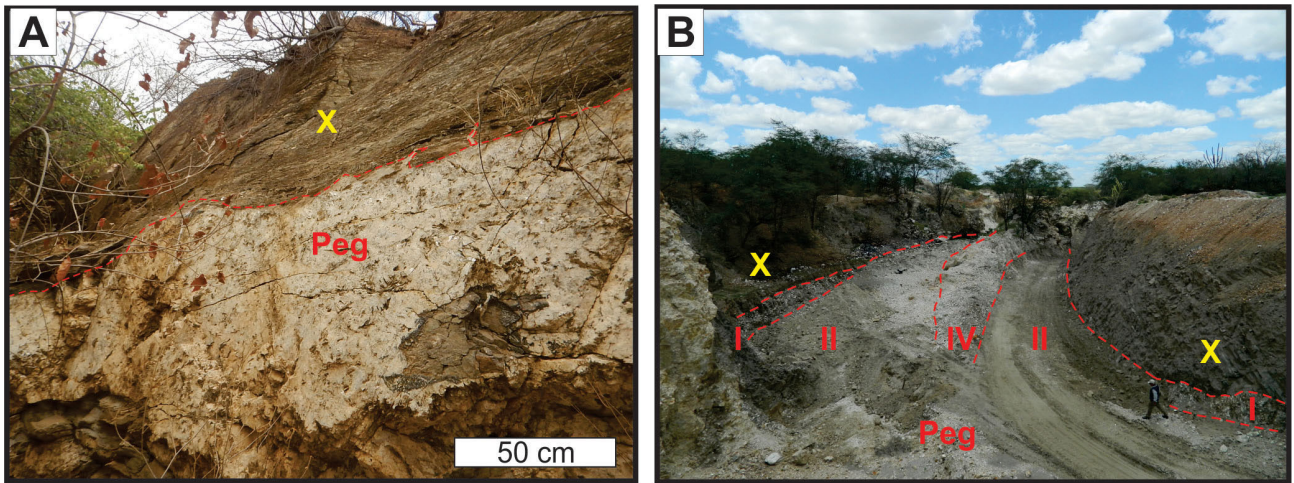


FIGURE 11. Example of homogeneous (A) and heterogeneous (B) intrusive pegmatite in mica schists from the Seridó Formation. Peg=pegmatite; X = mica schist; I, II and IV = pegmatite zones.

stands out for the production of industrial minerals (feldspar, kaolin and mica), Nb-Ta-bearing minerals, and gemstones (mainly tourmaline and aquamarine). Currently, its most noble product is the “Paraíba tourmaline”, a cupriferous elbaite with Mn, with a turquoise blue to green color (Abduriyim et al. 2006; Beurlen et al. 2014).

4. Geochronology

In order to collaborate with the stratigraphic positioning models of the Seridó Group formations, three samples of metasediments were object of U-Pb determination in detrital zircon (paragneiss from Fazenda Coqueiros/Equador-RN, quartzite from Fazenda Currais/Cruzeta-RN and quartzite from the Picuí River/Currais Novos-RN). The main objective was to check the degree of geochronological correlation between them and the lithotypes from the Seridó Group.

4.1. Paragneisses of the Coqueiros Farm (*Serra das Queimadas, Equador/RN*) - LS-17

The Paragneisses from Fazenda Coqueiros were considered in previous years/decades as being representatives of the Jucurutu Formation of the Seridó Group (Neoproterozoic, for example. Jardim de Sá et al. 1998, Angelim et al. 2006, Cavalcante et al. 2015) or the Caicó Complex (Rhyacian, Legrand et al. 2009). In the first hypothesis, the stratigraphic sequence of the Seridó Group (Jucurutu, Equador and Seridó formations, respectively from the bottom to the top) would be complete and in the order proposed by Jardim de Sá (1984, 1994), while in the second hypothesis, the sequence would be incomplete with the absence of the Jucurutu Formation, where such gneisses were correlated with the Caicó Complex.

The present study identified a medium-grained amphibole-biotite paragneiss with epidote, which showed alternations between mafic (rich in biotite and amphibole) and felsic (rich in quartz and feldspar) centimetric bands, in addition to levels of calc-silicate rocks parallel to the current banding of the rock (Fig. 12).

This paragneiss of Fazenda Coqueiros (Fig. 12) was subjected to U-Pb dating of zircon (LAM-MC-ICP-MS). The zircon extracted from the sample is represented by

short, medium and fragmented prisms, whose sizes range from 50 to 150 micrometers. Some inclusions and frequent fractures were identified. In a cathodoluminescence image, it can be seen that the predominant internal structure is a well-marked oscillatory zoning, but there was also zircon with sectorial zoning (Fig. 13A, zircon 38), blurred primary areas (Fig. 13A, zircon 2) and zircon with homogeneous texture (Fig. 13A, zircon 73). Many crystals have dark, homogeneous edges.

This study determined the U-Pb isotopic composition of eighty-two points on eighty zircon crystals from sample LS-17 (Table 3). Of these, data from nine were discarded owing to high analytical error (> 5% in 1 sigma) and another five as a result of common Pb content (<3%). The remaining sixty-eight data showed agreement for apparent ages $^{207}\text{Pb}/^{206}\text{Pb}$ and $^{206}\text{Pb}/^{238}\text{U}$ between 51 and 107%. The age distribution diagram (Fig. 13C) was designed with the points that presented disagreement of up to 10%. Data from the thirty-five points that passed through all filters mostly showed records of Archean to Paleoproterozoic ages (2704 Ma, 2463 Ma, 2323 Ma with main peak of 2177 Ma) but few Neoproterozoic results (mainly at 590 Ma). However, the distribution of all data in the concordia diagram (Fig. 13B) shows the clear effect of loss of lead to the Neoproterozoic. The few Neoproterozoic data were found on dark, homogeneous edges or crystals. Although only the spots 5.1 and 38.1 (Table 3) have low Th/U ratios (0.03 and 0.08 respectively), the few Neoproterozoic ages suggest that the sources of debris in the basin were mainly Paleoproterozoic and Archean, and the Neoproterozoic could represent the metamorphism imposed on the rock. According to this interpretation, the predominant peak of 2177 Ma would establish the maximum age of deposition. As for the Neoproterozoic data, the selection of the most concordant results allowed the calculation of the Concordia Age of 593 ± 4 Ma (MSWD of 0.18), which could be considered the best estimate for the age of metamorphism.

On the other hand, field data corroborate a Neoproterozoic sedimentation for this unit, allowing to correlate it with the lithotypes of the Jucurutu Formation from the Seridó Group. However, discordant values/ages may suggest a progressive loss of lead for the Neoproterozoic (Brasiliano) event.

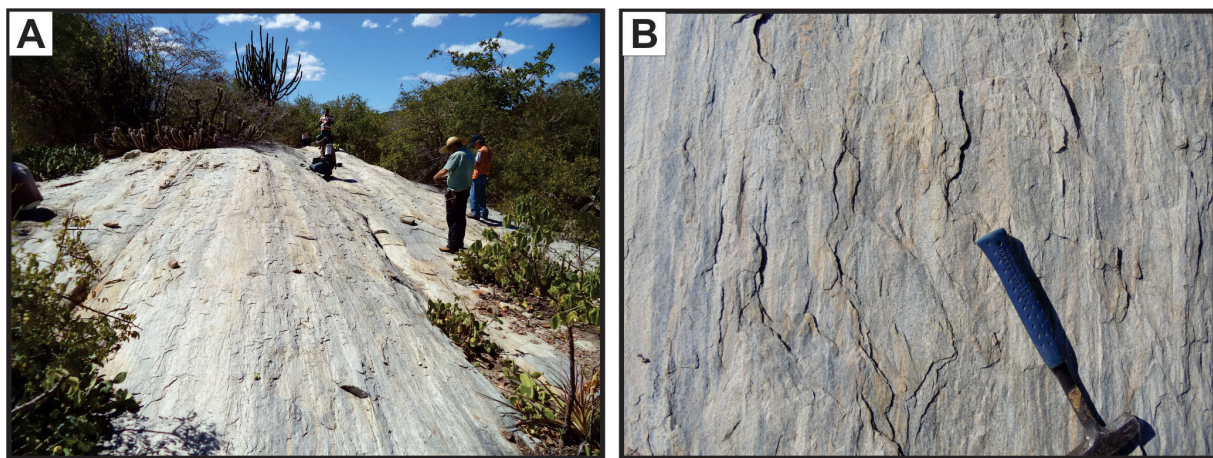


FIGURE 12. Features of the paragneiss of the Jucurutu Formation: (A) Overview of slab outcrop; (B) Detail of quartz-feldspathic bands intercalated by bands rich in biotite and amphibole in paragneiss (Coqueiros Farm in the Equador-RN region).

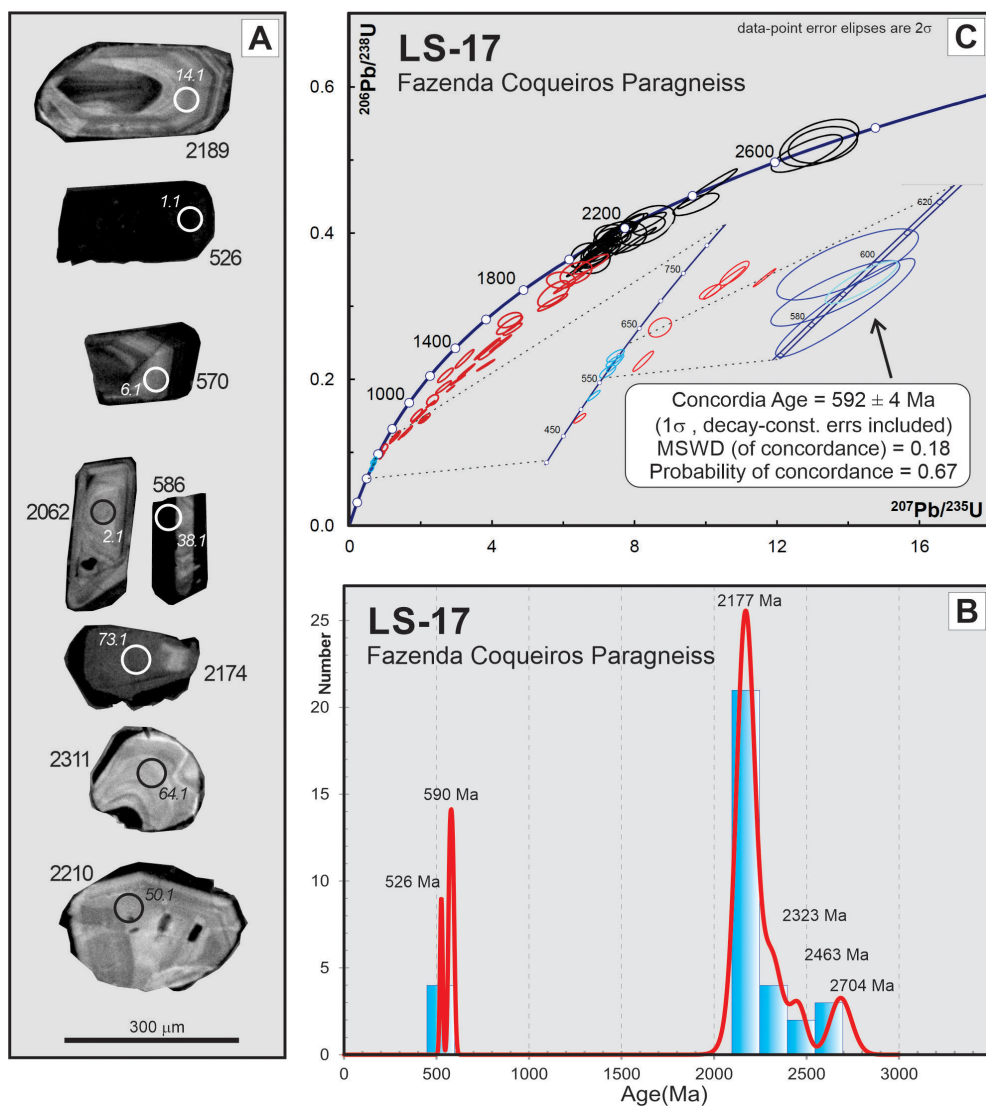


FIGURE 13. A) Cathodoluminescence image of zircon crystals from sample LS-17; ages in millions of years; spot number in italics; B) concordance diagram for concordant data used in concordance diagram (black and blue) and discordant (red) data; in detail, calculation of Concordia Age for Neoproterozoic data; C) frequency histogram of the concordant ages ($1000 \pm 10\%$). Apparent age, $^{207}\text{Pb}/^{206}\text{Pb}$ for ages greater than 1000 Ma and $^{206}\text{Pb}/^{238}\text{U}$ for the others.

TABLE 3 - U-Pb isotopic data in detrital zircons for the sample (LS-17) of paragneiss from Fazenda Coqueiros (Equador/RN), UTM coordinates: 752,969 mE; 9,237,224 mN (Datum WGS84, Zone 24).

| grain. spot | f(206) % | (ppm) | | | RATIOS | | | | | | Coef. corr | AGES (Ma) | | | | | |
|----------------|-------------|--------|-------|------|--------|---|------------|--|------------|--|---------------|-----------|---|--------------|---|------------|---|
| | | | | | Th/U | $\frac{^{207}\text{Pb}}{^{206}\text{Pb}}$ | err (%) | $\frac{^{207}\text{Pb}}{^{235}\text{U}}$ | err (%) | $\frac{^{206}\text{Pb}}{^{238}\text{U}}$ | err (%s) | | 206 Pb 238 U | err (abs) | $\frac{^{207}\text{Pb}}{^{206}\text{Pb}}$ | err (%) | 206 Pb 238 U |
| | | Pb rad | Th | U | | | | | | | | | | | | | |
| 1.1 | 1.80 | 173 | 765 | 1345 | 0.57 | 0.0592 | 2.20 | 0.693 | 2.76 | 0.0850 | 1.29 | 0.92 | 526 | 7 | 573 | 49 | 9 |
| 1.2 | 2.58 | 127 | 643 | 1272 | 0.51 | 0.0588 | 2.38 | 0.631 | 2.82 | 0.0779 | 1.28 | 0.87 | 483 | 6 | 559 | 53 | 14 |
| 2.1 | 0.12 | 74 | 73 | 140 | 0.52 | 0.1367 | 2.19 | 7.102 | 2.14 | 0.3769 | 1.17 | 0.99 | 2062 | 22 | 2185 | 42 | 6 |
| 3.1 | 0.11 | 66 | 52 | 128 | 0.40 | 0.1353 | 2.29 | 7.347 | 2.72 | 0.3938 | 1.40 | 0.36 | 2140 | 26 | 2168 | 40 | 2 |
| 4.1 | 0.01 | 61 | 73 | 117 | 0.63 | 0.1376 | 2.54 | 6.783 | 2.92 | 0.3574 | 1.54 | 0.87 | 1970 | 26 | 2197 | 44 | 11 |
| 5.1 | 0.91 | 48 | 7 | 236 | 0.03 | 0.1107 | 2.35 | 3.039 | 2.83 | 0.1990 | 1.46 | 0.99 | 1170 | 15 | 1812 | 42 | 36 |
| 6.1 | 0.01 | 64 | 362 | 465 | 0.78 | 0.0592 | 2.70 | 0.756 | 3.14 | 0.0925 | 1.41 | 0.71 | 570 | 8 | 575 | 60 | 1 |
| 6.2 | 0.56 | 27 | 219 | 181 | 1.21 | 0.0608 | 5.10 | 0.796 | 5.17 | 0.0950 | 1.89 | 0.78 | 585 | 11 | 631 | 115 | 8 |
| 7.1 | 1.05 | 173 | 416 | 1290 | 0.32 | 0.0748 | 2.27 | 1.213 | 2.64 | 0.1176 | 1.28 | 0.77 | 717 | 9 | 1064 | 45 | 33 |
| 8.1 | 0.28 | 60 | 55 | 118 | 0.47 | 0.1355 | 2.44 | 5.702 | 3.01 | 0.3051 | 1.57 | 0.94 | 1717 | 23 | 2171 | 42 | 21 |
| 9.1 | 0.36 | 54 | 91 | 104 | 0.87 | 0.1335 | 2.47 | 6.999 | 2.07 | 0.3802 | 1.13 | 0.99 | 2077 | 21 | 2145 | 44 | 4 |
| 10.1 | 9.68 | 95 | 242 | 285 | 0.85 | 0.1232 | 2.52 | 4.856 | 2.86 | 0.2859 | 1.47 | 0.98 | 1621 | 21 | 2003 | 44 | 20 |
| 11.1 | 0.35 | 81 | 39 | 196 | 0.20 | 0.1346 | 2.08 | 7.006 | 2.56 | 0.3777 | 1.32 | 0.66 | 2065 | 24 | 2158 | 37 | 5 |
| 12.1 | 0.06 | 42 | 34 | 76 | 0.45 | 0.1367 | 2.63 | 7.483 | 2.91 | 0.3970 | 1.46 | 0.81 | 2155 | 27 | 2186 | 45 | 2 |
| 13.1 | 0.04 | 72 | 57 | 140 | 0.41 | 0.1362 | 2.42 | 6.867 | 2.65 | 0.3656 | 1.37 | 0.73 | 2009 | 24 | 2180 | 42 | 8 |
| 14.1 | 0.10 | 65 | 54 | 120 | 0.45 | 0.1370 | 2.41 | 7.566 | 2.77 | 0.4006 | 1.40 | 0.76 | 2172 | 26 | 2189 | 42 | 1 |
| 15.1 | 0.10 | 64 | 61 | 115 | 0.53 | 0.1347 | 2.45 | 7.386 | 2.84 | 0.3977 | 1.41 | 0.01 | 2158 | 26 | 2160 | 42 | 1 |
| 16.1 | 0.08 | 61 | 34 | 117 | 0.29 | 0.1460 | 2.40 | 8.339 | 2.70 | 0.4142 | 1.40 | 0.89 | 2234 | 26 | 2300 | 41 | 3 |
| 17.1 | 0.19 | 38 | 12 | 61 | 0.19 | 0.1368 | 2.27 | 7.195 | 2.58 | 0.3815 | 1.34 | 0.67 | 2083 | 24 | 2187 | 41 | 5 |
| 18.1 | 0.06 | 52 | 23 | 88 | 0.26 | 0.1606 | 2.37 | 9.726 | 2.71 | 0.4393 | 1.41 | 0.76 | 2347 | 27 | 2462 | 40 | 5 |
| 19.1 | 0.31 | 56 | 50 | 115 | 0.43 | 0.1345 | 2.30 | 7.163 | 2.61 | 0.3863 | 1.35 | 0.83 | 2106 | 24 | 2158 | 40 | 3 |
| 20.1 | 2.84 | 80 | 317 | 631 | 0.50 | 0.0593 | 2.70 | 0.784 | 3.01 | 0.0959 | 1.25 | 0.85 | 590 | 7 | 577 | 61 | -2 |
| 21.1 | 0.21 | 32 | 13 | 42 | 0.30 | 0.1347 | 3.27 | 7.413 | 3.42 | 0.3991 | 1.60 | 0.99 | 2165 | 30 | 2160 | 57 | 0 |
| 22.1 | 2.04 | 10 | 10 | 18 | 0.56 | 0.1283 | 2.49 | 5.935 | 2.76 | 0.3356 | 1.34 | 0.01 | 1865 | 22 | 2074 | 41 | 11 |
| 23.1 | 3.31 | 59 | 247 | 434 | 0.57 | 0.0599 | 4.51 | 0.875 | 4.02 | 0.1059 | 1.98 | 0.98 | 649 | 12 | 600 | 99 | -8 |
| 24.1 | 0.82 | 85 | 123 | 239 | 0.51 | 0.1012 | 3.75 | 2.642 | 3.38 | 0.1893 | 1.85 | 0.94 | 1117 | 19 | 1647 | 74 | 33 |
| 25.1 | 0.13 | 73 | 76 | 130 | 0.58 | 0.1335 | 3.22 | 6.359 | 2.87 | 0.3455 | 1.79 | 0.42 | 1913 | 30 | 2144 | 57 | 11 |
| 26.1 | 0.12 | 47 | 35 | 94 | 0.37 | 0.1323 | 3.78 | 6.779 | 3.34 | 0.3716 | 1.99 | 0.82 | 2037 | 35 | 2129 | 67 | 5 |
| 27.1 | 0.71 | 40 | 34 | 54 | 0.64 | 0.1851 | 3.35 | 13.289 | 2.98 | 0.5207 | 1.96 | 0.32 | 2702 | 44 | 2699 | 60 | 0 |
| 28.1 | 0.64 | 35 | 29 | 72 | 0.40 | 0.1347 | 3.41 | 7.009 | 2.97 | 0.3773 | 1.86 | 0.61 | 2064 | 33 | 2160 | 58 | 5 |
| 29.1 | 0.16 | 27 | 18 | 50 | 0.37 | 0.1403 | 4.42 | 7.630 | 3.82 | 0.3944 | 2.26 | 0.24 | 2143 | 41 | 2231 | 77 | 4 |
| 30.1 | 0.15 | 50 | 28 | 69 | 0.41 | 0.1829 | 3.66 | 12.839 | 3.18 | 0.5090 | 2.06 | 0.76 | 2652 | 45 | 2680 | 60 | 2 |
| 31.1 | 0.27 | 39 | 76 | 112 | 0.68 | 0.1352 | 3.70 | 6.193 | 3.06 | 0.3322 | 1.84 | 0.99 | 1849 | 30 | 2167 | 65 | 15 |
| 32.1 | 6.97 | 9 | 45 | 79 | 0.56 | 0.0614 | 13.36 | 0.633 | 11.66 | 0.0748 | 3.21 | 0.74 | 465 | 15 | 655 | 300 | 30 |
| 33.1 | 0.69 | 48 | 23 | 230 | 0.10 | 0.0985 | 3.35 | 2.331 | 2.89 | 0.1716 | 1.75 | 0.51 | 1021 | 16 | 1596 | 63 | 37 |
| 34.1 | 0.69 | 35 | 49 | 70 | 0.70 | 0.1188 | 3.87 | 4.493 | 3.31 | 0.2742 | 1.90 | 0.85 | 1562 | 27 | 1939 | 71 | 20 |
| 35.1 | 0.61 | 133 | 933 | 859 | 1.09 | 0.0865 | 3.24 | 1.456 | 2.30 | 0.1220 | 1.56 | 0.99 | 742 | 11 | 1350 | 67 | 46 |
| 36.1 | 0.00 | 39 | 23 | 68 | 0.34 | 0.1497 | 3.74 | 8.028 | 2.97 | 0.3890 | 1.95 | 0.99 | 2118 | 35 | 2342 | 69 | 10 |
| 37.1 | 0.29 | 75 | 25 | 155 | 0.16 | 0.1236 | 3.56 | 4.242 | 2.94 | 0.2490 | 1.93 | 0.99 | 1433 | 24 | 2008 | 62 | 29 |
| 38.1 | 0.06 | 100 | 71 | 916 | 0.08 | 0.0602 | 3.99 | 0.789 | 3.23 | 0.0951 | 1.89 | 0.93 | 586 | 10 | 610 | 84 | 5 |
| 39.1 | 1.41 | 29 | 19 | 137 | 0.14 | 0.0674 | 4.01 | 0.989 | 3.43 | 0.1064 | 1.88 | 0.38 | 652 | 12 | 850 | 79 | 24 |
| 40.1 | 0.70 | 79 | 79 | 294 | 0.27 | 0.0777 | 3.73 | 1.321 | 3.27 | 0.1234 | 2.03 | 0.85 | 750 | 14 | 1139 | 69 | 35 |
| 41.1 | 1.28 | 108 | 168 | 304 | 0.55 | 0.1127 | 3.64 | 3.280 | 3.00 | 0.2111 | 1.94 | 0.99 | 1234 | 22 | 1844 | 63 | 34 |
| 42.1 | 0.06 | 86 | 276 | 163 | 1.70 | 0.1385 | 3.75 | 7.073 | 3.12 | 0.3703 | 2.03 | 0.82 | 2031 | 35 | 2209 | 64 | 9 |
| 43.1 | 0.55 | 70 | 337 | 346 | 0.97 | 0.1045 | 4.02 | 2.109 | 3.01 | 0.1464 | 1.84 | 0.85 | 881 | 15 | 1706 | 82 | 49 |
| 44.1 | 0.01 | 50 | 52 | 174 | 0.30 | 0.0951 | 4.42 | 2.694 | 3.33 | 0.2055 | 1.95 | 0.90 | 1205 | 22 | 1529 | 106 | 22 |
| 45.1 | 8.49 | 8 | 64 | 58 | 1.10 | 0.0685 | 15.91 | 0.726 | 13.37 | 0.0768 | 3.91 | 0.43 | 477 | 18 | 884 | 356 | 47 |
| 46.1 | 3.02 | 17 | 17 | 43 | 0.39 | 0.1279 | 3.52 | 5.433 | 2.86 | 0.3080 | 1.88 | 0.01 | 1731 | 29 | 2070 | 63 | 17 |
| 47.1 | 1.02 | 107 | 74 | 453 | 0.16 | 0.1099 | 1.91 | 2.839 | 1.58 | 0.1873 | 0.96 | 0.99 | 1107 | 10 | 1798 | 41 | 39 |
| 48.1 | 0.01 | 70 | 48 | 143 | 0.34 | 0.1265 | 2.37 | 3.824 | 2.70 | 0.2192 | 1.46 | 0.99 | 1278 | 16 | 2050 | 40 | 38 |
| 49.1 | 0.70 | 72 | 53 | 129 | 0.41 | 0.1486 | 2.29 | 8.400 | 2.24 | 0.4100 | 1.29 | 0.42 | 2215 | 24 | 2330 | 39 | 5 |
| 50.1 | 0.40 | 50 | 47 | 90 | 0.53 | 0.1386 | 2.60 | 7.900 | 2.45 | 0.4135 | 1.33 | 0.92 | 2231 | 25 | 2210 | 45 | 0 |
| 51.1 | 2.69 | 40 | 412 | 283 | 1.45 | 0.0588 | 3.40 | 0.790 | 3.28 | 0.0975 | 1.33 | 0.76 | 600 | 8 | 559 | 72 | -7 |
| 52.1 | 4.22 | 71 | 112 | 191 | 0.59 | 0.1305 | 2.15 | 5.767 | 2.12 | 0.3205 | 1.22 | 0.99 | 1792 | 19 | 2104 | 39 | 15 |
| 53.1 | 0.69 | 84 | 77 | 146 | 0.53 | 0.1331 | 2.25 | 6.452 | 2.27 | 0.3515 | 1.28 | 0.98 | 1942 | 21 | 2140 | 40 | 10 |
| 54.1 | 1.86 | 68 | 170 | 289 | 0.59 | 0.0820 | 3.17 | 1.163 | 7.31 | 0.1028 | 2.82 | 0.99 | 631 | 15 | 1246 | 39 | 50 |
| 55.1 | 0.21 | 73 | 75 | 216 | 0.35 | 0.1237 | 2.26 | 4.579 | 2.34 | 0.2685 | 1.27 | 0.92 | 1533 | 17 | 2010 | 39 | 24 |
| 56.1 | 1.10 | 99 | 216 | 416 | 0.52 | 0.0994 | 2.21 | 2.275 | 2.26 | 0.1659 | 1.21 | 0.99 | 989 | 11 | 1614 | 41 | 39 |
| 57.1 | 0.15 | 420 | 12576 | 793 | 15.86 | 0.1035 | 2.51 | 2.065 | 2.57 | 0.1447 | 1.31 | 0.99 | 871 | 11 | 1688 | 42 | 49 |

TABLE 3 - U-Pb isotopic data in detrital zircons for the sample (LS-17) of paragneiss from Fazenda Coqueiros (Equador/RN), UTM coordinates: 752,969 mE; 9,237,224 mN (Datum WGS84, Zone 24). (continued)

| grain. spot | f(206) %* | (ppm) | | | RATIOS | | | | | | | AGES (Ma) | | | | | |
|----------------|--------------|-------|-----|-----|--------|---|------------|--|------------|--|-------------|---------------|--|--------------|---|--------------|----------------|
| | | | | | Th/U | $\frac{^{207}\text{Pb}}{^{206}\text{Pb}}$ | err (%) | $\frac{^{207}\text{Pb}}{^{235}\text{U}}$ | err (%) | $\frac{^{206}\text{Pb}}{^{238}\text{U}}$ | err (%s) | Coef. corr | $\frac{^{206}\text{Pb}}{^{238}\text{U}}$ | err (abs) | $\frac{^{207}\text{Pb}}{^{206}\text{Pb}}$ | err (abs) | Disc. (%)** |
| 58.1 | 0.04 | 116 | 106 | 232 | 0.46 | 0.1162 | 2.67 | 4.502 | 2.99 | 0.2810 | 1.49 | 0.52 | 1596 | 21 | 1899 | 43 | 16 |
| 59.1 | 0.52 | 83 | 118 | 143 | 0.82 | 0.1375 | 2.98 | 7.640 | 3.30 | 0.4030 | 2.36 | 0.91 | 2183 | 43 | 2196 | 52 | 1 |
| 60.1 | 1.52 | 57 | 79 | 127 | 0.63 | 0.0695 | 4.32 | 1.138 | 6.19 | 0.1188 | 2.95 | 0.99 | 724 | 20 | 913 | 56 | 21 |
| 61.1 | 0.15 | 70 | 108 | 171 | 0.63 | 0.1312 | 2.90 | 5.732 | 3.18 | 0.3170 | 2.27 | 0.67 | 1775 | 36 | 2113 | 51 | 17 |
| 62.1 | 5.89 | 10 | 55 | 98 | 0.56 | 0.0563 | 12.26 | 0.571 | 11.67 | 0.0736 | 3.67 | 0.85 | 458 | 16 | 464 | 260 | 2 |
| 63.1 | 0.83 | 78 | 84 | 306 | 0.28 | 0.0769 | 3.90 | 1.277 | 4.88 | 0.1204 | 2.82 | 0.98 | 733 | 19 | 1119 | 57 | 35 |
| 64.1 | 0.76 | 32 | 21 | 55 | 0.39 | 0.1470 | 3.81 | 8.317 | 4.01 | 0.4105 | 2.70 | 0.48 | 2217 | 51 | 2311 | 66 | 5 |
| 65.1 | 0.52 | 91 | 92 | 173 | 0.53 | 0.1113 | 3.32 | 2.558 | 5.68 | 0.1667 | 3.60 | 0.99 | 994 | 30 | 1820 | 52 | 46 |
| 66.1 | 0.82 | 100 | 293 | 771 | 0.38 | 0.0692 | 3.03 | 0.914 | 3.34 | 0.0958 | 2.19 | 0.94 | 590 | 12 | 905 | 67 | 35 |
| 67.1 | 16.74 | 4 | 22 | 38 | 0.56 | 0.0602 | 23.09 | 0.635 | 19.97 | 0.0765 | 5.10 | 0.42 | 475 | 24 | 609 | 442 | 23 |
| 68.1 | 0.60 | 88 | 323 | 440 | 0.74 | 0.0905 | 3.20 | 1.881 | 3.54 | 0.1508 | 2.25 | 0.90 | 906 | 19 | 1435 | 72 | 37 |
| 69.1 | 1.29 | 47 | 27 | 64 | 0.42 | 0.1828 | 3.23 | 13.188 | 3.43 | 0.5234 | 2.52 | 0.49 | 2713 | 56 | 2678 | 53 | -1 |
| 70.1 | 0.91 | 81 | 166 | 173 | 0.96 | 0.1160 | 3.19 | 3.866 | 3.81 | 0.2416 | 2.52 | 0.99 | 1395 | 31 | 1896 | 56 | 27 |
| 71.1 | 1.05 | 79 | 134 | 203 | 0.66 | 0.0755 | 4.50 | 1.264 | 5.02 | 0.1213 | 2.80 | 0.99 | 738 | 19 | 1083 | 60 | 32 |
| 72.1 | 1.54 | 77 | 113 | 184 | 0.61 | 0.0950 | 3.37 | 1.958 | 4.25 | 0.1496 | 2.61 | 0.99 | 899 | 22 | 1527 | 56 | 42 |
| 73.1 | 0.34 | 75 | 48 | 156 | 0.31 | 0.1342 | 2.98 | 6.766 | 3.33 | 0.3656 | 2.32 | 0.01 | 2009 | 40 | 2154 | 51 | 7 |
| 74.1 | 0.66 | 99 | 107 | 324 | 0.33 | 0.1028 | 3.11 | 3.229 | 3.33 | 0.2279 | 2.28 | 0.96 | 1323 | 27 | 1675 | 58 | 21 |
| 75.1 | 0.14 | 50 | 55 | 77 | 0.71 | 0.1583 | 3.10 | 10.051 | 3.39 | 0.4606 | 2.41 | 0.98 | 2442 | 49 | 2437 | 53 | 0 |
| 76.1 | 0.26 | 40 | 48 | 76 | 0.64 | 0.1356 | 3.39 | 7.166 | 3.25 | 0.3834 | 2.32 | 0.99 | 2092 | 42 | 2171 | 61 | 4 |
| 77.1 | 1.08 | 51 | 44 | 135 | 0.33 | 0.1190 | 2.86 | 3.937 | 3.23 | 0.2400 | 2.25 | 0.93 | 1386 | 28 | 1941 | 52 | 29 |
| 78.1 | 0.01 | 90 | 95 | 185 | 0.51 | 0.1352 | 3.03 | 6.917 | 3.43 | 0.3712 | 2.37 | 0.96 | 2035 | 41 | 2166 | 53 | 7 |
| 79.1 | 2.63 | 82 | 163 | 278 | 0.59 | 0.0910 | 3.08 | 1.615 | 3.83 | 0.1287 | 2.41 | 0.97 | 780 | 18 | 1446 | 57 | 47 |
| 80.1 | 10.47 | 5 | -1 | 11 | -0.05 | 0.1201 | 3.00 | 3.860 | 3.66 | 0.2331 | 2.45 | 0.42 | 1351 | 29 | 1957 | 52 | 31 |

Errors are in 1 sigma

* Fraction of common lead

** Discordance, calculated as $(1 - \frac{^{206}\text{Pb}}{^{238}\text{U}} \text{ age} / \frac{^{207}\text{Pb}}{^{206}\text{Pb}} \text{ age}) * 100$

4.2. Quartzites from the Picuí River (Serra da Umburana, Currais Novos/RN) and from the Currais Farm (Cruzeta/RN)

To add isotopic determinations in these lithotypes considered in the literature as belonging to the Equador Formation, U-Pb dating of zircon (LAM-MC-ICP-MS) was carried out in a quartzite located in the Picuí River (Serra da Umburana, Currais Novos/RN) and also on Fazenda Currais (Cruzeta/RN). The Picuí River unit corresponds to quartzites with little muscovite, medium granulation and gray-white color (Fig. 14A), positioned in the western portion of the Serra da Umburana (40 continuous km of quartzite in the municipalities of Currais Novos-Carnaúba dos Dantas/RN).

A granoblastic, medium-grained, muscovite-poor whitish quartzite was found at Fazenda Currais (Fig. 14B), representing a layer positioned between mica schists of the Seridó Formation at the top and paragneisses of the Jucuruçu Formation at the base of the Seridó Group, outcropping for at least 35 km, especially between the towns of São José do Seridó and São Vicente (RN).

Zircon crystals from the quartzite sample from Picuí River (LS-05) are short to medium prisms with few transport features, ranging from 100 to 300 mm, with frequent fractures and inclusions. Their internal structure, revealed in cathodoluminescence imaging (Fig. 15A), is varied and complex, with the presence of nuclei and edges (Fig. 15A, zircon 44), oscillatory zoning (Fig. 15A, zircon 3), nebulitic and chaotic features (Fig. 15A, zircon 28), in addition to complex sectorial zoning (Fig. 15A, zircon 1, 21 and 47).

For this sample, the isotopic compositions of fifty-one spots were determined in forty-seven crystals (Table 4),

although in many other points, the analysis started but was canceled owing to the large content of common Pb. Among the completed analyses, only forty-eight were considered to be analytically adequate (error < 5%) and with little common Pb (<3%), whose apparent ages $^{207}\text{Pb}/^{206}\text{Pb}$ range between 2492 and 3032 Ma (Fig. 15D). The most concordant data (disagreement < 10%) were used in the frequency diagram plot (Fig. 15C), which indicated two main populations, a Neoarchean of 2701 and a Mesoarchean of 2980 Ma.

The quartzite zircon concentrate (LS-03) from Fazenda Currais presents zircon crystals in the form of prisms, rounded prisms and fragments, have few fractures, rare inclusions and different levels of wear, relative to the transport of sediments, with sizes ranging from approximately 50 to 300 µm. The internal structure includes the presence of a core and edge, with a predominance of oscillatory zoning (Fig. 15B, zircon 1), including concentric zoning (Fig. 15B, zircon 53), although there were some areas with complex sectorial zoning (Fig. 15B, zircon 41 and 23).

U-Pb isotopic composition was determined for ninety points (Table 5), but only seventy-nine had acceptable parameters of analytical error, common lead content and disagreement. The apparent ages $^{207}\text{Pb}/^{206}\text{Pb}$ range from 1033 to 3312 Ma, but paleoproterozoic data predominate, which in the frequency diagram (Fig. 15E) show the main peak at 2144 Ma and the secondary peak at 1910 Ma. The ages determined in these samples are predominantly in agreement (Fig. 15F) and only two determinations present Stenian ages, indicating the maximum age of deposition; this is significant, since geological data are more favorable for the beginning of sedimentation at the end of the Neoproterozoic.

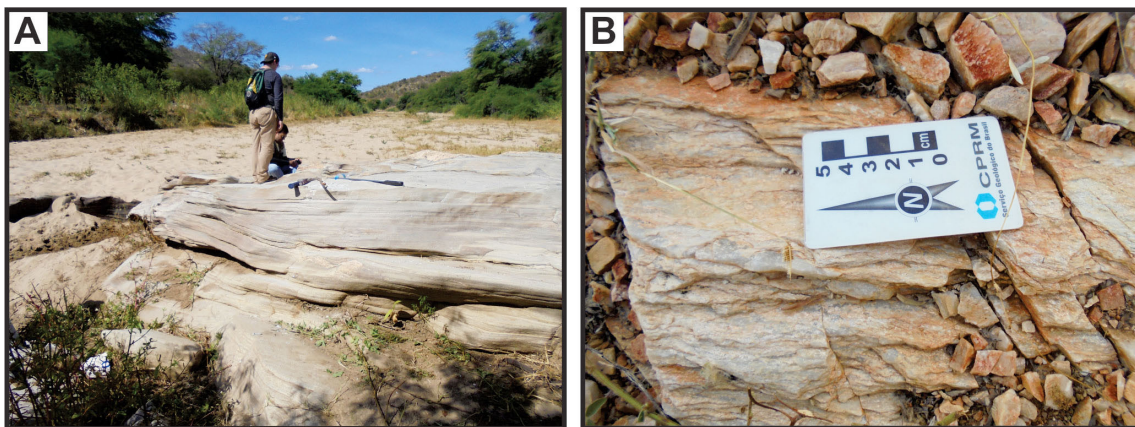


FIGURE 14. Characteristics of quartzites from the Equador Formation: (A) Overview of the quartzite outcrop at the bottom of the Picuí River (Currais Novos/RN); (B) Detail of quartzite from Fazenda Currais (Cruzeta/RN).

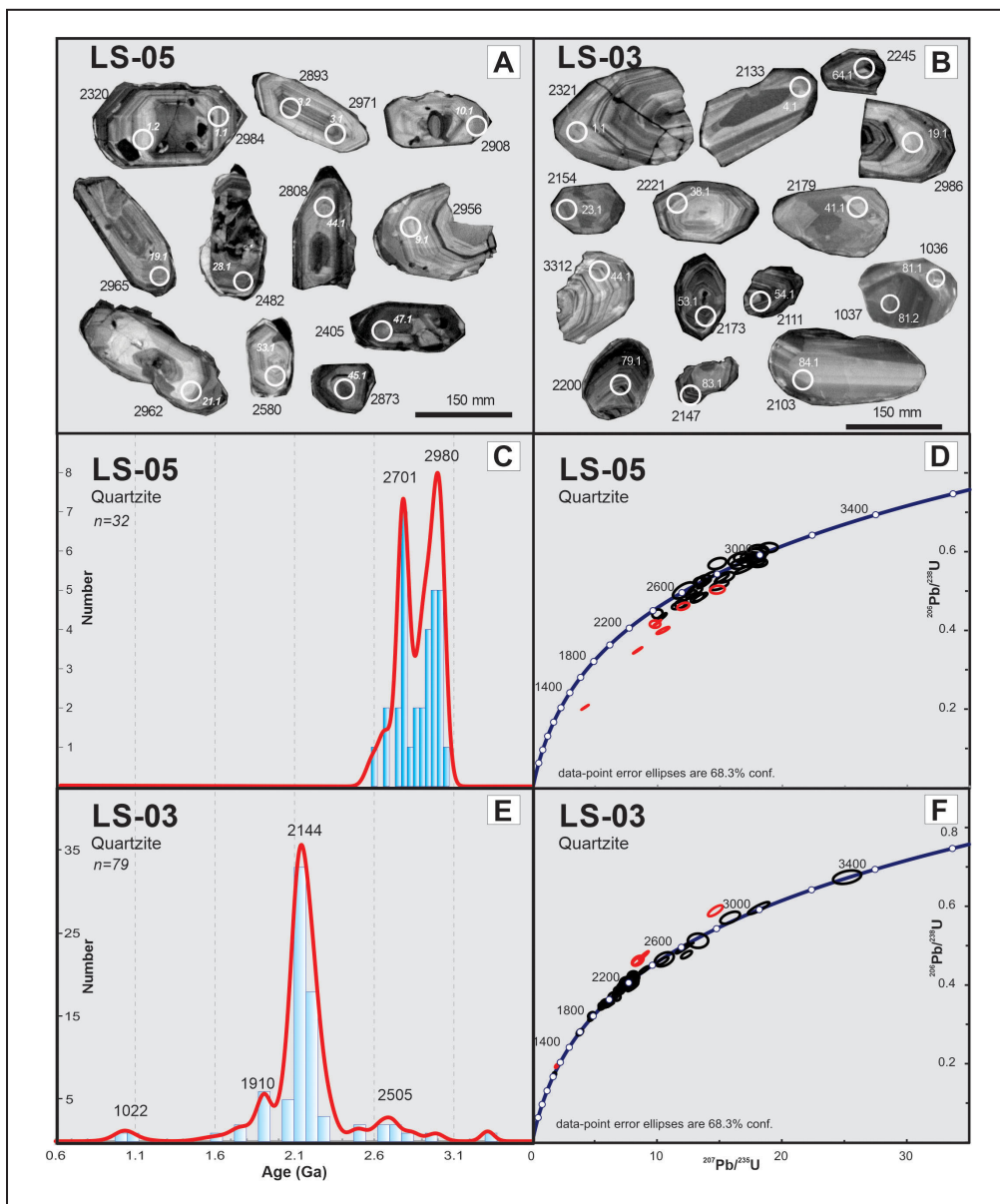


FIGURE 15. Cathodoluminescence images of zircon crystals from sample LS-05 (A) and LS-03 (B) of quartzites from the Equador Formation, aged in millions of years; spot number in italic/white color. Frequency histogram of concordant ages for samples LS-05 (C) and LS-03 (E), using apparent age, $^{207}\text{Pb}/^{206}\text{Pb}$ for ages greater than 1000 Ma and $^{206}\text{Pb}/^{238}\text{U}$ for the others. Concordance diagrams for the concordant data used in the concordance diagram (black) and discordant (red) for the LS-05 (D) and LS-03 (F) samples.

TABLE 4 - U-Pb isotopic data in detrital zircons from the sample (LS-05) of muscovite quartzite in the Picuí River (Serra das Umburanas, Currais Novos/RN), UTM coordinates: 780,366 mE; 9,299,710 mN (Datum WGS84, Zone 24).

| grain. spot | $f(206\text{Pb})^*$ | (ppm) | | | RATIOS | | | | | | AGES (Ma) | | | | | | | |
|----------------|---------------------|--------|----|-----|--------|-------------------|------------|-------------------|------------|-------------------|-------------|-------------------|------|-------------------|--------------|-------------------|--------------|-------|
| | | Pb rad | Th | U | Th/U | ^{207}Pb | err (%) | ^{207}Pb | err (%) | ^{206}Pb | err (%s) | Coef. | corr | ^{206}Pb | err (abs) | ^{207}Pb | err (abs) | Disc. |
| | | | | | | ^{206}Pb | | ^{235}U | | ^{238}U | | ^{206}Pb | | | | | | |
| 1.1 | 0.54 | 38 | 30 | 51 | 0.59 | 0.22040 | 2.50 | 16.878 | 2.74 | 0.5554 | 1.24 | 0.89 | | 2.848 | 0.029 | 2.984 | 0.041 | 5 |
| 1.2 | 0.78 | 39 | 16 | 61 | 0.27 | 0.14770 | 3.11 | 4.188 | 4.53 | 0.2056 | 1.95 | 0.99 | | 1.206 | 0.020 | 2.320 | 0.046 | 49 |
| 2.1 | 4.75 | 10 | 3 | 16 | 0.22 | 0.18520 | 2.75 | 12.329 | 2.96 | 0.4829 | 1.37 | 0.97 | | 2.540 | 0.029 | 2.700 | 0.046 | 6 |
| 2.2 | 0.62 | 41 | 20 | 54 | 0.37 | 0.18950 | 2.69 | 14.084 | 2.62 | 0.5392 | 1.34 | 0.82 | | 2.780 | 0.030 | 2.738 | 0.044 | -1 |
| 3.1 | 1.18 | 26 | 19 | 29 | 0.64 | 0.21860 | 2.74 | 18.023 | 3.00 | 0.5978 | 1.44 | 0.21 | | 3.021 | 0.035 | 2.971 | 0.049 | -1 |
| 3.2 | 0.32 | 45 | 45 | 49 | 0.93 | 0.20840 | 2.83 | 16.863 | 2.90 | 0.5868 | 1.50 | 0.17 | | 2.977 | 0.036 | 2.893 | 0.046 | -2 |
| 4.1 | 13.11 | 4 | 1 | 9 | 0.09 | 0.18370 | 2.56 | 11.988 | 2.89 | 0.4732 | 1.29 | 0.45 | | 2.498 | 0.027 | 2.687 | 0.042 | 8 |
| 5.1 | 0.07 | 73 | 56 | 81 | 0.69 | 0.22720 | 2.60 | 17.984 | 2.88 | 0.5741 | 1.38 | 0.01 | | 2.925 | 0.032 | 3.032 | 0.043 | 4 |
| 6.1 | 4.04 | 9 | 4 | 15 | 0.26 | 0.19270 | 3.11 | 11.751 | 3.28 | 0.4422 | 1.61 | 0.32 | | 2.360 | 0.032 | 2.766 | 0.052 | 15 |
| 7.1 | 9.72 | 4 | 3 | 4 | 0.81 | 0.17730 | 3.78 | 13.339 | 3.75 | 0.5456 | 1.85 | 0.14 | | 2.807 | 0.043 | 2.628 | 0.057 | -6 |
| 8.1 | 2.52 | 11 | 5 | 17 | 0.32 | 0.18250 | 2.63 | 11.683 | 3.05 | 0.4643 | 1.34 | 0.50 | | 2.459 | 0.027 | 2.676 | 0.043 | 9 |
| 9.1 | 0.51 | 36 | 14 | 42 | 0.34 | 0.21660 | 2.82 | 17.512 | 3.17 | 0.5862 | 1.45 | 0.01 | | 2.974 | 0.034 | 2.956 | 0.044 | 0 |
| 10.1 | 0.57 | 25 | 17 | 27 | 0.62 | 0.21030 | 2.81 | 14.943 | 3.19 | 0.5153 | 1.49 | 0.62 | | 2.679 | 0.033 | 2.908 | 0.045 | 8 |
| 11.1 | 2.72 | 15 | 9 | 21 | 0.44 | 0.17460 | 4.58 | 12.096 | 4.73 | 0.5024 | 2.69 | 0.62 | | 2.624 | 0.056 | 2.603 | 0.079 | 0 |
| 12.1 | 1.59 | 23 | 19 | 28 | 0.66 | 0.21160 | 2.84 | 16.628 | 3.02 | 0.5699 | 1.46 | 0.36 | | 2.907 | 0.035 | 2.918 | 0.046 | 1 |
| 13.1 | 0.86 | 25 | 21 | 23 | 0.92 | 0.21760 | 2.25 | 17.833 | 2.67 | 0.5944 | 1.48 | 0.01 | | 3.007 | 0.035 | 2.963 | 0.037 | -1 |
| 13.2 | 1.91 | 10 | 4 | 12 | 0.37 | 0.22070 | 2.54 | 17.837 | 2.62 | 0.5863 | 1.36 | 0.01 | | 2.974 | 0.032 | 2.986 | 0.042 | 1 |
| 14.1 | 1.36 | 28 | 25 | 28 | 0.90 | 0.20470 | 2.64 | 16.389 | 2.94 | 0.5808 | 1.74 | 0.39 | | 2.952 | 0.041 | 2.864 | 0.046 | -3 |
| 15.1 | 1.00 | 37 | 35 | 41 | 0.86 | 0.20070 | 2.39 | 13.431 | 2.70 | 0.4853 | 1.48 | 0.82 | | 2.550 | 0.031 | 2.832 | 0.040 | 10 |
| 16.1 | 1.30 | 46 | 28 | 64 | 0.44 | 0.17040 | 2.52 | 9.797 | 2.86 | 0.4169 | 1.46 | 0.01 | | 2.247 | 0.028 | 2.562 | 0.041 | 13 |
| 17.1 | 0.22 | 40 | 29 | 43 | 0.68 | 0.18750 | 2.61 | 13.666 | 2.86 | 0.5287 | 1.55 | 0.45 | | 2.736 | 0.035 | 2.720 | 0.042 | 0 |
| 18.1 | 4.59 | 11 | 11 | 13 | 0.79 | 0.21420 | 2.52 | 15.849 | 2.63 | 0.5366 | 1.55 | 0.82 | | 2.769 | 0.035 | 2.938 | 0.041 | 6 |
| 19.1 | 1.14 | 24 | 21 | 23 | 0.93 | 0.21790 | 2.29 | 17.296 | 2.67 | 0.5758 | 1.48 | 0.19 | | 2.931 | 0.035 | 2.965 | 0.037 | 2 |
| 20.1 | 0.26 | 45 | 28 | 51 | 0.55 | 0.18610 | 2.31 | 13.444 | 2.69 | 0.5240 | 1.45 | 0.11 | | 2.716 | 0.032 | 2.708 | 0.038 | 0 |
| 21.1 | 0.49 | 28 | 17 | 25 | 0.70 | 0.21750 | 2.57 | 18.074 | 2.93 | 0.6026 | 1.64 | 0.01 | | 3.040 | 0.040 | 2.962 | 0.042 | -2 |
| 22.1 | 1.72 | 23 | 29 | 26 | 1.12 | 0.20870 | 2.68 | 15.414 | 3.06 | 0.5358 | 1.62 | 0.49 | | 2.766 | 0.037 | 2.895 | 0.043 | 5 |
| 23.1 | 0.55 | 37 | 21 | 36 | 0.60 | 0.18790 | 2.98 | 14.788 | 3.19 | 0.5707 | 1.63 | 0.37 | | 2.911 | 0.038 | 2.724 | 0.047 | -6 |
| 24.1 | 1.64 | 23 | 18 | 27 | 0.65 | 0.18520 | 2.32 | 11.918 | 2.75 | 0.4669 | 1.56 | 0.11 | | 2.470 | 0.031 | 2.700 | 0.039 | 9 |
| 25.1 | 4.44 | 9 | 6 | 14 | 0.40 | 0.18520 | 2.05 | 12.528 | 2.27 | 0.4907 | 1.39 | 0.01 | | 2.574 | 0.029 | 2.700 | 0.036 | 5 |
| 26.1 | 1.08 | 23 | 16 | 32 | 0.51 | 0.18720 | 2.19 | 12.714 | 2.36 | 0.4925 | 1.38 | 0.38 | | 2.582 | 0.029 | 2.718 | 0.036 | 6 |
| 27.1 | 0.75 | 20 | 13 | 26 | 0.52 | 0.19140 | 2.56 | 13.712 | 2.64 | 0.5195 | 1.48 | 0.90 | | 2.697 | 0.032 | 2.754 | 0.039 | 3 |
| 28.1 | 2.28 | 18 | 10 | 29 | 0.36 | 0.16350 | 2.69 | 9.987 | 2.71 | 0.4431 | 1.67 | 0.19 | | 2.364 | 0.033 | 2.492 | 0.052 | 6 |
| 29.1 | 4.86 | 11 | 11 | 16 | 0.73 | 0.18400 | 2.99 | 11.226 | 3.04 | 0.4424 | 1.74 | 0.08 | | 2.362 | 0.034 | 2.689 | 0.048 | 13 |
| 30.1 | 5.64 | 14 | 8 | 24 | 0.33 | 0.16590 | 2.65 | 9.280 | 2.84 | 0.4056 | 1.60 | 0.47 | | 2.195 | 0.030 | 2.517 | 0.045 | 13 |
| 31.1 | 0.22 | 65 | 51 | 93 | 0.55 | 0.18820 | 2.07 | 12.657 | 2.19 | 0.4878 | 1.31 | 0.99 | | 2.561 | 0.028 | 2.726 | 0.035 | 7 |
| 32.1 | 0.33 | 68 | 36 | 79 | 0.45 | 0.22410 | 1.92 | 18.071 | 2.11 | 0.5848 | 1.32 | 0.53 | | 2.968 | 0.031 | 3.011 | 0.031 | 2 |
| 33.1 | 0.37 | 42 | 26 | 67 | 0.39 | 0.17230 | 2.38 | 10.337 | 2.44 | 0.4352 | 1.42 | 0.88 | | 2.329 | 0.028 | 2.580 | 0.040 | 10 |
| 34.1 | 0.91 | 65 | 32 | 110 | 0.29 | 0.17220 | 2.09 | 9.958 | 2.12 | 0.4194 | 1.26 | 0.98 | | 2.258 | 0.024 | 2.579 | 0.035 | 13 |
| 35.1 | 0.06 | 56 | 50 | 81 | 0.62 | 0.18920 | 2.54 | 12.058 | 2.62 | 0.4622 | 1.30 | 0.43 | | 2.449 | 0.026 | 2.735 | 0.042 | 11 |
| 36.1 | 6.26 | 32 | 20 | 49 | 0.41 | 0.18550 | 3.02 | 12.291 | 2.78 | 0.4805 | 1.56 | 0.99 | | 2.530 | 0.033 | 2.703 | 0.050 | 7 |
| 37.1 | 0.85 | 32 | 19 | 53 | 0.37 | 0.17400 | 2.82 | 8.400 | 2.86 | 0.3502 | 1.48 | 0.98 | | 1.935 | 0.024 | 2.596 | 0.047 | 26 |
| 38.1 | 0.43 | 34 | 23 | 37 | 0.63 | 0.22430 | 2.45 | 18.900 | 2.53 | 0.6111 | 1.26 | 0.06 | | 3.074 | 0.031 | 3.012 | 0.039 | -2 |
| 39.1 | 2.66 | 19 | 15 | 26 | 0.58 | 0.21260 | 2.54 | 14.787 | 2.63 | 0.5044 | 1.31 | 0.17 | | 2.633 | 0.028 | 2.926 | 0.040 | 11 |
| 40.1 | 2.50 | 14 | 11 | 21 | 0.51 | 0.18870 | 3.02 | 10.430 | 3.23 | 0.4008 | 1.45 | 0.88 | | 2.173 | 0.026 | 2.731 | 0.043 | 21 |
| 41.1 | 11.83 | 21 | 20 | 33 | 0.60 | 0.14270 | 2.80 | 6.083 | 2.90 | 0.3091 | 1.46 | 0.79 | | 1.736 | 0.021 | 2.260 | 0.045 | 24 |
| 42.1 | 5.35 | 13 | 8 | 22 | 0.37 | 0.20560 | 2.72 | 13.605 | 2.67 | 0.4799 | 1.48 | 0.78 | | 2.527 | 0.031 | 2.871 | 0.048 | 12 |
| 43.1 | 0.23 | 44 | 40 | 50 | 0.81 | 0.22440 | 2.45 | 17.924 | 2.45 | 0.5794 | 1.47 | 0.03 | | 2.946 | 0.035 | 3.012 | 0.040 | 3 |
| 44.1 | 1.21 | 19 | 18 | 30 | 0.61 | 0.19770 | 2.83 | 13.183 | 2.64 | 0.4835 | 1.57 | 0.61 | | 2.543 | 0.033 | 2.808 | 0.045 | 10 |
| 45.1 | 0.00 | 14 | 12 | 22 | 0.56 | 0.20580 | 2.48 | 15.133 | 2.44 | 0.5333 | 1.41 | 0.86 | | 2.755 | 0.032 | 2.873 | 0.040 | 5 |
| 46.1 | 0.54 | 28 | 33 | 34 | 0.97 | 0.18800 | 3.19 | 13.023 | 2.77 | 0.5023 | 1.61 | 0.45 | | 2.624 | 0.036 | 2.725 | 0.050 | 4 |
| 47.1 | 7.27 | 30 | 43 | 55 | 0.78 | 0.15530 | 2.90 | 6.746 | 2.76 | 0.3150 | 1.65 | 0.29 | | 1.765 | 0.025 | 2.405 | 0.051 | 27 |

Errors are in 1 sigma

* Fraction of common lead

** Discordance, calculated as $(1 - (\frac{^{206}\text{Pb}}{^{238}\text{U}} \text{ age} / \frac{^{207}\text{Pb}}{^{206}\text{Pb}} \text{ age})) * 100$

TABLE 5 - U-Pb isotopic data in detrital zircons from the sample (LS-03) of quartzite from Fazenda Currais (Cruzeta/RN), UTM coordinates: 737,325 mE; 9,295,128 mN (Datum WGS84, Zone 24).

| grain. spot | f(206) % | (ppm) | | | RATIOS | | | | | | AGES (Ma) | | | | | | | |
|----------------|-------------|-------|-----|-----|--------|------|-----------|------------|-----------|------------|-----------|------------|---------------|-----------|--------------|-----------|--------------|----------------|
| | | Pb | rad | Th | U | Th/U | 207 Pb | err (%) | 207 Pb | err (%) | 206 Pb | err (%) | Coef. corr | 206 Pb | err (abs) | 207 Pb | err (abs) | Disc. (%)** |
| | | | | | | | 206 Pb | (%) | 235 U | (%) | 238 U | (%s) | | 238 U | (abs) | 206 Pb | (abs) | |
| 1.1 | 1.02 | 40 | 27 | 67 | | 0.40 | 0.14790 | 3.11 | 8.951 | 2.86 | 0.4390 | 1.44 | 0.88 | 2346 | 28 | 2321 | 54 | -1 |
| 2.1 | 1.38 | 25 | 31 | 46 | | 0.68 | 0.12620 | 4.04 | 6.475 | 3.64 | 0.3722 | 1.77 | 0.21 | 2040 | 31 | 2045 | 73 | 1 |
| 3.1 | 3.82 | 8 | 5 | 15 | | 0.31 | 0.13910 | 6.76 | 7.597 | 5.99 | 0.3961 | 3.08 | 0.04 | 2151 | 56 | 2216 | 121 | 3 |
| 4.1 | 0.17 | 41 | 40 | 70 | | 0.57 | 0.13260 | 3.02 | 7.384 | 2.83 | 0.4038 | 1.36 | 0.84 | 2187 | 25 | 2133 | 52 | -2 |
| 5.1 | 0.57 | 13 | 22 | 21 | | 1.08 | 0.13530 | 5.40 | 7.576 | 4.78 | 0.4060 | 2.39 | 0.01 | 2197 | 44 | 2168 | 97 | -1 |
| 6.1 | 0.45 | 15 | 11 | 28 | | 0.39 | 0.13770 | 4.43 | 7.769 | 3.93 | 0.4092 | 1.93 | 0.76 | 2211 | 36 | 2198 | 75 | 0 |
| 7.1 | 2.05 | 16 | 6 | 35 | | 0.17 | 0.12950 | 6.80 | 6.540 | 4.67 | 0.3662 | 2.27 | 0.96 | 2011 | 41 | 2092 | 123 | 4 |
| 7.2 | 0.95 | 44 | 31 | 89 | | 0.35 | 0.13200 | 3.64 | 6.748 | 3.22 | 0.3706 | 1.70 | 0.01 | 2032 | 29 | 2125 | 73 | 5 |
| 8.1 | 0.92 | 16 | 12 | 31 | | 0.37 | 0.13440 | 4.09 | 7.402 | 3.60 | 0.3993 | 1.78 | 0.64 | 2166 | 33 | 2157 | 72 | 0 |
| 9.1 | 0.56 | 12 | 14 | 32 | | 0.44 | 0.09870 | 4.96 | 3.821 | 4.34 | 0.2808 | 1.82 | 0.42 | 1595 | 26 | 1599 | 93 | 1 |
| 10.1 | 0.15 | 41 | 40 | 55 | | 0.73 | 0.16400 | 3.05 | 10.446 | 2.91 | 0.4619 | 1.43 | 0.78 | 2448 | 29 | 2498 | 50 | 2 |
| 11.1 | 0.18 | 69 | 60 | 123 | | 0.49 | 0.13610 | 2.72 | 8.008 | 2.49 | 0.4268 | 1.22 | 0.26 | 2291 | 23 | 2178 | 47 | -5 |
| 12.1 | 0.69 | 74 | 60 | 137 | | 0.44 | 0.13590 | 2.65 | 7.720 | 2.74 | 0.4120 | 1.26 | 0.45 | 2224 | 24 | 2176 | 47 | -2 |
| 13.1 | 0.09 | 33 | 60 | 63 | | 0.95 | 0.11770 | 3.57 | 5.627 | 3.51 | 0.3467 | 1.62 | 0.61 | 1919 | 27 | 1922 | 65 | 1 |
| 14.1 | 0.55 | 23 | 23 | 40 | | 0.58 | 0.13660 | 3.51 | 7.792 | 3.42 | 0.4138 | 1.62 | 0.79 | 2232 | 31 | 2184 | 61 | -2 |
| 15.1 | 0.55 | 17 | 30 | 20 | | 1.52 | 0.18770 | 4.42 | 13.284 | 4.06 | 0.5134 | 2.34 | 0.01 | 2671 | 51 | 2722 | 74 | 2 |
| 16.1 | 0.61 | 17 | 15 | 32 | | 0.48 | 0.14180 | 4.80 | 8.024 | 4.42 | 0.4105 | 2.19 | 0.80 | 2217 | 41 | 2249 | 83 | 2 |
| 17.1 | 0.70 | 7 | 1 | 11 | | 0.11 | 0.17140 | 7.18 | 11.127 | 6.19 | 0.4707 | 3.55 | 0.03 | 2487 | 73 | 2572 | 121 | 4 |
| 18.1 | 0.49 | 30 | 24 | 55 | | 0.43 | 0.13360 | 3.67 | 7.371 | 3.59 | 0.4002 | 1.72 | 0.74 | 2170 | 32 | 2146 | 64 | -1 |
| 19.1 | 0.31 | 39 | 30 | 46 | | 0.65 | 0.22070 | 3.17 | 18.138 | 3.12 | 0.5962 | 1.69 | 0.87 | 3014 | 41 | 2986 | 51 | 0 |
| 20.1 | 0.43 | 26 | 32 | 58 | | 0.54 | 0.10660 | 4.03 | 4.761 | 3.83 | 0.3238 | 1.67 | 0.31 | 1808 | 26 | 1743 | 74 | -3 |
| 21.1 | 0.44 | 26 | 21 | 47 | | 0.45 | 0.13390 | 3.73 | 7.608 | 3.59 | 0.4121 | 1.72 | 0.84 | 2225 | 32 | 2150 | 66 | -3 |
| 22.1 | 0.49 | 39 | 43 | 48 | | 0.90 | 0.18170 | 2.53 | 12.547 | 1.96 | 0.5007 | 1.04 | 0.99 | 2617 | 24 | 2669 | 47 | 2 |
| 23.1 | 0.36 | 32 | 39 | 57 | | 0.68 | 0.13420 | 3.50 | 7.309 | 3.45 | 0.3949 | 1.65 | 0.22 | 2145 | 30 | 2154 | 61 | 1 |
| 24.1 | 3.28 | 25 | 32 | 51 | | 0.62 | 0.11010 | 4.36 | 4.106 | 4.87 | 0.2705 | 2.18 | 0.98 | 1543 | 29 | 1801 | 75 | 15 |
| 25.1 | 0.51 | 35 | 27 | 60 | | 0.45 | 0.13880 | 3.67 | 8.109 | 3.65 | 0.4239 | 1.82 | 0.01 | 2278 | 35 | 2212 | 64 | -2 |
| 26.1 | 0.37 | 45 | 42 | 52 | | 0.81 | 0.20110 | 3.13 | 15.855 | 3.27 | 0.5719 | 1.77 | 0.54 | 2916 | 41 | 2835 | 51 | -2 |
| 27.1 | 0.11 | 61 | 58 | 103 | | 0.57 | 0.13300 | 3.23 | 7.481 | 3.34 | 0.4081 | 1.64 | 0.13 | 2206 | 31 | 2137 | 56 | -3 |
| 28.1 | 0.07 | 38 | 22 | 69 | | 0.31 | 0.13400 | 3.36 | 7.300 | 3.45 | 0.3951 | 1.70 | 0.71 | 2147 | 31 | 2151 | 59 | 1 |
| 29.1 | 0.36 | 17 | 28 | 27 | | 1.03 | 0.13480 | 5.27 | 7.622 | 4.96 | 0.4100 | 2.39 | 0.90 | 2215 | 45 | 2162 | 93 | -2 |
| 30.1 | 0.24 | 40 | 27 | 74 | | 0.37 | 0.13380 | 3.44 | 7.484 | 3.48 | 0.4058 | 1.72 | 0.32 | 2196 | 32 | 2148 | 60 | -2 |
| 31.1 | 0.74 | 13 | 4 | 21 | | 0.17 | 0.16460 | 5.35 | 10.579 | 4.76 | 0.4661 | 2.53 | 0.40 | 2466 | 52 | 2504 | 90 | 2 |
| 32.1 | 0.44 | 29 | 35 | 50 | | 0.70 | 0.13490 | 4.08 | 7.533 | 3.94 | 0.4049 | 1.93 | 0.51 | 2192 | 36 | 2163 | 70 | -1 |
| 33.1 | 0.19 | 63 | 63 | 109 | | 0.58 | 0.13240 | 2.95 | 7.402 | 3.05 | 0.4054 | 1.53 | 0.01 | 2194 | 28 | 2130 | 51 | -2 |
| 34.1 | 0.96 | 12 | 8 | 22 | | 0.37 | 0.13510 | 6.74 | 7.383 | 6.27 | 0.3964 | 3.00 | 0.45 | 2152 | 54 | 2165 | 119 | 1 |
| 35.1 | 0.16 | 54 | 46 | 92 | | 0.50 | 0.13940 | 3.01 | 8.079 | 3.15 | 0.4204 | 1.59 | 0.03 | 2263 | 30 | 2219 | 53 | -1 |
| 36.1 | 0.98 | 23 | 16 | 41 | | 0.40 | 0.13480 | 3.93 | 7.588 | 4.09 | 0.4081 | 1.91 | 0.41 | 2206 | 36 | 2162 | 68 | -2 |
| 37.1 | 0.44 | 21 | 16 | 38 | | 0.43 | 0.13590 | 4.05 | 7.669 | 4.21 | 0.4094 | 1.98 | 0.58 | 2212 | 37 | 2175 | 70 | -1 |
| 38.1 | 0.27 | 30 | 17 | 54 | | 0.31 | 0.13950 | 3.15 | 7.862 | 3.43 | 0.4087 | 1.69 | 0.63 | 2209 | 32 | 2221 | 55 | 1 |
| 39.1 | 0.25 | 38 | 27 | 70 | | 0.38 | 0.13380 | 3.06 | 7.452 | 3.35 | 0.4039 | 1.66 | 0.10 | 2187 | 31 | 2149 | 53 | -1 |
| 40.1 | 1.61 | 33 | 25 | 45 | | 0.54 | 0.14740 | 2.85 | 8.048 | 3.65 | 0.3959 | 1.77 | 0.87 | 2150 | 32 | 2316 | 44 | 8 |
| 41.1 | 0.16 | 20 | 14 | 36 | | 0.38 | 0.13620 | 4.11 | 7.472 | 4.22 | 0.3980 | 2.01 | 0.63 | 2160 | 37 | 2179 | 73 | 1 |
| 42.1 | 1.07 | 31 | 59 | 61 | | 0.98 | 0.11880 | 3.70 | 5.773 | 3.88 | 0.3525 | 1.79 | 0.67 | 1946 | 30 | 1938 | 68 | 0 |
| 43.1 | 0.30 | 21 | 16 | 38 | | 0.42 | 0.13340 | 4.20 | 7.352 | 4.29 | 0.3998 | 2.00 | 0.34 | 2168 | 37 | 2143 | 73 | -1 |
| 44.1 | 0.15 | 52 | 31 | 51 | | 0.60 | 0.27110 | 2.58 | 25.228 | 2.95 | 0.6749 | 1.66 | 0.36 | 3325 | 43 | 3312 | 40 | 0 |
| 45.1 | 1.57 | 87 | 105 | 159 | | 0.66 | 0.13070 | 2.60 | 6.734 | 2.97 | 0.3736 | 1.50 | 0.98 | 2046 | 26 | 2108 | 46 | 3 |
| 46.1 | 0.90 | 21 | 19 | 37 | | 0.51 | 0.14090 | 3.90 | 8.075 | 4.06 | 0.4156 | 2.00 | 0.38 | 2241 | 37 | 2238 | 69 | 0 |
| 47.1 | 0.18 | 94 | 57 | 175 | | 0.33 | 0.13260 | 2.41 | 7.061 | 2.92 | 0.3862 | 1.50 | 0.25 | 2105 | 27 | 2133 | 43 | 2 |
| 48.1 | 0.02 | 90 | 65 | 111 | | 0.58 | 0.18050 | 2.94 | 14.674 | 2.65 | 0.5895 | 1.54 | 0.75 | 2988 | 37 | 2658 | 50 | -12 |
| 49.1 | 0.34 | 27 | 19 | 48 | | 0.39 | 0.13260 | 4.07 | 8.456 | 3.64 | 0.4625 | 1.79 | 0.44 | 2451 | 37 | 2133 | 70 | -14 |
| 50.1 | 0.52 | 54 | 51 | 89 | | 0.57 | 0.13630 | 3.30 | 8.942 | 2.85 | 0.4759 | 1.51 | 0.94 | 2509 | 32 | 2180 | 60 | -15 |
| 51.1 | 0.30 | 42 | 186 | 140 | | 1.32 | 0.07260 | 4.41 | 1.952 | 3.96 | 0.1951 | 1.54 | 0.58 | 1149 | 16 | 1001 | 89 | -14 |
| 52.1 | 0.51 | 62 | 56 | 105 | | 0.53 | 0.13180 | 2.96 | 8.389 | 2.77 | 0.4617 | 1.45 | 0.72 | 2447 | 30 | 2122 | 51 | -15 |
| 53.1 | 0.36 | 54 | 50 | 106 | | 0.47 | 0.13570 | 3.02 | 7.792 | 2.85 | 0.4164 | 1.49 | 0.59 | 2244 | 28 | 2173 | 53 | -3 |
| 54.1 | 0.54 | 56 | 47 | 114 | | 0.41 | 0.13090 | 3.59 | 7.361 | 3.18 | 0.4077 | 1.59 | 0.68 | 2204 | 30 | 2111 | 62 | -4 |
| 55.1 | 0.56 | 20 | 22 | 37 | | 0.59 | 0.13700 | 4.53 | 7.873 | 3.92 | 0.4167 | 1.97 | 0.45 | 2245 | 37 | 2190 | 78 | -2 |
| 56.1 | 0.09 | 63 | 59 | 100 | | 0.59 | 0.18750 | 2.51 | 12.359 | 2.31 | 0.4780 | 1.32 | 0.71 | 2518 | 28 | 2721 | 41 | 8 |
| 57.1 | 1.67 | 27 | 16 | 56 | | 0.29 | 0.13460 | 4.09 | 7.535 | 3.71 | 0.4060 | 1.87 | 0.62 | 2197 | 35 | 2159 | 72 | -1 |
| 58.1 | 0.11 | 31 | 19 | 65 | | 0.29 | 0.13370 | 3.81 | 7.439 | 3.43 | 0.4035 | 1.73 | 0.07 | 2185 | 32 | 2147 | 67 | -1 |
| 59.1 | 2.53 | 55 | 34 | 114 | | 0.30 | 0.13790 | 2.90 | 7.847 | 2.64 | 0.4127 | 1.41 | 0.88 | 2227 | 26 | 2201 | 51 | -1 |

TABLE 5 - U-Pb isotopic data in detrital zircons from the sample (LS-03) of quartzite from Fazenda Currais (Cruzeta/RN), UTM coordinates: 737,325 mE; 9,295,128 mN (Datum WGS84, Zone 24)(continued).

| grain. spot | f(206) % | (ppm) | | | RATIOS | | | | | | AGES (Ma) | | | | | | |
|----------------|-------------|--------|-----|-----|--------|---|------------|--|------------|--|-------------|---------------|--|--------------|---|--------------|----------------|
| | | Pb rad | Th | U | Th/U | $\frac{^{207}\text{Pb}}{^{206}\text{Pb}}$ | err (%) | $\frac{^{207}\text{Pb}}{^{235}\text{U}}$ | err (%) | $\frac{^{206}\text{Pb}}{^{238}\text{U}}$ | err (%s) | Coef. corr | $\frac{^{206}\text{Pb}}{^{238}\text{U}}$ | err (abs) | $\frac{^{207}\text{Pb}}{^{206}\text{Pb}}$ | err (abs) | Disc. (%)** |
| 65.1 | 2.07 | 100 | 112 | 212 | 0.53 | 0.11570 | 2.33 | 5.734 | 2.46 | 0.3593 | 0.95 | 0.69 | 1979 | 16 | 1891 | 42 | -4 |
| 66.1 | 0.26 | 44 | 63 | 86 | 0.73 | 0.11690 | 3.42 | 5.693 | 3.31 | 0.3533 | 1.56 | 0.84 | 1950 | 26 | 1909 | 62 | -2 |
| 67.1 | 0.26 | 52 | 64 | 113 | 0.56 | 0.10810 | 2.96 | 4.718 | 2.99 | 0.3167 | 1.42 | 0.53 | 1773 | 22 | 1767 | 54 | 0 |
| 68.1 | 1.07 | 30 | 30 | 50 | 0.61 | 0.14380 | 3.89 | 8.072 | 3.72 | 0.4070 | 1.84 | 0.41 | 2201 | 34 | 2274 | 70 | 4 |
| 69.1 | 0.00 | 68 | 27 | 134 | 0.20 | 0.13010 | 2.15 | 6.901 | 2.23 | 0.3848 | 1.25 | 0.01 | 2099 | 22 | 2099 | 38 | 1 |
| 70.1 | 0.00 | 41 | 55 | 49 | 1.13 | 0.17730 | 2.93 | 12.078 | 3.09 | 0.4939 | 1.70 | 0.92 | 2588 | 35 | 2628 | 49 | 2 |
| 71.1 | 0.19 | 74 | 59 | 134 | 0.44 | 0.13210 | 2.50 | 7.082 | 2.54 | 0.3888 | 1.34 | 0.13 | 2117 | 24 | 2126 | 43 | 1 |
| 72.1 | 0.35 | 85 | 158 | 143 | 1.11 | 0.12550 | 2.31 | 6.067 | 2.41 | 0.3505 | 1.28 | 0.89 | 1937 | 21 | 2036 | 41 | 5 |
| 73.1 | 0.19 | 51 | 46 | 93 | 0.50 | 0.13240 | 2.64 | 7.246 | 2.63 | 0.3970 | 1.36 | 0.65 | 2155 | 25 | 2130 | 46 | -1 |
| 74.1 | 0.09 | 70 | 45 | 132 | 0.34 | 0.13150 | 2.43 | 7.174 | 2.52 | 0.3956 | 1.34 | 0.69 | 2149 | 24 | 2118 | 43 | -1 |
| 75.1 | 0.26 | 44 | 43 | 90 | 0.48 | 0.11620 | 3.01 | 5.577 | 2.97 | 0.3482 | 1.44 | 0.01 | 1926 | 24 | 1898 | 54 | -1 |
| 76.1 | 1.49 | 12 | 7 | 23 | 0.33 | 0.13710 | 5.69 | 7.555 | 5.33 | 0.3998 | 2.38 | 0.36 | 2168 | 43 | 2190 | 102 | 2 |
| 77.1 | 0.31 | 62 | 22 | 124 | 0.18 | 0.12690 | 2.29 | 6.798 | 2.33 | 0.3884 | 1.24 | 0.22 | 2115 | 22 | 2056 | 39 | -2 |
| 78.1 | 0.69 | 13 | 13 | 21 | 0.63 | 0.13450 | 5.43 | 7.616 | 5.00 | 0.4106 | 2.70 | 0.01 | 2218 | 51 | 2158 | 94 | -2 |
| 79.1 | 0.13 | 52 | 70 | 80 | 0.89 | 0.13780 | 2.39 | 7.951 | 2.61 | 0.4184 | 1.51 | 0.35 | 2253 | 29 | 2200 | 42 | -2 |
| 80.1 | 0.18 | 76 | 92 | 129 | 0.71 | 0.13430 | 2.38 | 7.270 | 2.58 | 0.3926 | 1.48 | 0.61 | 2135 | 27 | 2155 | 41 | 1 |
| 81.1 | 0.56 | 22 | 49 | 89 | 0.55 | 0.07430 | 4.71 | 1.785 | 4.70 | 0.1743 | 1.89 | 0.18 | 1036 | 18 | 1050 | 98 | 2 |
| 81.2 | 0.09 | 58 | 125 | 232 | 0.54 | 0.07370 | 2.85 | 1.773 | 3.01 | 0.1745 | 1.49 | 0.49 | 1037 | 14 | 1033 | 59 | 0 |
| 82.1 | 0.28 | 35 | 25 | 62 | 0.41 | 0.14110 | 2.69 | 7.869 | 2.86 | 0.4045 | 1.68 | 0.53 | 2190 | 31 | 2241 | 48 | 3 |
| 83.1 | 0.36 | 69 | 66 | 129 | 0.51 | 0.13370 | 2.32 | 7.087 | 2.49 | 0.3844 | 1.46 | 0.95 | 2097 | 26 | 2147 | 41 | 3 |
| 84.1 | 0.89 | 23 | 24 | 40 | 0.60 | 0.13030 | 3.76 | 7.182 | 3.74 | 0.3997 | 2.03 | 0.65 | 2167 | 37 | 2103 | 65 | -3 |
| 85.1 | 0.07 | 112 | 70 | 203 | 0.34 | 0.13190 | 2.05 | 7.272 | 2.28 | 0.3999 | 1.35 | 0.67 | 2169 | 25 | 2123 | 35 | -2 |
| 86.1 | 0.17 | 65 | 91 | 109 | 0.83 | 0.13070 | 2.37 | 6.949 | 2.60 | 0.3856 | 1.50 | 0.26 | 2102 | 27 | 2107 | 42 | 1 |
| 87.1 | 0.28 | 55 | 73 | 91 | 0.80 | 0.13220 | 2.57 | 7.213 | 2.72 | 0.3957 | 1.54 | 0.47 | 2149 | 28 | 2128 | 45 | -1 |
| 88.1 | 0.13 | 150 | 103 | 320 | 0.32 | 0.11720 | 1.96 | 5.661 | 2.24 | 0.3502 | 1.31 | 0.01 | 1936 | 22 | 1914 | 35 | -1 |

Errors are in 1 sigma

* Fraction of common lead

** Discordance, calculated as $(1 - \frac{^{206}\text{Pb}}{^{238}\text{U}} \text{ age} / \frac{^{207}\text{Pb}}{^{206}\text{Pb}} \text{ age}) * 100$

5. Study of the provenance of Neoproterozoic supracrustal rocks (Seridó Group)

In the context of the Seridó Group, the ages (U-Pb) of 696 detrital zircons found in paragneisses of the Jucurutu Formation, quartzites and conglomerates of the Equador Formation and schists of the Seridó Formation, by Van Schmus et al. (2003), Hollanda et al. (2015) and in the present study (Fig. 16), allow us to indicate sources with ages ranging from Archean to Neoproterozoic, with a major contribution of Paleoproterozoic and Neoproterozoic to these metasediments. Some considerations are presented below.

(1) U/Pb determinations in detrital zircon crystals found in paragneisses of the Jucurutu Formation by Van Schmus et al. (2003), Hollanda et al. (2011) and in this study (Fig. 16) show sources from Neoproterozoic to Mesoarchean, with peak contribution from Ediacaran to Tonian (0.57 to 1.1 Ga) and in Rhyacian (2.1 to 2.2 Ga), corroborating a deposition model of this unit in Ediacaran with Neoproterozoic sources that may be from the PSD itself, in addition to the Zona Transversal Domain. The Rhyacian provenance may represent contributions from rocks from the Caicó Complex and the Serra da Formiga Suite.

(2) U-Pb data in detrital zircon found in quartzites and conglomerates of the Equador Formation (Hollanda et al. 2011 and this study, Fig. 16), indicate Paleoarchean to Paleoproterozoic sources (1.6 to 3.5 Ga), with a major Rhyacian source (2.1 to 2.3 Ga). Younger ages (ca. 1.05 Ga) suggest the deposition of the formation after the end of the Tonian. In general, the data are consistent in indicating a large contribution of Mesoproterozoic

units and another smaller portion of Archean units, despite the field relations pointing to the Neoproterozoic/Ediacaran deposition. In this context, the few younger ages become significant, with rocks located south of the PSD as a possible source, more precisely in the Zona Transversal Domain.

(3) The U-Pb ages determined in detrital zircons of mica schists from the Seridó Formation (Van Schmus et al 2003; Hollanda et al. 2011) shown in Fig. 16, present Neoproterozoic sources as the main contribution to these metasediments (600 to 1000 Ma), and Paleoproterozoic (1700 to 2100 Ma) and Neoarchean (2700 to 2800 Ma) secondary sources. Such characteristics are consistent with the model of deposition of this unit in the Ediacaran, on the basis of sources that can be from within the PSD and/or from adjacent domains, such as the Zona Transversal and the Jaguariabeano.

The U-Pb ages in detrital zircons presented for each formation of the Seridó Group corroborate the field data as they are considered to belong to the same Neoproterozoic entity/group. Regarding the source of the sediments, it can be assumed that they come mainly from Rhyacian and Neoproterozoic rocks, although we have a contribution of ages from the Mesoarchean to the Neoproterozoic, which for the most part have representatives in the PSD itself (Fig. 17) or in adjacent domains.

6. Evolution of the Rio Piranhas-Seridó Domain

Data available to date (field, petrography, lithochemistry, isotopes, geological maps, etc.) collected by several authors

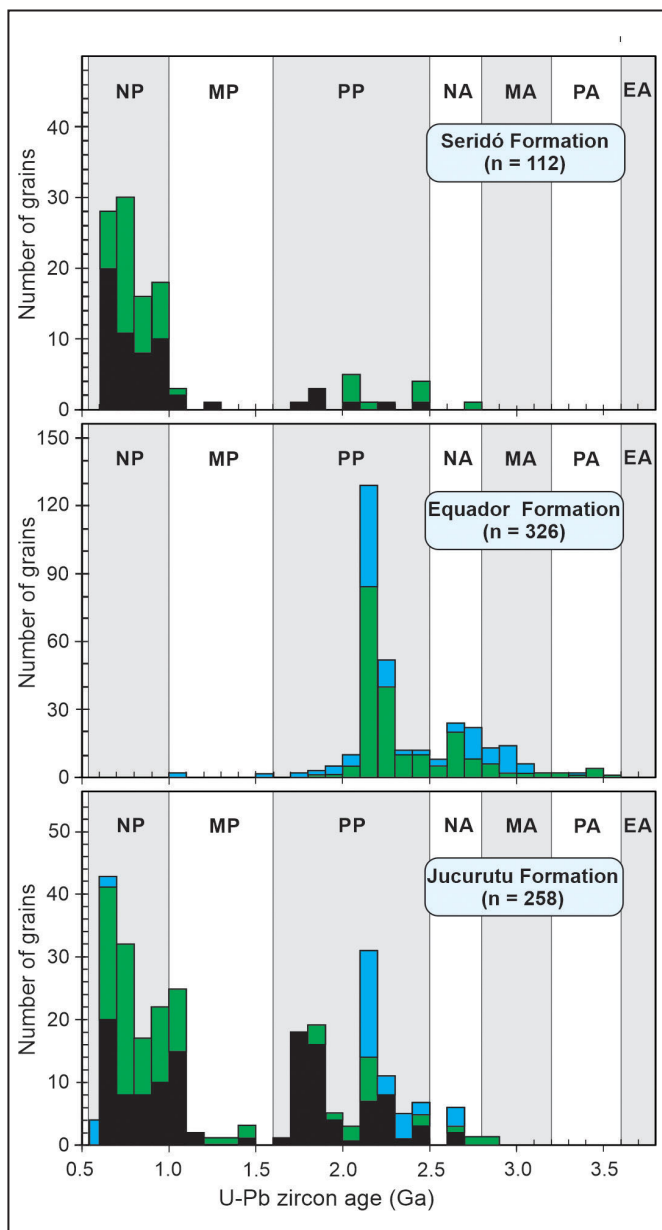


FIGURE 16. Histogram of U-Pb ages in detrital zircons (696) of paragneisses from the Jucurutu Formation, quartzites and conglomerates from the Ecuador Formation and schists from the Seridó Formation. Data from Van Schmus et al. (2003) in black, Hollanda et al. (2015) in green and this study in blue. NP=Neoproterozoic, MP=Mesoproterozoic, PP=Paleoproterozoic, NA=Neoarchean, MA=Mesoarchean, PA=Paleoarchean, EA=Eoarchean.

(Souza et al. 2007, 2016; Oliveira et al. 2013; Ruiz et al. 2019; Cavalcante et al. 2018; Santos et al. 2020; Ferreira et al. 2020a; Ferreira et al. 2020b), allowed us to suggest that the Archean units of the PSD would represent rocks with juvenile sources added to the crust, and may represent collages of blocks and/or terrains (including ocean arches) during or up to the Paleoproterozoic, in line with the proposals by Ferreira et al. (2020a, 2020b) for the Campo Grande Block region in Rio Grande do Norte (Fig. 18A).

The Paleoproterozoic accretionary process culminated in the collision between the Caicó Plate and the Benin-Nigeria Shield (Fig. 18B), where the Caicó plate would be represented by the Arabia Complex (2.50-2.30 Ga) and the Caicó Complex - Serra da Formiga Suite (2.28-2.00 Ga). The metaplutonic rocks of the

Arabia Complex are still poorly studied, but those of the Caicó Complex, according to Jardim de Sá (1994) and Souza et al. (2007, 2016), are predominantly K-calc-alkaline metaluminous units, representing a TTG-like sequence, generated from a metasomatized mantle, as represented in Fig. 18B.

Fig. 18B shows an adaptation of the proposed configuration of Jardim de Sá (1994) to the Paleoproterozoic, especially by the inclusion of Archean fragments in the model, currently recognized in the PSD through U-Pb dating of zircon (e.g., regions of Granjeiro/CE, Campo Grande/RN and São Tomé-Bonfim/RN). The final configuration considers the evolution from the generation of oceanic arches, their addition by successive collisions and generation of the Caicó protocrust (see Jardim de Sá 1994), also including probable units/sediments representing former passive margins (partially or fully obliterated).

Supracrustal sequences (paragneisses, quartzites, marbles, etc.) are attributed to both the Arabia Complex and the Caicó Complex. Despite the absence of field relationships and geochronological data in these lithotypes, these sequences are attributed as possible representatives of both the passive margin (later positioned in a convergent environment) and the arc+graben environment (Fig. 18B).

The unit representing the end of the Paleoproterozoic is materialized by the augen gneisses from the Poço da Cruz Suite, dated by Legrand et al. (1991) and Jardim de Sá et al. (1995) as Orosirian (1934-1990 Ma) and as Statherian (1741 Ma) by Hollanda et al. (2011). This Statherian age implies considering the deformation found in this unit as related to a younger event, in the Ediacaran/Brasiliano case (650-530 Ma), as there are no records of the Tonian/Cariris Velhos event from Ca. 1.0 Ga (Santos et al 2010) in the PSD.

There is a gap in the geological record in the PSD in the Mesoproterozoic, although some detrital zircons from this period have been identified in Neoproterozoic metasediments (Seridó Group), but they can be attributed to sources in domains adjacent to the PSD, e.g., in the Jaguaretama Domain, which has Calymmian age rocks (Orós Belt), and in the Zona Transversal Domain, where Calymmian rocks (e.g., augen gneiss from Taquaritinga do Norte and the Carnoí Suite) as well as Tonian rocks (lithotypes associated with the Cariris Velhos event) have also been dated.

The Seridó Basin was implemented at the end of the Neoproterozoic period, after the collision between the Caicó and Benin-Nigeria blocks had been completed, in association with the Brasiliano/Pan-African Orogenesis. Initially, it occurred in a passive margin environment (Atlantic type) with the deposition of the Jucurutu and Ecuador; then it moved on to an environment with more energy, culminating in the deposition of turbidites from the Seridó Formation (Fig. 18C). In this case, some authors (Van Schmus et al. 2003) also suggest an alternative model for the Neoproterozoic supracrustals, starting from a continental rift followed by the closure of a small oceanic basin.

Associated with this orogeny, there was also the intrusion of several magmatic bodies/suites. The predominantly strike-slip shear zones (at least in the final kinematic regime) are also part of this lithological context; they also represent the current configuration of the SPD, as shown in Fig. 19. There is a greater presence of these structures in the south-east segment of the PSD, reworking previous structures.

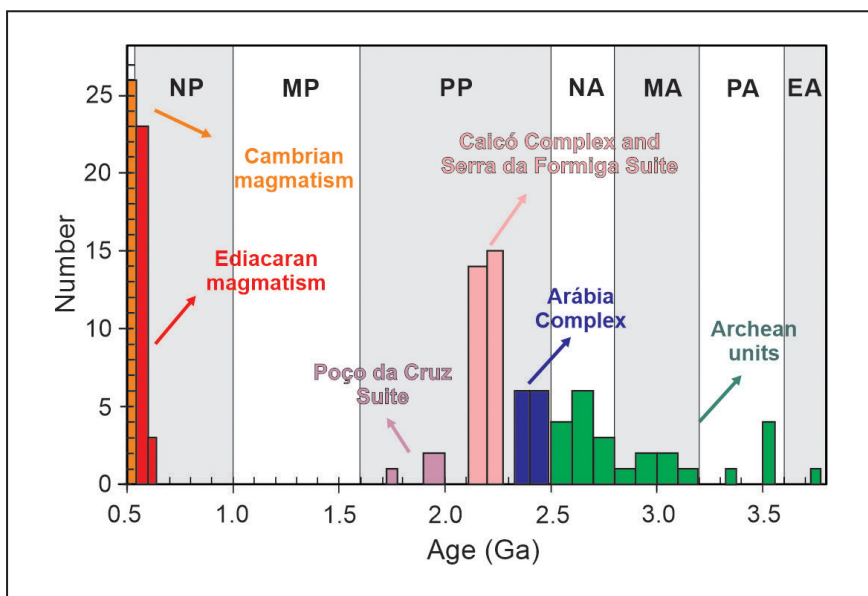


FIGURE 17. Histogram of U-Pb zircon ages (115) of PSD orthogneisses and granitoids. NP=Neoproterozoic, MP=Mesoproterozoic, PP=Paleoproterozoic, NA=Neoarchean, MA=Mesoarchean, PA=Paleoarchean, EA-Eoarchean.

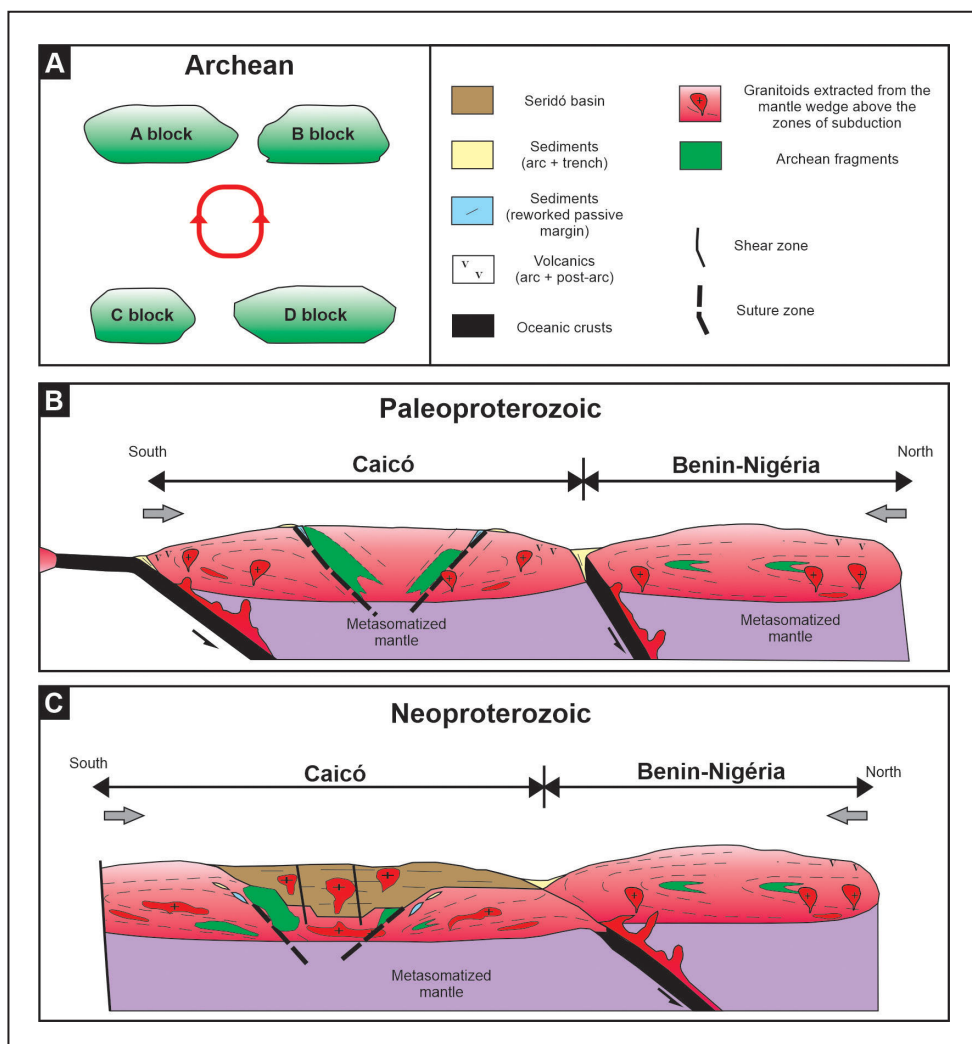


FIGURE 18. Geodynamic evolution model of the PSD, based on accretion of ocean arcs (which may contain peripheral continental arcs) and magmatism generation (Arabia and Caicó complexes, and Serra da Formiga Suite), forming the Caicó crust from fragments/Archean units (A) – Paleoproterozoic (B) and the implementation of the Seridó basin in the Neoproterozoic (C).

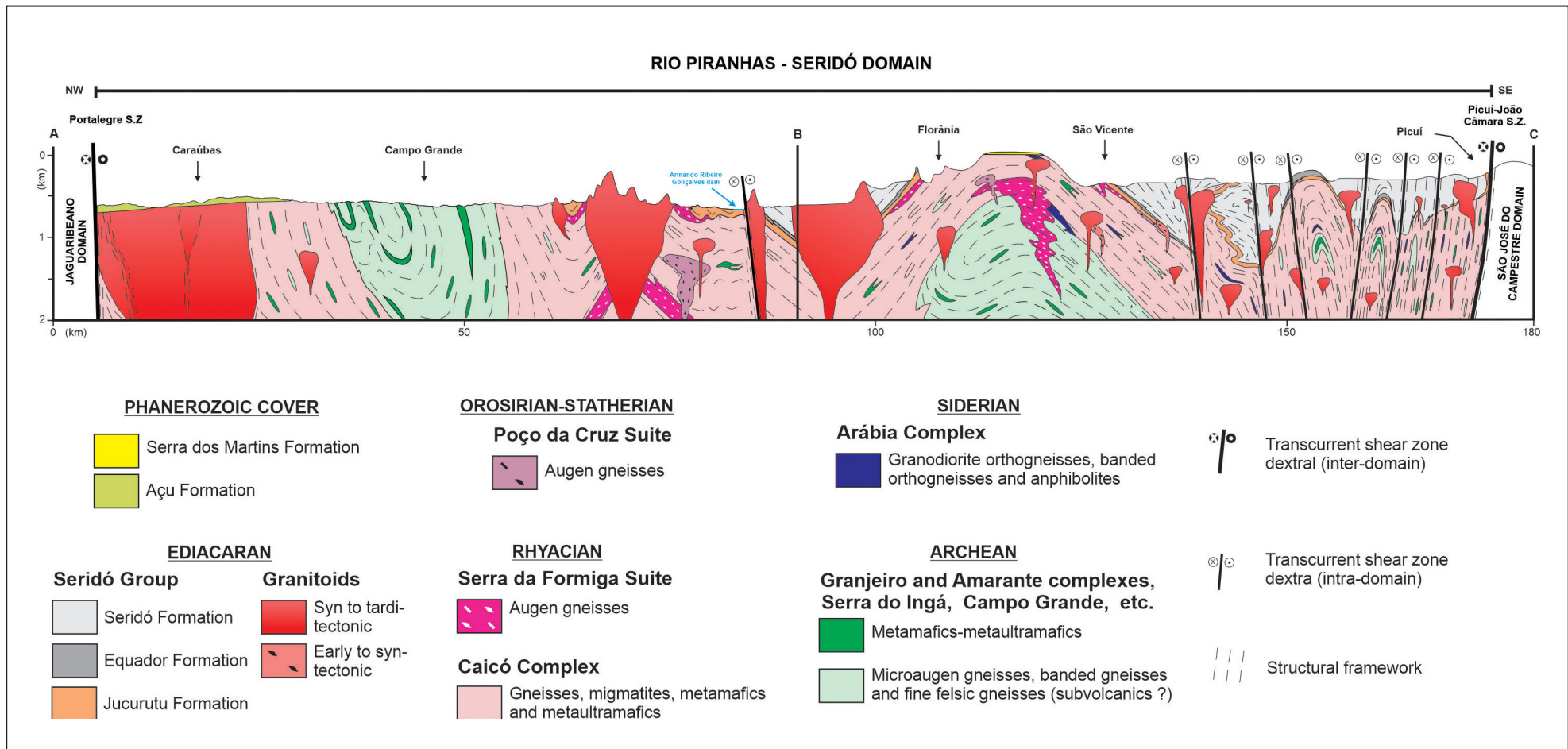


FIGURE 19. Geological profile of the PSD between the towns of Picuí-São Vicente-Florânia-Campo Grande-Caraúbas (PB/RN). S.Z. = Shear Zone. See spatial location of the profile in Fig. 3.

Geochronological data to date suggest a gap between the sedimentation of the Seridó Group (paragneisses of the Jucurutu Formation, quartzites and conglomerates of the Ecuador Formation and schists of the Seridó Formation) and the Brasiliano granitoids around 30 Ma (630 to 600 Ma.). In this context, the younger ages cited in the literature of 590–570 Ma in detrital zircons from the Seridó Group could characterize a later sedimentation/interfingering of the Seridó basin; alternatively, they could be zircons/ages affected by the Ediacaran/Brasiliano metamorphic event.

7. Final remarks

The collection of a great amount of geochronological data (U-Pb dating of zircon) in the last decades in the region allowed the recognition/characterization of Archean and Siderian units in the context of the PSD (Granjeiro, Campo Grande, Amarante and Arabia complexes, in addition to the metamafic units from Serra do Ingá). Thus, owing to continuous evolution of geochronological mapping in the region, one can expect recognition of lithotypes with these ages, especially within the Caicó Complex.

The ages found in detrital zircons indicate that the sedimentation of the Paragneisses of Fazenda Coqueiros occurred in the Neoproterozoic (Ediacaran), and they were considered as belonging to the Jucurutu Formation of the Seridó Group, although discordant values/ages may suggest a progressive loss of lead for the Neoproterozoic event (Brasiliano).

The detrital zircons of the quartzites from the Picuí River (Currais Novos/RN) dated in the present study had essentially Archean sources, while the quartzites from the Fazenda Currais (Cruzeta/RN) indicate a major Rhyacian source (about 2100 Ma) and secondarily younger sources. (~1900 and 1033 Ma). With these data, we can consider the maximum deposition of these lithotypes in the Stenian-Tonian boundary, which corroborates not only the field data, which are considered as an intermediate unit of the Seridó Group (Brasiliano), but also the model for stratigraphic stacking pattern proposed/used by Jardim de Sá (1994) and Medeiros et al. (2017) for this group.

According to the data above and those from the literature, the Seridó Group can be considered to originate from Rhyacian and Neoproterozoic sources, although there are contributions from sources ranging from the Mesoarchean to the Neoproterozoic.

In line with previous proposals, the evolution of the PSD is considered to occur as of the addition of oceanic arcs, probably between the Archean and the Paleoproterozoic, with the generation of juvenile magmas, followed by their reworking, essentially in the Neoproterozoic.

8. Acknowledgements

The authors are thankful to the Geological Survey of Brazil-CPRM for releasing the data/information reported in this study, in particular the team of the Crustal Evolution and Metallogeny Project of the Seridó Mineral Province and the team of the Geology and Mineral Potential Project of the Borborema Province. We would also like to thank the Laboratory of Grinding, Department of Geology, Federal University of Rio Grande do Norte. We are also grateful to Prof. Claudia Regina Passarelli (PhD) and to the blind reviewer for the suggestions that contributed to the improvement of this manuscript.

References

- Abduriyim A., Kitawaki H., Furuya M., Schwarz D. 2006. Paraiba-type Copper-bearing Tourmaline from Brazil, Nigeria, and Mozambique: chemical fingerprinting by LA-ICP-MS. *Gems and Gemology*, 42(1), 4–21. <https://doi.org/10.5741/GEMS.42.1.4>.
- Almeida F.F.M., Hasui Y., Brito Neves B.B., Fuck R.A. 1977. Províncias estruturais brasileiras. In: Simpósio de Geologia do Nordeste, 8, Campina Grande, p. 363–391.
- Ancelmi M.F. 2016. Geocronologia e geoquímica das rochas arqueanas do Complexo Granjeiro, Província Borborema. PhD Thesis, Instituto de Geociências, Universidade Estadual de Campinas, Campinas, 159 p. Available online at: <http://www.repositorio.unicamp.br/handle/REPOSIPI/330571> / (accessed on 30 August 2021).
- Angelim L.A.A., Medeiros V.C., Nesi, J.R. 2006. Mapa geológico do Estado do Rio Grande do Norte, Escala 1:500.000. Programa Geologia do Brasil, Recife, CPRM, FAPERN. Available online at: <https://rigeo.cprm.gov.br/handle/doc/10234> / (accessed on 1 September 2021).
- Archango C.J., Viegas L.G.F., Hollanda M.H.B.M., Souza L.C., Liu D. 2013. Timing of the HT/LP transpression in the Neoproterozoic Seridó belt (Borborema Province, NE Brazil): constraints from U-Pb (SHRIMP) geochronology and implications for the connections between NE Brazil and West Africa. *Gondwana Research*, 23(2), 701–714. <https://doi.org/10.1016/j.gr.2012.05.005>.
- Baumgartner R., Romer R.L., Moritz R., Sallet R., Chiaradia M. 2006. Columbite-tantalite-bearing granitic pegmatites from the Serido belt, Northeastern Brazil: genetic constraints from U-Pb dating and Pb isotopes. *The Canadian Mineralogist*, 44(1), 69–86. <https://doi.org/10.2113/gscanmin.44.1.69>.
- Beurlen H., Rhede D., Silva M.R.R., Thomas R., Guimarães I.P. 2009. Petrography, geochemistry and chemical electron microprobe U-Pb-Th dating of pegmatitic granites in the Borborema Pegmatite Province, NE-Brazil: a possible source of the rare-element granitic pegmatites. *Terraer* 6(1), 59–71. Available online at: <https://www.ige.unicamp.br/terrae/V6/PDF-N6/T-a6i.pdf> / (accessed on 1 September 2021).
- Beurlen H., Thomas R., Silva M.R.R., Müller A., Rhede D., Soares D.R. 2014. Perspectives for Li- and Ta-Mineralization in the Borborema Pegmatite Province, NE-Brazil: a review. *Journal of South American Earth Sciences*, 56, 110–127. <https://doi.org/10.1016/j.jsames.2014.08.007>.
- Black L.P., Kamo S.L., Allen C.M., Aleinikoff J.N., Davis D.W., Korsch R.J., Foudolis C. 2003. TEMORA 1: a new zircon standard for Phanerozoic U/Pb geochronology. *Chemical Geology*, 200(1–2), 155–170. [https://doi.org/10.1016/S0009-2541\(03\)00165-7](https://doi.org/10.1016/S0009-2541(03)00165-7).
- Brito Neves B.B. 1975. Regionalização geotectônica do pré-cambriano nordestino. PhD Thesis, Instituto de Geociências, Universidade de São Paulo, São Paulo, 198 p. Available online at: <https://teses.usp.br/teses/disponiveis/44/44132/tde-21062013-104857/pt-br.php> / (accessed on 31 August 2021).
- Cabral Neto I., Silveira F.V., Fernandes P.R., Paes V.J., Santos L.D., Medeiros V.C. 2018. Mapa geológico e de recursos minerais de lítio – Província Pegmatítica da Borborema, Escala 1:250.000. Natal, CPRM. Available online at: <http://rigeo.cprm.gov.br/jspui/handle/doc/20512> / (accessed on 1 September 2021).
- Cabral Neto I., Medeiros V.C., Cavalcante R., Fernandes P.R., Silveira F.V., Dantas E.L., Rodrigues J.B., Bahiense I.C., Paes V.J.C., Santos L.D. 2019. Jardim do Seridó Suite: first example of Ediacaran peraluminous magmatism in the Rio Piranhas-Seridó Domain, Borborema Province, Northeast Brazil. *Journal of the Geological Survey of Brazil*, 2(2), 119–136. <https://doi.org/10.29396/jgsb.2019.v2.n2.3>.
- Campos M.S. 2011. Químicoestratigrafia isotópica de carbono e estrôncio e geoquímica de elementos terras raras em formações carbonáticas e ferríferas do Cinturão Seridó, Nordeste do Brasil. MSc Dissertation, Programa de Pós-Graduação em Geociências, Universidade Federal de Pernambuco, Recife, 99 p. Available online at: <https://repositorio.ufpe.br/handle/123456789/6477> / (accessed on 1 September 2021).
- Cavalcante R., Cunha A.L.C., Medeiros V.C. 2015. Mapa geológico do Projeto Províncias Metalogenéticas do Brasil: área PB - RN (Borborema Leste), Escala 1:250.000. Programa Geologia do Brasil, Recife, CPRM. Available online at: <https://rigeo.cprm.gov.br/handle/doc/17659> / (accessed on 2 September 2021).
- Cavalcante R., Medeiros V. C., Costa A.P., Sá J.M., Santos R.V., Rodrigues J.B., Dantas A.R., Nascimento M.A.L., Cunha A.L.C. 2018. Neoarchean, Rhyacian and Neoproterozoic units of the Saquinho region, eastern Rio Piranhas-Seridó domain, Borborema Province

- (northeastern Brazil): implications for the stratigraphic model. *Journal of the Geological Survey of Brazil*, 1(1), 11-29. <https://doi.org/10.29396/jgsb.2018.v1.n1.2>.
- Cavalcante R., Medeiros V.C., Costa A.P., Dantas A.R., Cunha A.L.C., Lima R.B., Spisila A.L., Lages G.A., Rodrigues J.B. 2019. Caracterização das rochas metáficas-ultramáficas da região de Saquinho (Cruzeta/RN), Domínio Rio Piranhas-Seridó. In: Simpósio de Geologia do Nordeste, 28, Aracaju, p. 314. Available online at: http://www.28sgn.com.br/assets/files/Anais_28o_Simpasio_de_Geologia_do_Nordeste-ISBN.pdf / (accessed on 26 November 2019).
- Caçalvanti Neto M.T.O. 2008. A faixa cuprífera do Rio Grande do Norte e Paraíba e as relações de contato entre as formações Equador e Seridó. *Holos*, 24(3), 105-118. Available online at: www2.ifrn.edu.br/ojs/index.php/HOLOS/article/view/210 / (accessed on 31 August 2021).
- Corrêa R.S., Oliveira C.G., Dantas E.L., Della Giustina M.E.S., Hollanda M.H.B.M. 2021. The root zones of the Seridó W-skarn system, northeastern Brazil: constraints on the metallogenesis of a large Ediacaran tungsten Province. *Ore Geology Reviews*, 128, 103884. <https://doi.org/10.1016/j.oregeorev.2020.103884>.
- Costa A.P., Dantas A.R. 2012. Cartografia geológica de uma área na região de Pedra Preta-RN. In: Congresso Brasileiro de Geologia, 46, Santos.
- Costa A.P., Dantas A.R. 2014. Carta geológica da folha Lajes SB.24-X-D-VI, Estado do Rio Grande do Norte, Escala 1:100.000. Programa Geologia do Brasil, Recife, CPRM. [Available online at: https://rigeo.cprm.gov.br/handle/doc/20238](https://rigeo.cprm.gov.br/handle/doc/20238) / (accessed on 6 September 2021).
- Costa A.P., Dantas A.R. 2018. Geologia e recursos minerais da folha Lajes SB.24-X-D-VI, Estado do Rio Grandedo Norte, Escala 1:100.000. Recife, CPRM, 163 p. Available online at: <http://rigeo.cprm.gov.br/jspui/handle/doc/20238> / (accessed on 31 August 2021).
- Costa A.P., Nascimento M.A.L., Galindo A.C., Dantas A.R. 2015. Geologia, petrologia e geocronologia U-Pb do Plutônio Granítico Serra da Rajada: implicações sobre a evolução magmática ediacarana na porção NE do Domínio Rio Piranhas-Seridó (NE da Província Borborema). *Geologia USP*, Série Científica, 15(3-4), 83-105. <https://doi.org/10.11606/issn.2316-9095.v15i3-4p83-105>
- Cunha A.L.C., Cavalcante R., Mariano G. 2017. Idade U-Pb do Plutônio Serra da Lagoa Seca (PSLS), folha Currais Novos - RN. In: Simpósio de Geologia do Nordeste, 27, João Pessoa. Available online at: <http://www.geologiadonordeste.com.br/anais/> / (accessed on 31 August 2021).
- Dantas A.R., Cavalcante R., Costa A.P., Cunha A.L.C., Lages G.A., Spisila A.L., Rodrigues J.B. 2019. Unidades arqueanas na porção norte da Faixa Seridó – Corpo máfico Serra do Ingá e Complexo Amarante. In: Simpósio de Geologia do Nordeste, 28, Aracaju, p. 482. Available online at: http://www.28sgn.com.br/assets/files/Anais_28o_Simpasio_de_Geologia_do_Nordeste-ISBN.pdf / (accessed on 26 November 2019).
- Dantas A.R., Nascimento M.A.L., Costa A.P., Cavalcante R. 2017. Petrografia e litioquímica de rochas ferríferas na região central do estado do Rio Grande do Norte (Domínio Rio Piranhas – Seridó, NE da Província Borborema). *Geologia USP*, Série Científica, 17(3), 163-187. <https://doi.org/10.11606/issn.2316-9095.v17-125622>.
- Dantas E.L. 1988. Mapeamento geológico da região de Florânia-RN. Graduation work, Departamento de Geologia, Universidade Federal do Rio Grande do Norte, Natal, 270 p.
- Dantas E.L., Negrão M.M., Buhn B. 2008. 2,3 Ga continental crust generation in the Rio Grande do Norte terrane, NE-Brazil. In: South American Symposium on Isotope Geology, 7, San Carlos de Bariloche, p. 40.
- Degen S., Franz L., Krzemnicki M.S., Wang H.A.O., Berger A. 2019. Petrology and mineralogy of gem-quality “Paraíba-type” tourmaline bearing granitic pegmatite from Parelhas, Brazil. Swiss Geoscience Meeting, 17, Fribourg, p. 49-50. Available online at: https://geoscience-meeting.ch/sgm2019/wp-content/uploads/abstract_volumes/SGM_2019_Symposium_02.pdf / (accessed 2 September 2021).
- Ebert H. 1969. Geologia do Alto Seridó: nota explicativa da folha geológica de Currais Novos. Série Geologia Regional, 11, Recife, SUDENE, 120 p.
- Ebert H. 1970. The Precambrian geology of the “Borborema”- Belt (States of Paraíba and Rio Grande do Norte; northeastern Brazil) and the origin of its mineral provinces. *Geologische Rundschau*, 59, 1292-1326. <https://doi.org/10.1007/BF02042293>.
- Ferreira A.C.D., Ferreira Filho C.F., Dantas E.L., Souza V.S. 2019. Paleoproterozoic mafic-ultramafic magmatism in the Northern Borborema Province, Northeast Brazil: tectonic setting and potential for deposits. *The Journal of Geology*, 127(5), 483-504. <https://doi.org/10.1086/704256>.
- Ferreira A.C.D., Dantas E.L., Fuck R.A., Nedel I.M. 2020a. Arc accretion and crustal reworking from late Archean to Neoproterozoic in Northeast Brazil. *Scientific Reports*, 10, 7855. <https://doi.org/10.1038/s41598-020-64688-9>.
- Ferreira A.C.D., Dantas E.L., Santos T.J.S., Fuck R.A., Tedeschi M. 2020b. High-pressure metamorphic rocks in the Borborema Province, Northeast Brazil: reworking of archean oceanic crust during proterozoic orogenies. *Geoscience Frontiers*, 11(6), 2221-2241. <https://doi.org/10.1016/j.gsf.2020.03.004>.
- Ferreira C.A. 1998. Caicó folha SB.24-Z-B, Estados da Paraíba e Rio Grande do Norte. Programa Levantamentos Geológicos Básicos do Brasil, Brasília, CPRM, 152 p. Available online at: <http://rigeo.cprm.gov.br/jspui/handle/doc/8867> / (accessed on 31 August 2021).
- Ferreira J.A.M. 1967. Considerações sobre uma nova estratigrafia do Seridó. *Eng. Min. Metal.*, 45(265), 25-28.
- Ferreira J.A.M., Albuquerque J.P.T. 1969. Sinopse da geologia da folha Seridó. Série Geologia Regional, 18, Recife, SUDENE, 47 p.
- Fonseca G.D.A. 2019. Caracterização petrográfica e litioquímica do Stock Serra do Capuxu, SW do Domínio Rio Piranhas-Seridó, Província Borborema. MSc Dissertation. Programa de Pós-Graduação em Geodinâmica e Geofísica, Universidade Federal do Rio Grande do Norte, Natal, 97p. Available online at: <https://repositorio.ufrn.br/handle/123456789/27994> / (accessed on 6 September 2021).
- Freimann M.A. 2014. Geocronologia e petrótrama de quartzo milonitos do duplex transcorrente de Lavras da Mangabeira. MSc Dissertation, Instituto de Geociências, Universidade de São Paulo, São Paulo, 83 p. <https://doi.org/10.11606/D.44.2014-144455>.
- Gomes I.P., Palheta E.S.M., Braga I.F., Rocha J.M.A. 2019. Geologia e geocronologia dos complexos Arábia e Granjeiro, região sul do Ceará. In: Simpósio de Geologia do Nordeste, 28, Aracaju, p. 501. Available online at: http://www.28sgn.com.br/assets/files/Anais_28o_Simpasio_de_Geologia_do_Nordeste-ISBN.pdf / (accessed on 26 November 2019).
- Hackspacher P.C., Van Schmus W.R., Dantas E.L. 1990. Um embasamento transamazônico na Província Borborema. In: Congresso Brasileiro de Geologia, 36, Natal, p. 2683-2696.
- Hollanda M.H.B.M., Archanjo C.J., Souza L.C., Dunyi L., Armstrong L. 2011. Long-lived Paleoproterozoic granitic magmatism in the Seridó-Jaguaribe domain, Borborema Province-NE Brazil. *Journal of South American Earth Sciences*, 32(4), 287-300. <https://doi.org/10.1016/j.jsames.2011.02.008>.
- Hollanda M.H.B.M., Archanjo C.J., Bautista J.R., Souza L.C. 2015. Detrital zircon ages and Nd isotope compositions of the Seridó and Lavras da Mangabeira basins (Borborema Province, NE Brazil): evidence for exhumation and recycling associated with a major shift in sedimentary provenance. *Journal of South American Earth Sciences*, 258, 186-207. <https://doi.org/10.1016/j.precamres.2014.12.009>.
- Hollanda M.H.B.M., Souza Neto J.A.S., Archanjo J.C., Stein H., Maia A.C. 2017. Age of the granitic magmatism and the W-Mo mineralization in skarns of the Seridó belt (NE Brazil) based on zircon U-Pb (SHRIMP) and molybdenite Re-Os dating. *Journal of South American Earth Sciences*, 79, 1-11. <https://doi.org/10.1016/j.jsames.2017.07.011>.
- Jardim de Sá E.F. 1984. Geologia da região Seridó: reavaliação de dados. In: Simpósio de Geologia do Nordeste, 11, Natal, p. 278-296.
- Jardim de Sá E.F. 1994. A Faixa Seridó (Província Borborema, NE do Brasil) e o seu significado geodinâmico na Cadeia Brasiliiana/Pan-Africana. PhD Thesis, Instituto de Geociências, Universidade de Brasília, Brasília, 803 p.
- Jardim de Sá E.F., Salim J. 1980. Reavaliação dos conceitos estratigráficos na região do Seridó (RN-PB). *Mineração e Metalurgia*, 80(421), 16-28.
- Jardim de Sá E.F., Fuck R.A., Macedo M.H.F., Peucat J.J., Kawashita K., Souza Z.S., Bertrand J.M. 1995. Pre-brasiliense orogenic evolution in the Seridó belt, NE Brazil: conliting geochronological and structural data. *Revista Brasileira de Geociências*, 25(4), 307-314. Available online at: <http://www.ppegeo.igc.usp.br/index.php/rbg/article/view/11539> / (accessed on 31 August 2021).
- Jardim de Sá E.F., Matos R.M.D., Oliveira D.C., Rêgo J.M., Monteiro E.T., Dantas J.R.A., Xavier C.B., Hollanda M.H.B.M. 1998. Mapa Geológico do Estado do Rio Grande do Norte, Escala 1:500.000. Natal, DNPM, UFRN, PETROBRÁS, CRM.
- Johnston Jr. W.D. 1945. Os pegmatitos berilo-tantalíferos da Paraíba e Rio Grande do Norte, no Nordeste do Brasil. *Boletim*, 72, Rio de

- Janeiro, Departamento Nacional de Produção Mineral, Divisão de Geologia, 85 p.
- Legrand J.M., Liégois J.P., Deutsch S. 1991. Datação U/Pb e Rb/Sr das rochas precambrianas da região de Caicó: reavaliação da definição de um embasamento arqueano. In: Simpósio de Geologia do Nordeste, 14, Recife, p. 276-279.
- Legrand J.M., Sá J.M., Maia H.N., Souza L.C. 2009. Carta geológica da folha Jardim do Seridó SB.24-Z-B-V, Estados do Rio Grande do Norte e Paraíba, Escala 1:100.000. Programa Geologia do Brasil, Recife, CPRM. Available online at: <http://rigeo.cprm.gov.br/jspui/handle/doc/18296> / (accessed on 6 September 2021).
- Long L.E., Ketcham D.H., Fanning C.M., Sial A.N. 2019. The unregenerate São Rafael pluton, Borborema Province, Northeastern Brazil. *Lithos*, 332–333, 192–206.
- Ludwig K.R. 2003. Isoplot 3.00 - A Geochronological Toolkit for Microsoft Excel. Special Publication, 4, Berkeley, Berkeley Geochronology Center, 70 p.
- McReath I., Galindo A.C., Dall'Agnol R. 2002. The Umarizal igneous association, Borborema Province, NE Brazil: implications for the genesis of A-type granites. *Gondwana Research*, 5(2), 339-353. [https://doi.org/10.1016/S1342-937X\(05\)70727-9](https://doi.org/10.1016/S1342-937X(05)70727-9).
- Medeiros V.C., Rocha D.E.G.A., Amaral, C.A., Lins C.A.C., Souza F.J.C., Santos R.B., Barbosa A.J., Mendes V.A., Galvão M.J.T.G., Costa Filho W.D. 2008. Geologia e recursos minerais da folha Sousa SB.24-Z-A. Recife, CPRM, 312 p. Available online at: <https://rigeo.cprm.gov.br/jspui/handle/doc/10861> / (accessed on 6 September 2021).
- Medeiros V.C., Nascimento M.A.L., Dantas E.L., Cunha A.L.C. 2012a. Carta Geológica da folha Currais Novos SB.24-Z-B-II, Estados do Rio Grande do Norte e da Paraíba, Escala 1:100.000. Programa Geologia do Brasil, Recife, CPRM. Available online at: <http://rigeo.cprm.gov.br/jspui/handle/doc/18452> / (accessed on 31 August 2021).
- Medeiros V.C., Nascimento M.A.L., Galindo A.C., Dantas E.L. 2012b. Augen gnaisses riacianos no Domínio Rio Piranhas-Seridó, Província Borborema, Nordeste do Brasil. *Geologia USP, Série Científica*, 12(2), 3-14. <https://doi.org/10.5327/Z1519-874X201200020001>.
- Medeiros V.C., Cavalcante R., Cunha A.L.C., Dantas A.R., Costa A.P., Brito A.A., Rodrigues J.B., Silva M.A. 2017. O furo estratigráfico de Riacho Fechado (Currais Novos/RN), domínio Rio Piranhas-Seridó (província Borborema, NE Brasil): procedimentos e resultados. *Estudos Geológicos*, 27(3), 3-44. <https://doi.org/10.18190/1980-8208.estudosgeologicos.v27n3p1-40>.
- Meunier A.R. 1964. Sucession stratigraphique et passages latéraux deus au métamorphisme dans la Série Ceará, Antecabriens du Nord-Est brésilien. *Comptes Rendus de l'Académie des Sciences Paris*, 259, p. 3796-3799.
- Nascimento M.A.L., Dantas E.L., Medeiros V.C. 2011. Integração de dados geocronológicos do Domínio Rio Piranhas-Seridó (RN-PB, NE do Brasil), com base em idades U-Pb. In: Simpósio de Geologia do Nordeste, 24, Aracaju, p. 391. Available online at: <http://www.sbgc.org.br/home/pages/44#Simp%C3%B3sios%20Regionais> / (accessed on 6 September 2021).
- Nascimento M.A.L., Galindo A.C., Medeiros V.C. 2015. Ediacaran to cambrian magmatic suites in the Rio Grande do Norte domain, extreme Northeastern Borborema Province (NE of Brazil): current knowledge. *Journal of South American Earth Sciences*, 58, 281-299. <https://doi.org/10.1016/j.jsames.2014.09.008>.
- Nascimento M.A.L., Medeiros V.C., Galindo A.C. 2018. Plutón Serra da Garganta como registro de magmatismo cálcio-alcalino no Domínio Rio Piranhas – Seridó, Nordeste da Província Borborema. *Pesquisas em Geociências*, 45(1), 1-27. <https://doi.org/10.22456/1807-9806.85638>.
- Oliveira C.G., Dantas E.L., Souza V.S., Rodrigues Neto I., Dantas R., Silva J.C. 2013. Contribuição ao enquadramento metalogenético da Província Mineral do Seridó. In: Seminário das Províncias Metalogenéticas Brasileiras, 1, Currais Novos. CD-ROM.
- Oliveira S.F., Cunha A.L.C. 2018. Geologia e recursos minerais da folha Santa Cruz SB.24-Z-B, Estados do Rio Grande do Norte e Paraíba. Recife, CPRM, 167 p. Available online at: <http://rigeo.cprm.gov.br/jspui/handle/doc/20239> / (accessed on 6 September 2021).
- Palheta E.S.M., Gomes I.P., Braga I.F., Rocha J.M.A., Besser M.L., Freire D.P.C., Filho D.V., Holanda J.L.R. 2019. Mapa geológico Granjeiro-Cococi, Escala 1:250.000. Projeto Granjeiro Cococi, Fortaleza, CPRM. Available online at: <http://rigeo.cprm.gov.br/jspui/handle/doc/18691> / (accessed on 30 August 2021).
- Rolff P.M.A. 1945. Contribuição ao estudo da cassiterita no Nordeste. *Boletim*, 73, Rio de Janeiro, Departamento Nacional de Produção Mineral, Divisão de Geologia, 71 p.
- Roy P.L.D., Madon H.L. 1964. Estudo dos pegmatitos do Rio Grande do Norte e da Paraíba. Série Geologia Econômica, 1, Recife, SUDENE, 129 p.
- Ruiz F.V., Giustina M.E.S.D., Oliveira C.G., Dantas E.L., Hollanda M.H.B. 2019. The 3.5 Ga São Tomé layered mafic-ultramafic intrusion, NE Brazil: insights into a Paleoproterozoic Fe-Ti-V oxide mineralization and its reworking during West Gondwana assembly. *Precambrian Research*, 326, 462-478. <https://doi.org/10.1016/j.precamres.2018.03.011>.
- Sá J.M., Galindo A.C., Legrand J.M., Souza L.C., Maia H.N., Costa L.S. 2013. U-Pb and Sm-Nd isotopic data in Ediacaran granites in western Rio Grande Norte. In: Simpósio de Geologia do Nordeste, 25, Gravatá, p. 521-522.
- Santiago J.S., Souza V.S., Dantas E.L., Oliveira C.G. 2019. Ediacaran emerald mineralization in Northeastern Brazil: the case of the Fazenda Bonfim deposit. *Brazilian Journal of Geology*, 49(4), e20190081. <https://doi.org/10.1590/2317-4889201920190081>.
- Santos E.J. 1973. Província scheelítifera do Nordeste. In: Congresso Brasileiro de Geologia, 27, Aracaju, p. 31-46.
- Santos E.J., Van Schmus W.R., Kozuch M., Brito Neves B.B. 2010. The Cariris Velhos tectonic event in northeast Brazil. *Journal of South American Earth Sciences*, 29(1), 61-76. <https://doi.org/10.1016/j.jsames.2009.07.003>.
- Santos F.G., Cavalcanti Neto M.T.O., Ferreira V.P., Bertotti A. 2020. Eo to Paleoarchean metamafic-ultramafic rocks from the central portion of the Rio Grande do Norte Domain, Borborema Province, northeast Brazil: the oldest South American platform rock. *Journal of South American Earth Sciences*, 97, 102410. <https://doi.org/10.1016/j.jsames.2019.102410>.
- Scorza E.P. 1944. Província Pegmatítica da Borborema. *Boletim*, 112, Rio de Janeiro, Departamento Nacional de Produção Mineral, Divisão de Geologia, 55 p.
- Sial A.N., Campos M.S., Gaucher C., Frei R., Ferreira V.P., Nascimento R.C., Pimentel M.M., Pereira N.S., Rodler A. 2015. Algoma-type Neoproterozoic BIF's and related marbles in the Seridó belt (NE Brazil): REE, C, O, Cr and Sr isotope evidence. *Journal of South American Earth Sciences*, 61, 33-52. <https://doi.org/10.1016/j.jsames.2015.04.001>.
- Silva L.C., McNaughton N.J., Vasconcelos A.M., Gomes J.R.C., Fletcher I.R. 1997. U-Pb SHRIMP ages in southern State of Ceará, Borborema Province, NE Brazil: Archean TTG accretion and Proterozoic crustal reworking. In: International Symposium on Granites and Associated Mineralizations, 2, Salvador, p. 280-281.
- Silva M.A., Galindo A.C., Cavalcante R., Cunha A.L.C., Medeiros V.C. 2017. Magmatismo granítico neoproterozoico no Domínio Rio-Piranhas-Seridó: geoquímica e geocronologia do plutão granítico Serra da Acauã. In: Simpósio de Geologia do Nordeste, 27, João Pessoa. Available online at: <http://www.geologiandonordeste.com.br/anais/> / (accessed on 31 August 2021).
- Silva M.R.R. 1993. Petrographical and geochemical investigations of pegmatites in the Borborema Pegmatitic Province of Northeastern Brazil. PhD Thesis, Ludwig-Maximilians-Universität München, München, 306 p.
- Silva M.R.R., Dantas J.R.A. 1997. Província Pegmatítica da Borborema - Seridó, Paraíba e Rio Grande do Norte. In: Schobbenhaus C., Queiroz E.T. (eds.). Principais depósitos minerais do Brasil. Brasília, DNPM, CPRM, p. 441-467.
- Silva M.R.R., Höll R., Beurlen H. 1995. Borborema Pegmatitic Province: geological and geochemical characteristics. *Journal of South American Earth Sciences*, 8(3-4), 355-364. [https://doi.org/10.1016/0895-9811\(95\)00019-C](https://doi.org/10.1016/0895-9811(95)00019-C).
- Souza Z.S. 1991. Petrogénèse des metagranitoides du Complexe de Caicó, Província Borborema (Etat du Rio Grande do Norte, Brésil). MSc Dissertation, CAESS, Université de Rennes, Rennes, 87 p.
- Souza Z.S., Martin H., Peucat J.-J., Jardim de Sá E.F., Macedo M.H.F. 2007. Calc-alkaline magmatism at the archean e proterozoic transition: the Caicó complex basement (NE Brazil). *Journal of Petrology*, 48(11), 2149-2185. <https://doi.org/10.1093/petrology/egm055>.
- Souza Z.S., Kalsbeek F., Deng X-D., Frei R., Kokfelt T.F., Dantas E.L., Li J-W., Pimentel M.M., Galindo A.C. 2016. Generation of continental crust in the northern part of the Borborema Province, northeastern Brazil, from Archean to Neoproterozoic. *Journal of South American Earth Sciences*, 68, 68-96. <https://doi.org/10.1016/j.jsames.2015.10.006>.
- Trindade R.I.F., Dantas E.L., Babinski M., Van Schmus W.R. 1999. Short-lived granitic magmatism along shear zones: evidence from

- U-Pb zircon and sphene ages of Caraúbas and Tourão granites. In: South American Symposium on Isotope Geology, 2, Córdoba, p. 143-144.
- Van Schmus W.R., Brito Neves B.B., William I.S., Hackspacher P.C., Fetter A.H., Dantas E.L., Babinski M. 2003. The Seridó group of NE Brazil, a late Neoproterozoic pré- to syncollisional basin in West Gondwana: insights from SHRIMP U-Pb detrital zircons ages and Sm-Nd crustal residence (TDM) ages. *Precambrian Research*, 127(4), 287-386. [https://doi.org/10.1016/S0301-9268\(03\)00197-9](https://doi.org/10.1016/S0301-9268(03)00197-9).
- Vasconcelos A.M., Gomes F.E.M. 1998. Mapa geológico da folha Iguatú SB.24-Y-B, Estado do Ceará, Escala 1:250.000. Programa Levantamentos Geológicos Básicos do Brasil, Fortaleza, CPRM. Available online at: <http://rigeo.cprm.gov.br/jspui/handle/doc/8840> / (accessed on 30 August 2021).